INTEGRATED GENERATOR PROTECTION

By

Yi Hu

A THESIS
Submitted to the Faculty of Graduate Studies
in partial fulfillment of the requirements for the degree of

DOCTOR OF PHILOSOPHY

Department of Electrical and Computer Engineering
The University of Manitoba
Winnipeg, Manitoba, Canada

ISBN 0-315-99127-5

INTEGRATED GENERATOR PROTECTION

BY

YI HU

A Thesis submitted to the Faculty of Graduate Studies of the University of Manitoba in partial fulfillment of the requirements for the degree of

DOCTOR OF PHILOSOPHY

To

My Wife

and

My Family

I hereby declare that I am the sole author of this thesis.

I authorize the University of Manitoba to lend this thesis to other institutions or individuals for the purpose of scholarly research.

YI HU

I further authorize the University of Manitoba to reproduce this thesis by photocopying or by other means, in total or in part, at the request of other institutions or individuals for the purpose of scholarly research.

YI HU

The University of Manitoba requires the signatures of all persons using or photocopying this thesis. Please sign below, and give address and date.

ABSTRACT

Modern large generators are equipped with complicated protection systems to protect them from being damaged by different abnormal operating conditions and faults. These systems normally include a large number of different protection functions. The protection functions included in a particular generator protection system are not only determined by the type of generator, but also by the power system to which it is connected. One such example is the protection system for generators supplying HVDC transmission lines. Besides standard protection functions, three special problems should be addressed. These are: wide local system operating frequency range, harmonics, and self–excitation.

As the studies in this thesis show, solutions can be provided for these problems. However, it is very difficult to solve them for existing protection systems, due to the fact that these systems are not designed for easy modification and addition of new functions. It will also be very costly to use additional separate devices to solve these problems. A low cost, Integrated Generator Protection System (IGPS) can provide a solution to the above problems and is the subject of this thesis.

The IGPS is designed to access all necessary input signals of a generator, to include all required protection functions and to have sufficient computational power reserved for future changes. It can either be used to replace existing systems having the above problems or for new installations. The IGPS has obvious economic advantages over existing generator protection systems. The thesis also analyzes the IGPS reliability and functionality advantages compared to non–integrated protection systems. A prototype of an IGPS has been successfully implemented in this research and has demonstrated the feasibility of implementing a practical IGPS using state–of–the–art computer technology.

ACKNOWLEDGEMENT

I wish to express my sincere thanks and gratitude to my research supervisor, Professor Peter G. McLaren at Department of Electrical & Computer Engineering, University of Manitoba, for his guidance and encouragement throughout the course of this research work.

I also wish to thank Professor A. M. Gole for his invaluable discussions and assistance in the study and simulation of the difficult self–excitation problems. Special thanks are due to Mr. Erwin Dirks for his support and assistance in the hardware and software development of this research project.

The financial support from Manitoba Hydro for this project is gratefully acknowledged. I owe special thanks to Mr. D. J. Fedirchuk and Mr. A. Castro of Manitoba Hydro for their discussions, suggestions and supply of necessary data which were invaluable to the success of this research project.

I also wish to express my appreciation to all professors, colleagues and technical staff at the Power System Group, Department of Electrical & Computer Engineering, University of Manitoba, for their support, assistance and friendship during the course of this study, which made my years in Winnipeg a very pleasant experience.

Finally, I wish to express my greatest thanks to my wife and my family for their patience and sacrifice, as well as their continuous support and encouragement, for which the author is in deep debt.

YI HU

Table of Contents

List of Figures

Figure **Page**

List of Tables

CHAPTER 1

INTRODUCTION

1–1 The Problem

Modern protection systems for large generators have become more and more complicated due to the tasks which need to be accomplished. In the past few decades, the capacity of a single generator has been increased steadily to achieve high operating efficiency/cost. Compared to the small and medium capacity generators, large generators (> 100 MW) are typically having larger d–axis and q–axis inductances, smaller overheat capacity, smaller mechanical inertia constant and relatively higher fault probabilities. All this requires that a large generator be protected by a more complicated protection system. The advancement of HV/EHV and HVDC transmission technologies further complicated the protection and monitoring tasks of a generator protection system [8] [60].

Because of the importance of a large generator in a system to which it is connected, and the high repair cost of a large generator if it were damaged, as well as the complexity of the task in protecting a large generator, there is a continuous effort to evaluate the performance of existing generator protection systems, to study different aspects of a power system which affect the design and operation of generator protection systems, as well as to search for new and enhanced methods to improve the existing generator protection systems. As a result of these efforts, changes and/or modifications to the installed generator protection systems may be required.

The need to modify the existing system or add some new functions to the existing system may arise because of some changes of a power system itself. It could arise when transmission systems have been changed due to the addition of new lines, installation of series capacitors etc., or system operating requirements were changed.

Thus a common problem for an installed generator protection system is that no matter how much efforts was made in the design of the original system, it is often found that there is a need to modify the system or add some new functions to it. Normally, complete redesign and replacing the

existing system are not considered because the cost involved hardly can be justified, especially when most protection functions in the existing system still work properly. Making some modifications to the existing system and/or adding new protection schemes to the system are the common solutions when some changes to it are required.

Modifying and/or adding new protection functions to an existing generator protection system is not an easy task. This is because most of the installed systems are designed to only have and perform the protection functions specified in the original design stage. Making any changes to an existing protection system will involve making changes to the original system design, arranging scheduled shutdown of the protection system, rewiring the system and conducting extensive tests after changes are made to ensure the system works properly.

Making changes to an existing protection system could also be a very costly task, due to the direct costs in purchasing cables, relays or new protection schemes and the indirect costs of scheduled shut–down, system rewiring and extensive after–change tests.

If a new protection function is a complex one, it will require a complex scheme to accomplish the task and the cost of providing it could be high. This in some cases may make the addition of a new protection function to the existing system not economically justifiable, thus leaving the generators not properly protected. Other problems one may encounter in adding a new protection function are that the cabinet of an existing protection system does not have enough space to put in the new scheme, and some signals required by the new scheme are not available at the existing protection system site. All these problems require additional cost to solve.

One possible solution to the above problems is to design a low–cost yet powerful integrated digital generator protection system. The system will have all necessary input signals from a generator and can perform all main and optional protection and monitoring functions for a generator. Besides the implemented protection functions, it also has sufficient computation power reserved for future modification and addition of new protection functions.

If a large generator is protected by such a system, no hardware redesign and rewiring will be required when any of the built–in protection functions needs to be modified. Only the software

modification is required. Adding a new protection function to such a system will also be easy, as only additional software for the new protection function needs to be written and added to the existing software. Both can result in substantial cost reduction in the modification and new protection function addition to an installed system.

If the cost of such a system is properly controlled, it could also make complete replacement of an existing system economically justifiable for some cases. Such a case would be where more than one new protection function needs to be added to the existing system and some of the protection functions are not working properly in the existing system.

1–2 The background

This research originated from the need to provide proper solutions to three special generator protection problems in the Northern Collector System of Manitoba Hydro.

Manitoba Hydro has long been known as a pioneer in the HVDC (High Voltage Direct Current) transmission technology. The Kettle and Long Spruce hydro stations at Nelson river transmit most of their power through two bipolar HVDC lines from Radisson and Henday converter stations to Dorsey inverter station near Winnipeg. Since 1993, Limestone generating station has joined Kettle and Long Spruce stations to deliver its power through the same two bipolar HVDC lines to the main Manitoba AC system. The system with the above three generating stations is called the Northern Collector System.

For generators in a generating station connected to the HVDC transmission lines, three special protection and monitoring problems have been identified. These problems are "wide system operating frequency", "harmonics monitoring" and "self–excitation due to load rejections".

The first special problem is caused by the fast load change due either to fast regulations of the DC load flow or to load rejections, and the slow response of generator mechanical input power. It is well known that the load flow in an HVDC transmission line can be regulated very fast (in milliseconds). This has been widely used to increase the main AC system's stability, damp

sub–synchronous oscillations and maintain main system operating frequency in a specified range. Also, faults on the DC line or failure of firing control circuit etc. could cause rectifiers to be blocked resulting in load rejections. However, the generator mechanical input power can not be changed instantly. This causes the system frequency in such a generating station to fluctuate widely. In the Northern Collector System of Manitoba Hydro, the system frequency fluctuation range was identified as from 45 Hz to 90 Hz, with 60 Hz as its nominal system operating frequency. This is quite different from a normal AC system, where the frequency is always kept close to its nominal value (60 Hz in North America).

The second problem is the need to monitor harmonics levels in the generator stator currents and voltages. The rectifier bridge of an HVDC transmission line is well known as a current harmonics generator. The harmonics normally are suppressed to acceptable levels by the filters installed at the rectifier AC busbar. But imperfect system conditions, system operating frequency fluctuation and system impedance off designed value could cause the harmonics levels to increase. The high level harmonics will induce extra heat in generator rotor and stator, as well as high frequency vibrations and noise, thus it is necessary to continuously monitor the harmonics levels for generators operating in such a generating station.

Self–excitations and the consequent severe overvoltages, resulting from load rejections of HVDC lines is another major problem for generators operating in such a generating station. Self–excitation is a special problem for generators carrying dominantly capacitive load. A generator becomes self–excited when $X_C < X_d$ for d–axis and $X_C < X_q$ for q–axis [65] [69] [71], where X_C is the charging impedance seen at the generator terminal. When a self–excitation condition occurs, the system voltage will keep increasing limited only by the transformer saturation.

Because of the nature of AC–DC conversion, the rectifiers of an HVDC transmission line consume inductive VARs equivalent to 40 – 50% of active power converted. The rectification of AC power also generates high magnitude harmonic components. The AC filters are installed at the rectifier busbar both to suppress the harmonics and to supply part or all of the reactive power required for the AC–DC conversion. When there is a full load rejection, generators will be left connected only to the filters. The large capacitive load of the AC filters, previously consumed by the rectifiers,

will have to flow into the generators. This exposes the generators to the danger of self–excitation and the consequent system overvoltage. The generator field current will be reduced to a very low level close to zero or may attempt to go negative when a generator is close to or enters a self–excitation condition.

If negative current is not allowed to flow in generator exciters, which is the case for generators in the Northern Collector System, a self–excitation immediately after a load rejection could cause an immediate system overvoltage and induce very high reverse voltage across the exciter bridge. The high exciter reverse voltage is caused by the field current attempting to go negative, which is the combined effect of after–load–rejection low field current and superimposed oscillating components. The oscillating field current components are induced by the oscillations between filter capacitances and generator inductance. These oscillations are initiated by the load rejections.

Generator tripping after a load rejection exposes remaining generators in the system to even more danger of self–excitations. The remaining generators have to pick up more capacitive load left by the tripped machines and another burst of oscillations is initiated. Severe damage may result if the reverse overvoltage across an exciter bridge becomes too high [61]. In one incident on September 30, 1978 [61] at the Northern Collector System, the self–excitation after a full load rejection caused severe damage to the exciter of one generator at Kettle station.

These special protection problems, especially the self–excitation problem, at the Northern Collector System have long been known and studied. As the result of the self–excitation problem studies, a self–excitation protection system has been proposed [59] [60]. The proposed self–excitation protection is provided by (1) specifying different generator and filter combinations for different active and reactive load requirements, and (2) installing a "low field current + overvoltage relay" self–excitation protection system. Field tests were conducted at the Northern Collector System to investigate the feasibility and reliability of using field current level to detect self–excitation conditions after load rejection [60]. The proposed system is intended to remove strict

operating restrictions currently employed in the Northern Collector System to prevent self–excitation from occurring.

But to solve these problems separately has been shown to be too costly. Estimated cost of adding just "low field current + overvoltage relay" self–excitation protection system to all generators at Kettle and Long Spruce stations will be $200,000 in 1985 dollar value [59]. Adding harmonics monitoring schemes costs even more, as a 1987 survey [35] shows that the market price for commercially available harmonic measurement equipments is ranging from $8,000 to $33,000, and there are in total 22 generators in Kettle and Long Spruce generating stations.

It was decided to develop an integrated generator protection system for generators in the Northern Collector System. The system should provide adequate solutions to the above special protection problems with all standard generator protection functions. The cost of the system should be properly controlled so that it can be considered as a replacement option for the existing protection system. The project is named as the Integrated Generator Protection System (IGPS) project.

1–3 Goals of this research

This research has two major tasks. One is to study special protection problems related to generators connected to DC lines. Another task is to build a prototype of an integrated generator protection system.

The goal of the first task is to investigate proper solutions to special protection problems related to generators connected to DC lines. Though some aspects of these special generator protection problems have been studied previously, many other aspects of these problems have not been thoroughly studied. This research further investigates these problems with the focus of providing a proper solution to each of them. The investigation involves studying these problems, comparing different available techniques, and selecting practical algorithms or developing new algorithms when there is no suitable one available.

The goal of another task is to verify the feasibility of building an inexpensive integrated generator protection system using state–of–the–art computer technology. Although computer

technologies have advanced significantly in the past decade, whether the state–of–the–art technology is powerful enough to implement a low–cost yet powerful integrated generator protection system still remains as a question. The question can only be answered by building a prototype of such a system using the state–of–the–art technology. The initial goal is to build a prototype of an integrated generator protection system, which could provide adequate protections for the generators connected to the HVDC lines, and is also economically acceptable for replacing existing protection systems in the Northern Collector System of Manitoba Hydro.

The second goal also affects the considerations in selecting and developing proper solutions for the special protection problems in the first task of this research, i.e. the selected solutions should have little difficulty in being integrated into an integrated generator protection system.

1–4 The scope of the Thesis

The Thesis consists of two major parts corresponding to the two goals of this research. The first part is from chapter 2 to chapter 6 focusing on the generator protections including the study of special protection problems, and the second part includes chapter 7 to chapter 9 dealing with different issues of an integrated generator protection system. Chapter 10 presents the main achievements and conclusions of this research work, as well as some considerations and suggestions for the future development of a practical integrated generator protection system.

In the first part, Chapter 2 mainly describes the normal main and optional generator protection and monitoring functions. Chapters 3 to 6 analyze the three special protection problems and their solutions for generators connected to the HVDC lines. In the second part, Chapter 7 deals with the general aspects of an integrated protection system. Chapters 8 and 9 are concentrated on the considerations and actual hardware and software implementations of the first prototype of an integrated generator protection system, as well as the results obtained from the prototype regarding the feasibilities of building a practical integrated generator protection system. The contents of these chapters are briefly described as follows:

(1) Chapter 1: This chapter.

(2) Chapter 2: The basic structures of large generators and the common abnormal conditions and fault types of a large generator are presented in the beginning of this chapter. This is followed by the brief description of main and optional generator protection and monitoring functions. Then, the algorithms and criteria used by seven main protection and monitoring functions implemented in the first prototype of IGPS are presented in the last section of this chapter.

(3) Chapter 3: The sources of harmonics when a generating station is connected to DC lines and the adverse effects of harmonics on the generators are discussed at the beginning of this chapter. Different harmonic measurement techniques are presented and compared. The importance of synchronizing sampling frequency with the system frequency for fast and accurate harmonic measurement using an FFT algorithm in a digital system is also analyzed. The last section presents an efficient implementation technique for the FFT algorithm used by the first prototype of IGPS which reduces the computation time of a normal FFT by 15 – 30%.

(4) Chapter 4: As operating frequency in a generating station connected to DC lines fluctuates in a wide range (45 to 90 Hz) when load flow in the DC lines is fast regulated, frequency tracking is necessary for most of the digital systems so that they operate correctly. Different frequency tracking algorithms are discussed and compared. A fast and stable frequency tracking algorithm is developed in this research and implemented in the first prototype of IGPS. It ensures that the system can work properly when the system operating frequency changes in 45 – 90 Hz range. The power series expansion technique is used to implement the algorithm. The errors caused by utilizing this implementation technique are also analyzed.

(5) Chapter 5: This chapter analyzes the self–excitation problems in a generating station connected to DC lines from different aspects. The criteria used to determine self–excitations and a model system used for self–excitation simulations are described first. The classification between immediate and non–immediate self–excitations is introduced. This

is followed by the discussion of some consequences and possible problems which might be caused by the self–excitations. The generator operating constraints, which are determined by the self–excitation considerations, are derived and presented.

(6) Chapter 6: This chapter focuses on the self–excitation protection for generators in a generating station connected to DC lines. Different control measures are discussed. It analyzes some application problems of a commonly suggested "low field current + overvoltage relay" self–excitation protection system, and proposes a predictive self–excitation protection system based on the analysis results of Chapter 5. The last section discusses the integration of this predictive self–excitation protection system into the IGPS.

(7) Chapter 7: There are some common issues related to integrated protection systems in general, such as the economical and reliability comparisons between an integrated protection system and a non–integrated protection system, the other advantages of an integrated protection system and basic requirements for an integrated protection system. These issues are analyzed, discussed and presented in this chapter.

(8) Chapter 8: This chapter briefly describes considerations of selecting hardwares for an integrated generator protection system, and outlines the structure of the original AMPS hardware which is used by the first prototype of IGPS. During the process of development, some modifications to the original AMPS hardware have been made to further enhance its capability. These modifications are briefly described in this chapter. The adequacy of this hardware platform, and the considerations in selecting a future hardware platform for a practical integrated generator protection system are discussed in this chapter based on the implementation experience of the first prototype of IGPS and the development trend of computer technologies.

(9) Chapter 9: This chapter discusses the considerations and basic requirement of software structure for an integrated protection system. The software for the IGPS project consists of several programs, main preprocessing and protection program, man–machine interface

program, and fault records analysis and display program. In this chapter, the overall software structure for the first prototype of IGPS and the relationship among these programs are outlined first. Then, the structure, function and some implementation details of these programs are presented. Major algorithms and optimization methods used in these programs are also included in this chapter.

(10) Chapter 10: Achievements and conclusions are presented at the beginning of this chapter. This is followed by the considerations and suggestions for the future development of a practical integrated generator protection system.

CHAPTER 2

GENERATOR PROTECTION SYSTEMS

2–1 Introduction

The complexity of a generator protection system is determined by the importance of the protected generator in a power system to which it is connected, and the repair cost of the generator if it were damaged. Using fuses might be enough to protect a small generator, but for a large generator (> 100 MW), a more sophisticated protection system is required to prevent and limit the possible damage to it, because of the higher capital cost for a single machine, and the higher direct repair cost and indirect out–of–service cost if it were damaged. The repair cost for replacing one stator winding of a 100 MW hydro generator is well over $100,000.

Normally a protection system for a large generator consists of many different types of main and optional protection and monitoring functions, designed to protect different types of faults and monitor different abnormal conditions. The common practice is to divide these protection and monitoring functions into two groups or sub–systems. The two groups use separate power supplies, and are operated independently. Such arrangement is to ensure that the generator will not lose all protections when one of the groups is undergoing routine maintenance check or repair.

Not every generator is equipped with all main and optional protection and monitoring functions. The number of protection and monitoring functions needed for a generator is determined by the type of the generator and the system to which it is connected.

In the following sections, first the basic structure of generators and their main abnormal conditions and fault types will be described. The normal main and optional generator protection and monitoring functions will be listed thereafter. Then the seven main protection and monitoring functions implemented in the first prototype of IGPS will be presented in detail in the last section.

2–2 Basic generator structures

Generators can be categorized into different types. There are AC and DC generators. For AC generators, they could be operated synchronously or asynchronously. As three phase synchronous

AC generators are the dominant type of large generators, the basic generator structure discussed below is focused on this type of generators only.

Three phase synchronous AC generators could be further divided into different sub–types, such as Hydro generators, Turbine generators and Combustion generators. They could be further divided into sub–sub–types according to their capacity, cooling method, actual structure etc.. But as long as they are three phase synchronous AC generators, they all have the same basic structure.

Basically, a three phase synchronous AC generator consists of a stator and a rotor. The stator holds three phase windings and the rotor has one field winding. The rotor rotates at a designed speed driven by a prime mover, and at the same time a direct current flows in the field winding. This produces a rotating magnetic field in the generator. The rotating magnetic field then induces alternating currents in the three phase stator windings. The generated AC power in three phase stator windings is then the output to the system. The basic structure of a generator is shown in Fig. 2.2.1.

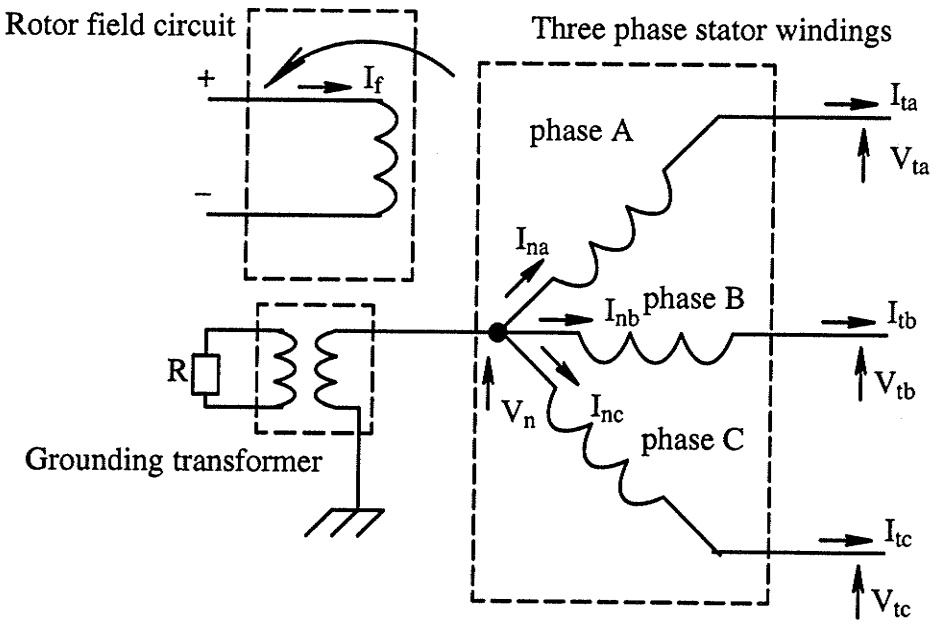

Fig. 2.2.1 Basic structure of the generators

Both stator and rotor are constructed by the special metal laminations to provide paths for field flux and reduce eddy current losses. These metal laminations are insulated from each other. They are also insulated from stator and rotor windings. The three phase stator windings are also insulated from each other. To keep a generator operating properly, the insulations between generator

three phase stator windings, stator phase windings to stator metal laminations, and rotor winding to rotor metal laminations must be intact.

2–3 Generator faults and abnormal conditions

Generators are vulnerable to damage due to different causes. The typical problem is due to the break down of generator insulations, which could be caused by the overheat, vibration, aging of insulation and extended abnormal conditions resulting from external faults, overload conditions, failure of cooling system and other abnormal conditions. To prevent an extended abnormal condition from damaging the generator, a generator should be continuously monitored to make sure it is operating within its limits. When a fault occurs, it should be cleared immediately. Otherwise, the fault will develop to further cause the melt down of stator and/or rotor windings and metal laminations. For any generator, to repair the melted windings and/or metal laminations is much more difficult and costly than to repair several small insulation breakdown spots. Reliable and fast response protections are necessary for preventing the development of such a fault.

In the following, the common abnormal conditions and internal fault types of a generator, which require dedicated monitoring and protections, are briefly described:

(1) *Phase to phase faults*: caused by insulation failure between stator phase windings. If not cleared, will further damage the windings and metal laminations.

(2) *Phase to ground faults*: caused by insulation failure between stator windings and metal laminations. If not cleared, will further damage the windings and metal laminations.

(3) *Current unbalance*: caused by uneven load or asymmetric external faults. The unbalanced three phase current contains a negative sequence component which will induce second harmonic current in the field winding and the rotor iron body. The heat generated by the second harmonic current causes the rotor temperature to increase. It may damage the field windings and rotor metal laminations if the temperature is too high.

(4) *Loss–of–excitation*: caused by excitation circuit failure due to various causes. The generator which has lost its excitation draws a large amount of reactive power from the system and may fall into the asynchronous operating state. This could cause voltage collapse if the system

that it is connected to does not have enough reactive power capability. It may also cause damage to the generator itself due to its asynchronous operation.

(5) *Motoring condition*: caused by loss of prime mover. The generator will consume active power instead of delivering it. Such an operating state is not allowed for a generator.

(6) *Over current*: could be caused by over–load conditions or external faults. Extended over–current will increase the temperature of the generator and cause damage to it.

(7) *Over voltage*: caused by load rejections, excessive capacitive load or other disturbances. It causes the increase of leakage flux in a generator and the consequent overheat problem which may damage the generator. Too high overvoltage could damage the insulation of a generator instantly.

(8) *Interturn faults*: caused by the insulation failure between turns in a winding. The short circuit current circulating in the shorted turns may be higher than the fault current of a three phase fault at the generator terminals, thus may cause severe damage to the generators.

(9) *Step–up transformer over–excitation*: caused by various misoperations during generator's start–up and shut–down, such as applying too high field current when a generator has not reached its rated speed etc. Over–excitation causes the leakage flux to increase and the consequent overheat problem. Extended over–excitation of a transformer could cause severe damage to it.

(10) *Pole slip*: After a large disturbance, generators, especially the large generators, may slip poles with the main system. It could damage boilers and subject the generators to equivalent fault current of a three phase fault close to the busbar.

(11) *Stator and rotor windings overload*: Though generators' stator and rotor windings are designed to sustain certain level overload condition for specified times, extended overload conditions will subject generators to high temperatures and cause damage to the generators.

Besides these common fault types and abnormal conditions, some other special protection and monitoring problems may arise when generators are connected to main power systems. The types of the problems are determined by the system they are connected to.

When a generator is connected to a HV or EHV AC transmission system, it may have other protection problems, such as "inadvertent energizing of off–line generators", "improper synchronizing", "transient instability", "dynamic instability", "unbalanced currents", "abnormal voltages" and "shaft torques". These problems and suggested protections for them are summarized in a paper [8]. These problems will not be further discussed in this thesis as they are beyond the scope of this study. Interested readers are advised to reference corresponding literatures.

When a generator is connected to an HVDC transmission system, three special problems, as having been mentioned in Chapter 1, must be considered. These problems will be analyzed and the solutions will be presented in the Chapters 3, 4, 5 and 6.

2–4 Main and optional generator protection and monitoring functions

In this section, common main and optional generator protection and monitoring functions for large generators are listed and briefly described. An example is given to show how these protection functions are divided into two groups. More detailed description of some of these protection functions, which have been implemented in the first prototype of IGPS, will be presented in the next section. The detailed description for other protection functions can be found in other literatures listed in the references.

(1) Generator differential: Main protection. It protects stator windings' internal faults.

(2) Unit differential: Main protection. It protects internal faults of a generator and its step–up transformer connected in a unit connection.

(3) Stator ground protection: Main protection. It protects stator windings' ground faults.

(4) Instantaneous overvoltage protection: Main protection. Protecting generators from being damaged by extremely high overvoltages.

(5) Inverse–time overvoltage protection: Main protection. Protecting generator from being damaged by extended low level overvoltages.

(6) Instantaneous overcurrent protection: Main protection. Protecting generator stator windings from being damaged by extremely high overcurrent.

(7) Inverse–time overcurrent protection: Main protection. Protecting generator from being damaged by extended low level overcurrent.

(8) Loss–of–excitation protection: Main protection. Used to prevent system undervoltage and the generator pole–slipping caused by its loss–of–excitation.

(9) Rotor ground fault protection: Main protection. Protecting generator rotor from being damaged by rotor winding ground fault.

(10) Current unbalance protection: Main protection. Use both definite time delay and inverse time delay.

(11) Motoring condition detection: Main monitoring function. Used to monitor generator power direction and prevent generators entering motoring condition due to prime mover failure.

(12) Overload protection: Main protection. Protecting generators from being damaged by overheat caused by extended overload condition.

(13) Rotor overload protection: Main protection. Protecting generator rotor from being damaged by overheat caused by extended overload condition.

(14) Pole slip protection: Main protection. Used to protect slip–pole generators from being damaged by intermittent overcurrent and pulsating shaft torque.

(15) Minimum impedance protection: Main protection. Used as main backup protection for generator internal faults.

(16) Interturn fault protection: Optional. Only necessary when several bars of same phase are in same slot or part of them are crossed.

(17) Over–excitation (U/f) protection: Optional. Use both definite time delay and inverse time delay. Prevent step–up transformers from being damaged by over–excitation.

(18) Over–/under–frequency protection: Optional. Necessary only for pumped stations.

(19) Overcurrent/undervoltage protection: Optional. Necessary when thyristor type excitation circuit using generator terminal voltages.

(20) Voltage unbalance protection: Optional. Used where voltage balance is important.

(21) Dead machine protection: Optional. It detects simultaneously occurred overcurrent and undervoltage phenomenon.

(22) Restricted ground fault protection: Optional. Only necessary under special conditions.

The following table is an example showing how these protection functions can be divided into two groups.

Table 2.4.1 Example of generator protection functions divided into two groups

Type of fault	Protection function	ANSI No.	System	
Generator stator			A	B
Short circuits	Generator differential	87G	X	
	Overall differential	87T		X
	Minimum impedance	21	X	
	Overcurrent/undervoltage	51/27		X
	Overcurrent	51		X
Asymmetry	Current unbalance	46	X	
Stator overload	Thermal overcurrent	49	X	
Stator ground fault	90% stator ground fault	59		X
	100% stator ground fault	64	X	
Loss–of–excitation	Minimum impedance / undervoltage	40		X
Pole slip	Out–of–step	78/21	X	
Motoring condition	Reverse power	32	X	
Interturn fault	Overvoltage or overcurrent	59	X	
Lower voltage	Undervoltage	27		X
Increased magnetization	Overexcitation	24		X
Higher voltage	Overvoltage	59	X	
Generator rotor				
Rotor overload	Thermal overcurrent	49		X
Rotor ground fault	Overvoltage	64R	X	
Step–up transformer				
Short circuits	Transformer differential	87T	X	
	Overcurrent	50/51		X
Ground fault	Ground fault overcurrent	51N	X	
	Restricted ground fault	87N		X

2–5 Main protection and monitoring functions implemented in IGPS

In the first prototype of IGPS, seven main protection and monitoring functions have been implemented. These functions are essential for protecting hydro generators. Thus implementing these functions are vital for realizing one of the primary goal of this research, i.e., to provide a low–cost replacement option for hydro generators operating at Northern Collector System of Manitoba Hydro.

The following subsections will give detailed criteria and algorithm descriptions for these seven functions, which have been successfully implemented in the first prototype of IGPS.

All these protection and monitoring functions only use 11 input signals shown in Fig. 2.2.1. These 11 input signals are three phase terminal voltages V_{ta}, V_{tb} and V_{tc}, three phase terminal currents I_{ta}, I_{tb} and I_{tc}, three phase neutral currents I_{na}, I_{nb} and I_{nc}, neutral voltage V_n and field current I_f. These signals are also used by three special protection and monitoring functions for generators connected to DC lines, as will be shown in the later chapters.

2–5–1 Generator differential protection

This function is used to protect generators from being damaged by phase–to–phase faults. There are two types of Generator Differential Protection algorithms implemented: one of them uses the magnitude of the sum of terminal current vector and neutral current vector as the restraining signal; another one uses the scalar–product of terminal current vector and neutral current vector as the restraining signal which makes it more sensitive than the former one [12]. To distinguish these two different protections, they will be called as type I and type II percentage differential protection respectively.

(1) The criterion of type I percentage differential protection is:

$$| \vec{I}_{t\phi} - \vec{I}_{n\phi} | > K_1 \frac{| \vec{I}_{t\phi} + \vec{I}_{n\phi} |}{2} \qquad (\phi = a, b, c) \qquad (2\text{–}5\text{–}1\text{–}1)$$

$\vec{I}_{t\phi}$: terminal phase current vector

$\vec{I}_{n\phi}$: neutral phase current vector

where K_1 is the differential percentage set point for type I percentage differential protection.

(2) The criterion of type II percentage differential protection is:

$$| \vec{I}_{t\phi} - \vec{I}_{n\phi} | > K'_1 \times (I_{t\phi.r} \times I_{n\phi.r} + I_{t\phi.i} \times I_{n\phi.i}) \qquad (2\text{–}5\text{–}1\text{–}2)$$

$\vec{I}_{t\phi}$: terminal phase current vector

$\vec{I}_{n\phi}$: neutral phase current vector

$I_{t\phi.r}$, $I_{n\phi.r}$, $I_{t\phi.i}$, $I_{n\phi.i}$: real and imaginary part of $\vec{I}_{t\phi}$ and $\vec{I}_{n\phi}$

where K'_1 is the differential percentage set point for type II percentage differential protection.

The Generator Differential Protection operates instantaneously whenever the criterion is met. They are evaluated for each phase. Any one of the three phase operating will trip the generator off the system.

2–5–2 Current–unbalance protection

The current–unbalance protection simply measures the magnitude of the negative sequence component of the stator current because that is the cause of temperature increase. According to symmetrical–components theory, the negative sequence component of a three phase system is equal to

$$\vec{I}_2 = \frac{1}{3} \left(\vec{I}_a + a^2 \vec{I}_b + a \vec{I}_c \right) \qquad (2\text{–}5\text{–}2\text{–}1)$$

where $a = 1 \angle 120°$, and the magnitude of it is

$$I_2 = | \vec{I}_2 | \qquad (2\text{–}5\text{–}2\text{–}2)$$

When I_2 is greater than the threshold value $I_{2.min}$, a trip signal will be sent out after a time delay "t" determined by

$$t = \frac{K_2}{\left[\frac{I_2}{I_{nom}} \right]^2} \qquad (2\text{–}5\text{–}2\text{–}3)$$

where I_{nom} is the rated phase current and K_2 is the time factor for the current unbalance protection.

2–5–3 Loss–of–excitation protection

The commonly used loss–of–excitation protection consists of a two–zone offset mho type impedance relay with the characteristics as shown in Fig. 2.5.3.1. In some applications, undervoltage relays are used with these impedance relays, so that the generator is tripped only when its continued operation will cause system voltage collapse. In the Fig. 2.5.3.1, the outer circle is the steady–state boundary, and the inner circle is the asynchronous boundary. The impedance is measured from phase–to–phase voltage and current, i.e.

$$\vec{Z} = \frac{\vec{V}_a - \vec{V}_b}{\vec{I}_a - \vec{I}_b} = \frac{\vec{V}_{ab}}{\vec{I}_{ab}} \qquad (2\text{–}5\text{–}3\text{–}1)$$

When the impedance locus enters the operating zone and stays there longer than a preset time, a trip signal will be sent out. In most applications, the trip signal is sent out after generator terminal voltage drops below a certain level to avoid unnecessary trips when system has sufficient reactive power support.

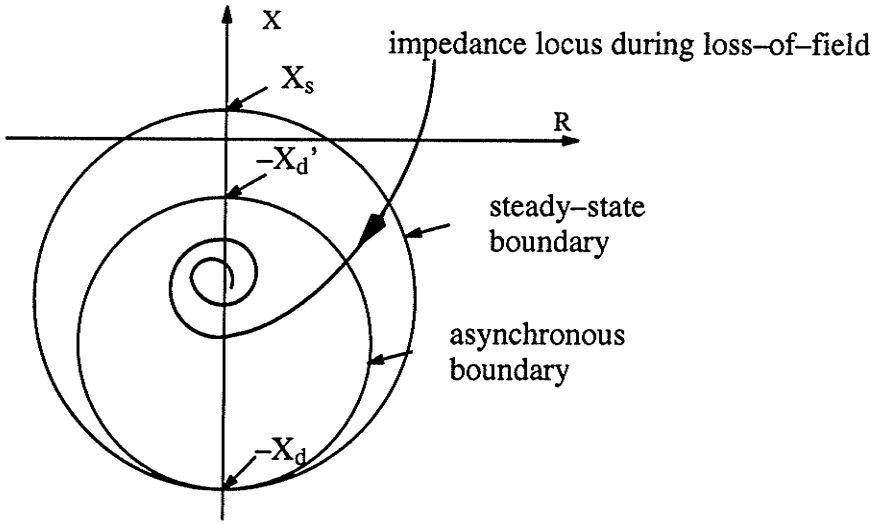

Fig. 2.5.3.1 Typical characteristics of a loss–of–field protection

2–5–4 Motoring condition detection

When a generator falls into motoring condition, it will absorb active power from the system instead of supplying energy to it. This can be easily detected by determining the sign of active power at the generator output terminal. The active power can be obtained from three–phase voltages and currents vectors by

$$P = \mathrm{Re}\left(\vec{V}_a \vec{I}^{*}_a + \vec{V}_b \vec{I}^{*}_b + \vec{V}_c \vec{I}^{*}_c \right) \qquad (2\text{–}5\text{–}4\text{–}1)$$

If the measured power P is less than a certain preset negative power level P_{inv}, i.e.

$$P < P_{inv} < 0 \qquad (2\text{–}5\text{–}4\text{–}2)$$

a signal will be generated after a certain time delay to warn the operator or trip the generator.

2–5–5 Over–voltage protection

The over–voltage protection in IGPS is implemented by measuring the positive sequence voltage at the generator output. The positive sequence voltage can be obtained from the three–phase voltage using the equation below:

$$\vec{V}_1 = \frac{1}{3}\left(\vec{V}_a + a\,\vec{V}_b + a^2\,\vec{V}_c \right) \qquad (2\text{–}5\text{–}5\text{–}1)$$

where $a = 1 \angle 120°$, and the magnitude V_1 is

$$V_1 = | \vec{V}_1 | \qquad (2\text{–}5\text{–}5\text{–}2)$$

A tripping signal will be sent out whenever the $V_1 > V_{1.set}$ for a time longer than

$$t = \frac{K_3}{\left[\frac{V_1}{V_{1.set}} \right] - 1} \qquad (2\text{–}5\text{–}5\text{–}3)$$

where $V_{1.set}$ is the rated phase voltage and K_3 is the time factor for over–voltage protection.

2–5–6 Voltage–restrained over–current protection

This is a standard generator over–current protection. It functions as the backup protection for the external faults. The voltage restraint is used to distinguish the over–current condition caused by normal over–load condition and external faults. The function is of the inverse–time delay characteristic as its tripping time is determined by the following equation

$$t = \frac{K_4}{\left[\frac{I_\phi \times V_{\phi.nom}}{V_\phi \times I_{set}} \right]^{0.5} - 1} \qquad (2\text{–}5\text{–}6\text{–}1)$$

where $V_{\phi.nom}$ is the rated phase voltage, I_{set} is the pick–up current and K_4 is the time factor for the over–current protection.

The above criterion will be processed three times in every calculation cycle, once for each phase. The relay starts to integrate "t" whenever

$$\frac{I_\phi \times V_{\phi.nom}}{V_\phi \times I_{set}} > 1 \qquad (2\text{–}5\text{–}6\text{–}2)$$

and the V_ϕ will be set to $V_{\phi.min}$ when $V_\phi < V_{\phi.min}$ to prevent overflow during calculation.

2–5–7 100% Ground fault protection

Two different algorithms were used to form a 100% stator ground fault protection. The first one is the definite–time–delay over–voltage algorithm which measures the neutral voltage. A tripping signal will be sent out when

$$V_n > K_5 \times V_{\phi.nom} \qquad (2\text{–}5\text{–}7\text{–}1)$$

where V_n is the neutral point voltage, $V_{\phi.nom}$ is the rated phase voltage and K_5 is the percentage factor. This is the main protection which could provide at least more than 85% coverage of the stator windings from the output end.

The second one utilizes the third harmonic components in the three–phase stator voltage and the neutral voltage to protect the remaining part of the windings. For protecting m% remaining part near the neutral point, an inequality below should be assessed

$$\frac{V_{n3}}{\frac{V_{p3}}{3} + V_{n3}} \leq \frac{m}{100} \qquad (2\text{–}5\text{–}7\text{–}2)$$

where V_{n3} is the third harmonic component in the neutral voltage and V_{p3} is the sum of the third harmonic components in the three–phase terminal voltages.

CHAPTER 3

HARMONICS MONITORING AND MEASUREMENT

3–1 Introduction

AC–DC conversion generates substantial harmonic components in three phase AC currents. A generator operating in a generating station connected to DC lines would experience high level of harmonics if no filters are installed. Under ideal conditions, these harmonic components are suppressed to acceptable levels by the carefully designed and installed filters on the rectifier AC busbar. But many non–perfect conditions of a system could cause the harmonics level to increase. As harmonics have many adverse effects to the generators, it is necessary to monitor harmonic levels continuously for generators connected to DC lines.

On the other hand, some harmonic components contained in the generator currents and voltages are of interest to relay engineers, as they can be used for certain relaying purposes. Several protection algorithms utilizing harmonic components have been successfully used by some protection systems, such as the third harmonic component being used by the generator stator ground fault protection. Extracting these harmonic components accurately will be very important for the correct operation of these protection systems.

There are many different harmonic measurement techniques that have been developed. They are of different complexities and suitabilities for different application areas. In selecting a proper harmonic measurement technique for IGPS, one important consideration is that it should be simple, easy to implement and be able to extract the required harmonics accurately in real–time (within a couple of milliseconds).

The harmonic measurement algorithm used in IGPS is the Fast Fourier Transform (FFT) algorithm with synchronized sampling. In the following sections, the errors and unstable results in harmonic measurement using the FFT algorithm which are caused by asynchronized sampling will be analyzed. An optimization technique is presented in this chapter which was used to implement the FFT algorithm in the first prototype of IGPS. Application of this technique results in 15% (16 point FFT) or 30% (32 point FFT) computation time reduction.

3–2 Harmonics in a generating station connected to DC lines

The main source of harmonics in a generating station connected to DC lines is from the rectifier bridges of an HVDC transmission line. The rectifier bridges of an HVDC transmission line are well known as harmonic current sources. The generation of harmonic current components is a characteristic of AC–DC rectification, thus cannot be avoided. Normally these harmonics are suppressed to acceptable levels by the installed filters on the rectifier AC busbar. But many non–perfect conditions and abnormalities could cause harmonic levels to increase. As will be shown later, since harmonics have many negative effects on generators as well as control and protection systems, it is necessary to monitor harmonic levels in a generating station connected to DC lines.

The characteristic harmonic components contained in the AC line currents, as having been analyzed and shown in the literature [78] [79] [24], are $6n \pm 1$ for a three phase 6–pulse rectifier bridge and $12n \pm 1$ for a three phase12–pulse rectifier bridge. Where $n = 1, 2, \ldots$ are integer numbers. The magnitudes of these characteristic harmonics decrease as the n increases. When a three phase system is symmetric and the firing angles of rectifier valves are equidistant and phase–locked, there will be no other non–characteristic harmonics generated by the three phase AC–DC rectification.

It is a common practice to install AC filters to suppress these harmonic components contained in the AC line currents. In a 6–pulse or a 12–pulse bridge rectifier station, typically the 5th, 7th, 11th, 13th and high–pass filters are installed. The high–pass filter is used to suppress all high frequency characteristic harmonics with the frequency higher than 13th harmonic. The 5th and 7th harmonic filters in a 12–pulse bridge rectifier station is necessary because a 12–pulse bridge is actually formed by two 6–pulse bridges. When one bridge is out–of–service, high level 5th and 7th harmonics will be present in the system.

But when a three phase system is not symmetric, or the firing angles of rectifier valves are not equidistant and phase–locked, the AC–DC rectification will not only generate characteristic harmonics but also non–characteristic harmonics. Because these non–characteristic harmonics usually have lower magnitude than that of characteristic harmonics, no filters are designed to suppress them.

Some factors could cause both characteristic and non–characteristic harmonics level to increase in a generating station connected to DC lines, in which characteristic harmonic and high–pass AC filters have already been installed.

One factor is the system frequency fluctuation in such a generating station. As will be discussed in the Chapter 4, the system frequency of such a generating station fluctuates widely (45 to 90 Hz) when the load flow in a DC line is adjusted very quickly or load rejection was occurred. An out–of–tune problem arises as all characteristic harmonic filters (5th, 7th, 11th and 13th) are tuned to best suppress these harmonics at the nominal system operating frequency (= 60 Hz). When the system frequency drifts, the harmonics frequencies drift as well. The out–of–tune problem arises because the center frequency of a filter is fixed. For example, a 5th harmonic filter is tuned to best suppress the 300 Hz harmonic component. It will leak some 5th harmonic when the system frequency drops to 50 Hz which results in the 5th harmonic becoming 250 Hz.

Another factor is the system impedance change. All characteristic harmonic filters are designed to best suppress targeted harmonic components at a specified system impedance. When the actual system impedance changes, the harmonics level will be higher than that at the designed system impedance. Unfortunately, in any generating station, the system impedance changes when the number of generators in operation and the system operating frequency are changed.

There are other harmonics sources other than the harmonics generated by the AC–DC rectification.

The generator itself generates some harmonics, such as slot harmonics. These harmonics are known as the voltage harmonic sources. Normally these harmonics are reduced to negligible levels by the careful design of the generator. But their existence may increase the Total Harmonics Distortion (THD) of generator voltages and currents.

Harmonic resonance is another source which causes harmonic levels to increase in such a system. Due to the existence of the above harmonic sources, a harmonic resonance could occur when one of the natural oscillation frequencies, which is determined by the system impedance and the filter capacitances, is close to one of the source harmonics.

The harmonic distortion in a generating station connected with AC systems has become a major concern of Utilities nowadays, because of the widespread application of electronically switched loads. This may, in the future, require generators connected to AC transmission systems to be equipped with harmonic monitoring functions. The study of the negative effects of harmonics on the generators and the analysis of the techniques for generator harmonic monitoring conducted in this research could also be of value for monitoring harmonics in generating stations connected to AC transmission lines.

3–3 The negative effects of harmonics on the generators

The negative effects of harmonics have been discussed in the literature [24] [34] [35], such as communication interference, heating losses, and solid–state device malfunctions. Among them, the major concern of harmonic monitoring in such a situation is their effects on the generators themselves.

The main negative effects of high level harmonic components in generator stator currents and voltages on a generator are the added losses, extra heat generation in rotor and stator, high frequency vibrations and noise.

Depending on the order of harmonics in the three phase stator currents, some of them produce positive sequence rotating fields rotating in the same direction as the rotor, others produce negative sequence rotating fields rotating in the opposite direction as the rotor, and some do not produce any rotating field.

All of these positive and negative sequence rotating fields could induce high frequency oscillating current components in the generator rotor winding superimposed onto the DC field current, as well as high frequency eddy currents in rotor and stator metal laminations. This will cause extra losses for the generator. Because of the skin effect, these high frequency oscillating current components experience higher resistance than that the low frequency ones. Extra heat will be produced by these high frequency current components on the top of other heat generating sources, thus decreasing the overheat capacity of a generator.

Besides the extra heat produced by these positive and negative sequence rotating fields, high frequency oscillating torques are also produced by them superimposed onto primary shaft torque,

causing high frequency vibrations of the generator shaft and generating unfavorable high frequency noises.

Other than the negative effects of harmonics on generators, the current and voltage waveform distortion due to harmonics affects the correct electrical quantities measurement and the correct operations of some generator control and protection systems.

Many studies and conducted tests [25] [26] [27] have shown that, depending on the algorithms to be used and the technologies used to implement these algorithms, current and voltage waveform distortion due to high level harmonics can cause large errors in the measurement of some electrical quantities. As the accurate measurement of electrical quantities is the basis of the correct operation of protection and control systems, this could affect the performance and may cause misoperation of some existing protection and control systems. One example is the generator overload protection.

Conventional overload protection is a thermal protection which only takes the RMS magnitude of phase current into account. When the current is distorted by the harmonics, the overheating and temperature increase pattern of a generator will be different. To make the overload protection operate more accurately, a new overload protection algorithm should be studied and developed to take into account the heat generating effect of harmonics.

Thus the levels of harmonics contained in the generator's stator currents and voltages should be monitored and measured, so that any abnormal harmonic level increase can be detected and corrected immediately. The harmonics should be within acceptable levels, such as those specified in [32], to ensure the proper operation of a generator as well as its control and protection systems.

3–4 Harmonic measurement techniques

Harmonic measurement techniques have been studied and developed for many years. Many dedicated and general harmonic analyzers are already commercially available [35]. Most of harmonic measurement techniques are in the frequency domain. With the advancement of digital computer technologies, different digital signal processing algorithms are used extensively in the

harmonic measurements. These algorithms include the DFT (Discrete Fourier Transform) or FFT (Fast Fourier Transform) [35] [36], anti–aliasing and low–pass filtering, band–pass filtering [38], Kalman filtering [34], frequency zooming [38], and so on. Among them, the DFT or FFT algorithm is the one most widely used. The FFT algorithm is most efficient when the number of input data points is a power of 2.

The actual selection and implementation of harmonic measurement techniques are affected by the requirement of the applications.

For applications where only one harmonic component is of interest and its frequency is stable, using a DFT algorithm with a narrow–band band–pass filter is sufficient.

But for applications where a full spectrum harmonic analysis across a wide frequency range is required for an input signal, a low–pass anti–aliasing filter and a large points FFT (1024 points FFT or even more) might be the only choice. The band–pass filters and the DFT will be too time consuming to be used.

When a narrow band of frequencies in a signal's spectrum is of interest and a high resolution of the spectral analysis is required for an application, the frequency zooming technique would be the proper one to use.

In applications where the magnitudes of harmonics are constantly changing and a fixed sampling frequency is used, the Kalman filtering technique could give very good estimations on the magnitudes of these harmonics, providing the number of harmonics and the characteristics of these harmonics are known.

There are other considerations in the implementation of harmonic measurement techniques. If only the magnitude is of interest or the harmonics have relatively large magnitudes, low resolution (10, 12 bit) A/D converters could be used. However, if the phase angle of harmonics is also important and the harmonic components of interest have a small magnitude which are superimposed onto a large magnitude fundamental component, some harmonic extracting techniques and/or high resolution (16 bit) A/D converter may be required.

In the first prototype of IGPS, analog low–pass anti–aliasing filters and an FFT algorithm are used to perform the harmonic measurement and extraction. This is based on the following considerations.

The number of harmonics needed to be monitored in a generating station connected to DC lines should contain all characteristic harmonics. However, when these factors are considered: (1) that the higher the order of a characteristic harmonic component generated by the AC–DC rectification is, the lower the magnitude of it will be, (2) the high–pass filter can effectively filter out these low magnitude high order characteristic harmonics, and (3) the harmonic monitoring for a generator is mainly concerned with their negative effects on the generator but not the communication interference (which is mainly caused by higher frequency harmonics), the task could be reduced to monitor only 5th, 7th, 11th and 13th harmonics. Because the 5th, 7th, 11th and 13th characteristic harmonics filters' "out–of–tune problem" and "the mis–match of system impedance problem" could cause the levels of these harmonic components to increase and may affect the normal operation of generators, they should be measured.

On the other hand, most of the generator protection functions require measuring the magnitude and phase angle of the fundamental component contained in the input signals. The third harmonic component of voltages is used to form a 100% stator ground fault protection. The second harmonic component of currents may be used, when a generator is in unit connection with a step–up transformer, to prevent the transformer protection's malfunction under in–rush current.

With both requirements considered, at least the fundamental, 2nd, 3rd, 5th, 7th, 11th and 13th harmonics should be measured for all stator current and voltage input signals. However, the number of harmonics needed to be measured could be more due to the following considerations.

If the field current of a generator is accessible and it is input into the protection system, the harmonics contained in it will be different from that in the stator currents and voltages. For example, the negative sequence fundamental component of stator currents induces a second harmonic component in the generator field current. Generally, the odd order harmonics in the stator current will generate even order harmonics in the field current, and vice versa.

As has been mentioned before, non–ideal rectification conditions could generate some low magnitude non–characteristic harmonics and there are no filters designed to suppress them. The magnitudes of them are the same as the characteristic harmonics, i.e. the higher the order of a non–characteristic harmonic component is, the lower its magnitude will be. Thus, if higher order non–characteristic harmonics are assumed to be suppressed by the high–pass filters, it would be better that the levels of these low order non–characteristic harmonics could also be monitored.

All considered, a range from fundamental to 13th harmonic is deemed to be a practical harmonics measurement range for generators in a generating station connected to DC lines. To obtain up to the 13th harmonic component and to avoid frequency aliasing, a sampling rate higher than 26 points/cycle is required according to the Nyquist theorem. As an FFT is most efficient when the number of input points is a power of 2, a 32 points/cycle sampling rate is the lowest one to meet the above requirement.

Using an FFT instead of individual DFTs is the most efficient approach. When only one harmonic component is needed, a DFT is faster than an FFT. When all harmonic components are needed, the FFT is definitely more efficient than multiple DFTs. The break–even point, i.e. when the time used by "n" DFTs is equal to the time needed by an FFT (where "n" is the number of harmonics required), depends on the actual implementation and the hardware being used.

For computers without hardware multiplier support, the break–even point of both algorithms could be estimated by the numbers of the multiplications needed by both algorithms. For computers with hardware multiplier support, the above estimation method can not be used. The actual implementation of the DFT and FFT algorithm in the first prototype of IGPS using the NEC 77230 DSP shows that the break–even point for 16 or 32 point DFT and FFT is about "n" = 3. That is, when more than three harmonic components are needed, an FFT uses less time than multiple DFTs use. With the harmonic monitoring requirement of at least up to the 13th, a 32 points FFT is necessary as it will provide up to the 15th harmonic monitoring capability.

In the first prototype of IGPS, it is designed to use a 32 points/cycle sampling rate and perform a 32 point FFT on each of the 11 input signals. A 32 point FFT will provide up to 15th harmonic measurement thus properly covering the desired harmonic monitoring range.

Because the main interest of harmonic monitoring in a generating station connected to DC lines is the harmonic magnitudes, a medium resolution A/D converter AD574 (12 bit) is used in the first prototype of IGPS.

3–5 Synchronized sampling: important for using FFT algorithm

One factor, which greatly affects fast and accurate harmonic measurement when DFT or FFT algorithms are used, is the synchronization of the sampling frequency with the system frequency. Synchronized sampling means that the sampling frequency is exactly N times the system frequency and exactly N samples are taken in one electric cycle and the samples must be equally spaced in time. When synchronized, the fundamental and harmonic components can be correctly extracted from the input signals using DFT or FFT algorithms. But if it is not synchronized, the so called "spectral leakage" problems will arise [33] [34]. In fact, in a digital protection system, the input signals are always sampled equidistantly at a certain sampling frequency which could be considered as synchronized to a "sample" system frequency. If this "sample" system frequency is equal to the actual system frequency, they are said to be synchronized, else they are not.

The "spectral leakage" problem arises when the "sample" system frequency is not equal to the actual frequency of a signal which contains only one pure sinusoidal component. The results of DFTs or FFT applied to the sampled data will be erroneous. Besides the fundamental vector, there are all other harmonic component vectors in the DFT or FFT results. One extreme example in [34] shows that a pure 60 Hz sine waveform

$$s\ (t) = \sin\ (\ 120\pi\ t + \theta\ ) \qquad (3\text{–}5\text{–}1)$$

sampled at a sampling frequency of 2 kHz, will produce a 8.89% or 15.74% THD in the results of a 32–point FFT or 64–point FFT performed on the sampled data.

The asynchronized sampling does not cause major problems to normal digital protection systems where only the fundamental component is used. It does cause some errors in the output vector of fundamental component (in the above example, the calculated magnitude of the fundamental component is 0.97898 for a 32–point FFT or 0.97394 for a 64–point FFT. The correct result is 1), but should not severely affect the final result. If the system frequency and the "sample"

system frequency only has a very small discrepancy, the effect of asychronized sampling for these protection systems is negligible.

When there are other harmonic components contained in the input signals along with the fundamental component, they also have the "spectral leakage" problems, as their frequencies are in integral numbers of the fundamental system frequency but not the "sample" system frequency. If no counter measures are used, their combined effects will cause a "cross representation" problem, i.e. each output vector of a DFT or FFT is not only the contribution of this harmonic component (which already has some errors), but also the contributions of all these "leaked" spectra of other harmonic components.

Though the "cross representation" problem can be effectively solved in a normal digital protection system by applying a low–pass anti–aliasing filter which has a lower cut–off frequency, it becomes a major problem for harmonics monitoring where a DFT or FFT algorithm is used. This is because the harmonic vectors of the DFT or FFT results are now of interest, thus the low–pass filter with a lower cut–off frequency can not be used.

There is another problem caused by asynchronous sampling which has not been found to be discussed in the literature. The problem is that the magnitudes of extracted harmonic components fluctuate when the sampling window moves along the time axis though the actual harmonic components contained in a signal have constant magnitudes. This problem could be called a "sampling window moving effect" problem and can be briefly analyzed as follows.

Assume y_k is a data series sampled equidistantly from a pure sine signal $s(t) = \sin(120\pi t + \theta)$, i.e. $y_k = \sin(120\pi (t_o + k \times \Delta t) + \theta)$, where t_o is the time when the sampling of s(t) is started and Δt is the time between two samples. If $\Delta t = 1 / (60 \times N)$, then the following DFT

$$F(k)_s = \frac{2}{N}\sum_{m=1}^{N} y_{k-N+m} \sin\left(2\pi\frac{m}{N}\right) \qquad (3\text{–}5\text{–}2)$$

$$F(k)_c = \frac{2}{N}\sum_{m=1}^{N} y_{k-N+m} \cos\left(2\pi\frac{m}{N}\right) \qquad (3\text{–}5\text{–}3)$$

applied to the sampled data gives a constant unit magnitude

$$F(k) = \sqrt{F(k)_s^2 + F(k)_c^2} = 1 \qquad (3\text{–}5\text{–}4)$$

when the k is incremented by 1 each time, as can be seen from the Fig. 3.5.1 curve F(sync). This is equivalent to the sampling window moving along the time axis one sample at a time and the "sample" system frequency is synchronized with the system frequency.

When the Δt is slightly greater or less than $1 / (60 \times N)$, then the same DFT applied to the sampled data will have an oscillating magnitude as can be seen clearly in the Fig. 3.5.1 curve F(async). The curve F(async) is obtained for $\Delta t = 1 / (65 \times N)$. The curve $10 \times (F(async) - F(sync))$ enlarges the difference between F(sync) and F(async), in which the oscillation of the F(async) is more evident.

The oscillation of magnitudes caused by "sampling window moving effect" further complicates the harmonic monitoring task. Some techniques will have to be used to reduce the effect of such oscillations. When there are several harmonic components contained in the input signals, the "cross representation" due to "spectral leakage" will make the problem even more complicated.

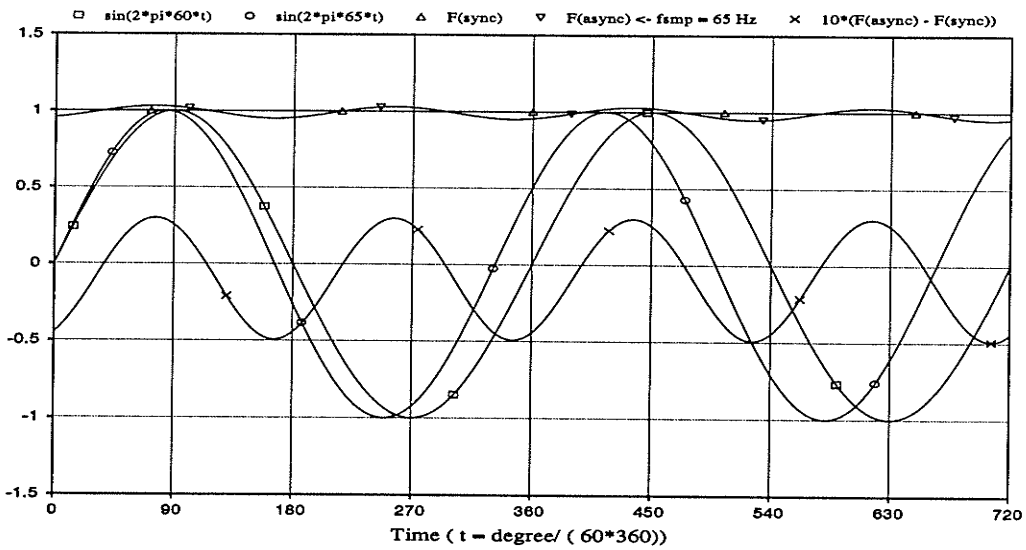

Fig. 3.5.1 "Sampling window moving effect"

Some solutions have been proposed in the literature in order to reduce the effects of asynchronized sampling on DFT or FFT results, such as "interpolation algorithms [39]",

"smoothing windows [40]", "rearranged sampled data sequence [41]", "frequency zooming [42]", and so on.

However, these methods can only reduce, but not completely remove the measurement errors caused by asynchronized sampling. They are also done at the cost of increased computation burden and added time delay. The best way to completely solve these problems is to keep the "sample" system frequency synchronized with the system fundamental frequency [33].

The above analysis clearly shows that to synchronize the sampling frequency with the sampled signal's fundamental frequency is very important for fast and accurate harmonic measurement using DFTs or FFTs. This requires the use of a fast and accurate frequency tracking algorithm which will be discussed in the next chapter.

3–6 Optimization of FFT calculation

Though using the FFT algorithm is more efficient than using separate DFTs to obtain several harmonic components, the FFT calculations on all 11 input signals of IGPS is still the most time consuming part of all the major computations in IGPS programs. As the following analysis shows, directly performing an FFT on each of the input signals is not efficient. An optimization technique is used in the implementation of the FFT algorithm in IGPS, which fully utilizes the properties of the FFT to further reduce the computation time required by the direct FFT.

Directly performing an FFT on each of the input signals is not efficient due to the fact that a Fast Fourier Transform (FFT) is a complex–to–complex transform, but an input signal's sampled data series is a real data series without an imaginary part. As we know, an FFT of 2^n input points can be divided into "n" butterfly operations, and each butterfly operation involves extensive multiplications and additions/subtractions. For a direct FFT on a real data series, the first two butterfly operations only involve addition/subtraction operations. Also, as will be shown later, the output vectors of an FFT on a real data series possess some symmetrical properties. Both imply that directly using a normal FFT program on a real data series is not efficient. Though some programming techniques can be applied to speed up the first two butterfly operations of an FFT on a real data series, butterfly operations after the first two are all complex–to–complex operations thus no optimization techniques can be applied.

In the first prototype of IGPS, the following optimization technique is utilized to reduce the total computation time of FFT computations on 11 input signals. Briefly, one FFT computation is performed on two signals' sampled data series and the result of the FFT computation is then converted into the two signals' FFT results utilizing the properties of FFT computations. The technique is explained in detail below. The properties of an FFT when applied to pure real or imaginary data series (which are used by this technique) will be shown before the explanation of this technique.

Assume a_i and A_k represent the input data series and its FFT transform (i = 0 ... N – 1, k = 0 ... N – 1). Then, by definition they have the relationship

$$A_k = \sum_{i=0}^{N-1} a_i \; W_N^{ik} \qquad (3\text{–}6\text{–}1)$$

$$a_i = \sum_{k=0}^{N-1} A_k \; W_N^{-ik} \qquad (3\text{–}6\text{–}2)$$

where

$$W_N^{ik} = e^{-j\frac{2\pi}{N} i k} = \cos\left(\frac{2\pi}{N} i k\right) - j \sin\left(\frac{2\pi}{N} i k\right) \qquad (3\text{–}6\text{–}3)$$

When a_i is a pure real data series, then the following properties exist

$$\mathrm{Re}(A_k) = \mathrm{Re}(A_{-k}) \qquad (3\text{–}6\text{–}4)$$

$$\mathrm{Im}(A_k) = -\mathrm{Im}(A_{-k}) \qquad (3\text{–}6\text{–}5)$$

and if a_i is a pure imaginary data series, we have

$$\mathrm{Re}(A_k) = -\mathrm{Re}(A_{-k}) \qquad (3\text{–}6\text{–}6)$$

$$\mathrm{Im}(A_k) = \mathrm{Im}(A_{-k}) \qquad (3\text{–}6\text{–}7)$$

Note that

$$A_{N-k} = A_{-k} \qquad (3\text{–}6\text{–}8)$$

and the above properties can be rewritten for pure real data series as

$$\text{Re}\ (\ A_k\ ) = \text{Re}\ (\ A_{N-k}\ ) \qquad (3\text{–}6\text{–}9)$$

$$\text{Im}\ (\ A_k\ ) = -\ \text{Im}\ (\ A_{N-k}\ ) \qquad (3\text{–}6\text{–}10)$$

and for pure imaginary data series as

$$\text{Re}\ (\ A_k\ ) = -\ \text{Re}\ (\ A_{N-k}\ ) \qquad (3\text{–}6\text{–}11)$$

$$\text{Im}\ (\ A_k\ ) = \text{Im}\ (\ A_{N-k}\ ) \qquad (3\text{–}6\text{–}12)$$

Assume a_i and b_i are two real data series. Let $c_i = a_i + j\ b_i$. Then

$$C_k = A_k + j\ B_k = [\ \text{Re}\ (A_k) + j\ \text{Im}\ (A_k)\ ] + j\ [\ \text{Re}\ (B_k) + j\ \text{Im}\ (B_k)\ ] \qquad (3\text{–}6\text{–}13)$$

and we have

$$\text{Re}\ (\ C_k\ ) = \text{Re}\ (\ A_k\ ) - \text{Im}\ (\ B_k\ ) \qquad (3\text{–}6\text{–}14)$$

$$\text{Im}\ (\ C_k\ ) = \text{Im}\ (\ A_k\ ) + \text{Re}\ (\ B_k\ ) \qquad (3\text{–}6\text{–}15)$$

By applying above properties, A_k and B_k could be calculated from C_k by the following equations

$$\text{Re}\ (\ A_k\ ) = \frac{1}{2}\ [\ \text{Re}\ (\ C_k\ ) + \text{Re}\ (\ C_{N-k}\ )\ ] \qquad (3\text{–}6\text{–}16)$$

$$\text{Im}\ (\ A_k\ ) = \frac{1}{2}\ [\ \text{Im}\ (\ C_k\ ) - \text{Im}\ (\ C_{N-k}\ )\ ] \qquad (3\text{–}6\text{–}17)$$

$$\text{Re}\ (\ B_k\ ) = \frac{1}{2}\ [\ \text{Im}\ (\ C_k\ ) + \text{Im}\ (\ C_{N-k}\ )\ ] \qquad (3\text{–}6\text{–}18)$$

$$\text{Im}\ (\ B_k\ ) = \frac{1}{2}\ [\ \text{Re}\ (\ C_{N-k}\ ) - \text{Re}\ (\ C_k\ )\ ] \qquad (3\text{–}6\text{–}19)$$

When the above technique is utilized, the calculation of two complete FFTs on two signals is reduced to one FFT computation plus the conversion process which only involves addition and subtraction. The coefficient 1/2 in the above conversion process could be easily combined with the coefficients of the FFT computation.

The time saved by utilizing the above technique is significant. In a 16 point FFT, the time needed for the FFT computation utilizing the above technique is 15% less than that of the two direct FFTs. And in a 32 point FFT, the time needed will be 30% less than that of two direct FFTs. The above

results are obtained from the actual implementation of these FFT subroutines on the NEC 77230 DSP chip in the first prototype of IGPS. And the above mentioned direct FFT subroutine has already been programmed to take advantage of the first two butterfly operations only involving arithmetic operations.

CHAPTER 4

FREQUENCY TRACKING

4–1 Introduction

The system operating frequency in a generating station connected to DC lines fluctuates in a wide range (45 – 90 Hz in the Northern Collector System), due to load rejections or fast load flow regulations of a DC line and the slow response of generators' mechanical input power. The rate of system frequency change in such a system is also higher than in a normal AC system.

The frequency fluctuation in such a station affects the proper operation of generators, filters, transformers and station auxiliary equipments. As the frequency fluctuation in such a station is unavoidable, these impacts should be properly considered during the system planning, designing and operating. However, these problems are not the focus of this research and will not be further discussed in this thesis.

The study of frequency fluctuation in this research is mainly focused on its impact on the digital integrated protection system under development and on providing a proper solution to it. The analysis in Chapter 3 has already shown the adverse effects of asynchronous sampling to the accurate harmonic components measurement. If the sampling frequency is fixed, then the sampling frequency will be out of synchronization with the system frequency when it fluctuates off its nominal value, thus causing harmonic "spectral leakage" and "sampling window moving effect" problems of DFT and FFT algorithms in a digital protection system. As all further calculations of an IGPS are based on the FFT phasor, this could cause erroneous results of these calculations, and lead to the improper operation of the system.

This problem could be best solved by frequency tracking [33], i.e. measuring the system frequency and adjusting the sampling frequency accordingly so that the sampling frequency is always synchronized with the system frequency. The main focus of this chapter is to compare different frequency tracking techniques and present a fast and accurate frequency tracking algorithm developed in this research and its implementation technique used in the first prototype of IGPS.

4–2 Frequency fluctuation in generating stations connected to DC lines

Two situations cause the fast load change in a generating station connected to a DC line: load rejections and fast load flow regulations of the DC line. The load rejections could be caused by the fault in the line, failure of firing control circuit, etc.. The fast regulation of load flow in a DC line is widely used to increase main systems stability and control the load flow distribution of main systems.

The frequency in such a generating station fluctuates widely due to the fact that the load can be changed almost instantly but the mechanical input of generators can not be changed immediately. This causes large torque unbalance in generators and hence the system frequency to increase or decrease. The frequency fluctuation in such a generating station has two distinct characteristics which are different from that in an AC system.

One characteristic is that the system operating frequency fluctuates in a much wider range than that in an AC system. In the Northern Collector System of Manitoba Hydro, a range of 45 – 90 Hz has been identified. In a normal AC system, the system operating frequency normally is kept close to its nominal value (60 Hz in North America) and $\pm$ 5 Hz off nominal value is considered to be extreme.

A load rejection field test was conducted on one 120 MVA generator at Kettle generating station of the Northern Collector System [60]. The recorded frequency change shows that the frequency increased from 60 Hz to a maximum 72 Hz (1.2 pu) after a full load rejection occurring at the time when the generator carried 80 MW load.

Another characteristic is the high df/dt (rate of change) of the system frequency when a large amount of load change is involved. In the same load rejection test, 4 Hz/second rate of system frequency change was observed. In a normal AC system, the load change is shared by the generators inter–connected to each other, thus the rate of frequency change usually is much smaller. In an AC system, 1 Hz/second may be considered as a fast frequency change.

Thus a frequency tracking algorithm to be used in an integrated generator protection system must consider these two requirements. It should be able to work properly in such a wide frequency range and should be able to dynamically follow the frequency change very quickly.

4–3 Different frequency tracking algorithms

There are some frequency measurement and frequency tracking algorithms which have been developed and proposed in the literature. Here is a brief review of these frequency measurement and frequency tracking algorithms.

"Zero–crossing" [45] [46] is a simple frequency measurement method. It could be implemented by using either a hardware solution or a software solution. The accuracy and stability of the hardware solution are prone to noise and waveform distortions. Also, when hardware solutions are used in a digital protection system, additional hardware is required. The software solution does not require additional hardware support but shows frequency deviations that exponentially approach the true value as the number of cycles considered approach infinity.

Least–mean–square (LMS) estimation algorithms have been proposed by several authors. Both stationary models [47] [48] and adaptive estimation models [57] [49] are used to track the system frequency without having to know any statistical property in advance. However, there is a compromise between the accuracy of the frequency measurement and the length of the observation period. This implies that low accuracy could be expected when these techniques are used in the fast frequency tracking of IGPS.

[52] describes a newly developed technique utilizing decomposition of the fundamental component contained in a distorted input signal for the fast and accurate measurement of power system frequency. This technique uses two finite impulse response bandpass–orthogonal filters with the band limited to 30 – 70 Hz (nominal frequency is 50 Hz). The orthogonal filters have a group time delay of 20 ms. After evaluation of frequency using the output of two orthogonal filters, another moving average filter, having a group delay of 20 ms is applied to the frequency estimates to remove any non–50 Hz components. As the results of [52] show, more than one cycle time delay should be expected in the application of this algorithm. Although the measurement speed of this algorithm is

acceptable, it requires additional software implementation and thus is not easy to integrate into the first prototype of IGPS where the FFT algorithm is to be used.

Most of the above algorithms did not show their dynamic performance during fast system frequency changes to be in the range required by IGPS. Nor did these algorithms adequately handle the system transients caused by switching operations and faults where there is no frequency change but large input signal's magnitude and phase angle change involved. Both problems are critical for a practical frequency tracking algorithm to be used in IGPS. A $\Delta\alpha/\Delta t$ frequency tracking algorithm is thus studied and developed in this research, which shows the speed and accuracy in tracking system frequency in a wide range. Furthermore, it is easy to integrate into IGPS using FFT results, and has been successfully implemented in the first prototype of IGPS.

4–4 $\Delta\alpha/\Delta t$ frequency tracking algorithm

The frequency tracking algorithm used in IGPS uses positive sequence voltage to track the system frequency. The sequence components are calculated from the fundamental components of the three phase voltages, and the positive sequence component is then used to perform the frequency tracking to adjust the sampling frequency.

The frequency tracking algorithm of IGPS is a very simple one. Once a cycle, the frequency tracking subroutine is called to compare the present positive sequence voltage phasor with the one of the previous cycle. If the phasor has rotated $2\pi + \alpha$, then the sampling interval T_s ($T_s = 1 / f_s$) will be adjusted according to the formula below:

$$T_{s(new)} = \frac{1}{1 + \frac{\alpha}{2\pi}} \times T_{s(old)} \qquad (4\text{–}4\text{–}1)$$

To understand how the above mentioned frequency tracking algorithm works, let us first examine some of the properties of the DFT on a sine waveform. As we know, the output of the DFT on a sine waveform has two components, a real and an imaginary part. It forms a vector on the X–Y plane. When the sampling window moves, the angle of the vector will rotate. If the sampling frequency is exactly N times that of the waveform and the sampling window moves "n" samples each time, the vector will rotate exactly $n\times 2\pi/N$ each time. The time used to rotate $n\times 2\pi/N$ radians

will be $T_n = n / (N \times f)$, where "f" is the input signal frequency. Fig. 4.3.1 shows a sine waveform sampled at 16 points/cycle with the sampling window moving 8 sample points each time.

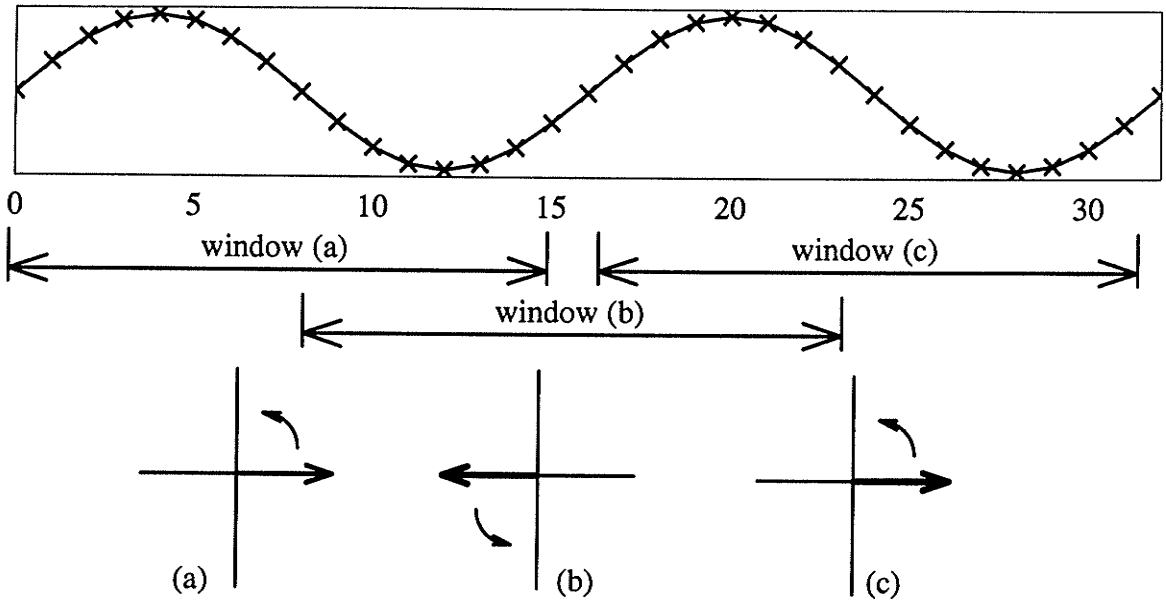

Fig. 4.3.1 DFT output vs. sampling window position

When the sampling frequency f_s is not exactly N times the input signal's frequency f, the vector of the DFT output will rotate $(n \times 2\pi/N) + \alpha$ instead of $n \times 2\pi/N$. The α will be less than zero if f_s is less than N times f, or it will be greater than zero when f_s is greater than N times f. As shown in Fig. 4.3.2. The sampling frequency should be changed such that at the next computation the vector of the DFT output will rotate just $n \times 2\pi/N$ when the sampling window moves n samples.

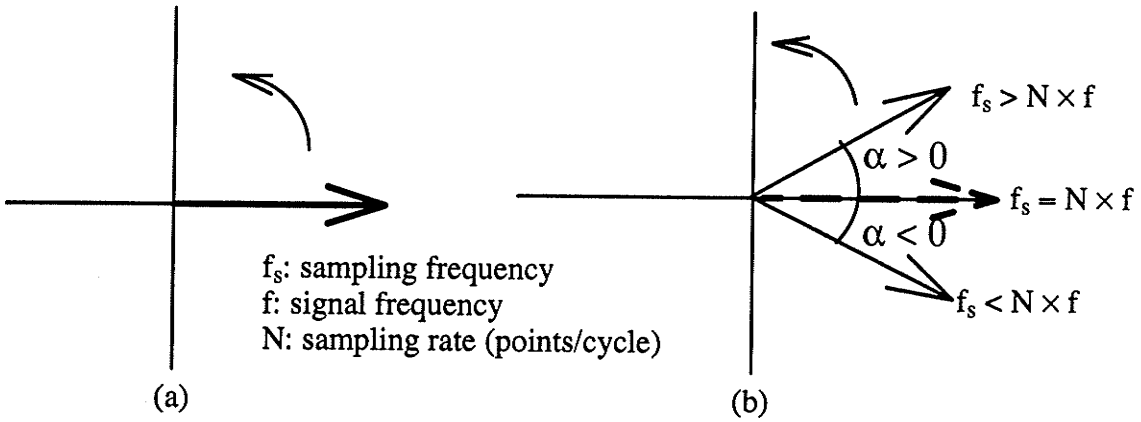

Fig. 4.3.2 DFT resultant vectors at $f_s \neq N \times f$

The calculation of the new sampling frequency $f_{s(new)}$ is simple if the phase difference α is known. Note that $T_s = 1 / f_s$. When $T_s = T_{s(old)}$, the vector rotates an angle of $(n\times 2\pi/N) + \alpha$ in time $n\times T_{s(old)}$. After T_s is changed from $T_{s(old)}$ to $T_{s(new)}$, it should rotate an angle of $n\times 2\pi/N$. So we have:

$$n \times T_{s(new)} = \left(\frac{n \times 2\pi}{N} \right) \div \left[\frac{\left(\frac{n\times 2\pi}{N} + \alpha \right)}{\left(n \times T_{s(old)} \right)} \right] \qquad (4\text{–}4\text{–}2)$$

i.e.

$$T_{s(new)} = \frac{\left(\frac{n\times 2\pi}{N} \right)}{\left(\frac{n\times 2\pi}{N} + \alpha \right)} \times T_{s(old)}$$

$$= \frac{1}{1 + \Delta\alpha} \times T_{s(old)} \qquad (4\text{–}4\text{–}3)$$

where

$$\Delta\alpha = \frac{\alpha}{\left(\frac{n\times 2\pi}{N} \right)} \qquad (4\text{–}4\text{–}4)$$

A special case is $\Delta\alpha = \alpha / 2\pi$ when $n = N$.

α should be calculated before calculating $\Delta\alpha$. It could be calculated from the present vector B and reference vector A. From Fig. 4.3.3, let

$$\theta_{nN} = \frac{n \times 2\pi}{N} \qquad (4\text{–}4\text{–}5)$$

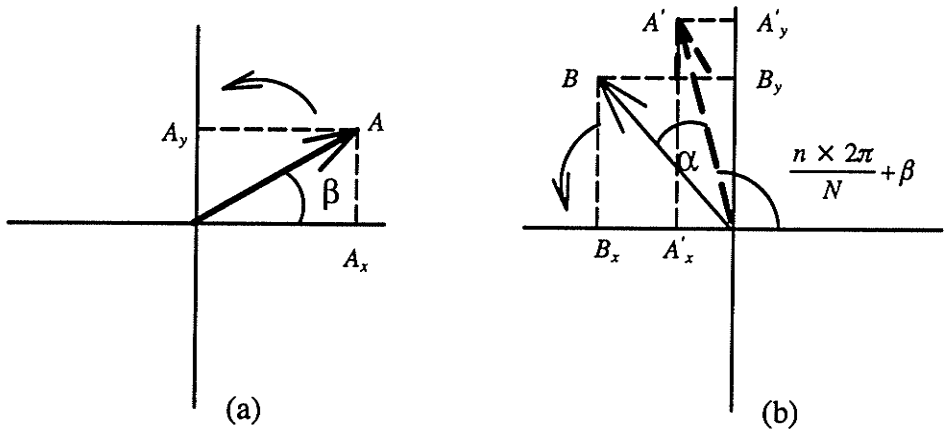

Fig. 4.3.3 Calculate α from vectors A and B

We have:

$$\tan(\alpha) = \tan\left[\left\{\left(\theta_{nN} + \beta\right) + \alpha\right\} - \left(\theta_{nN} + \beta\right)\right]$$

$$= \frac{\sin\left[\left\{(\theta_{nN} + \beta) + \alpha\right\} - (\theta_{nN} + \beta)\right]}{\cos\left[\left\{(\theta_{nN} + \beta) + \alpha\right\} - (\theta_{nN} + \beta)\right]}$$

$$= \frac{\sin\left[(\theta_{nN} + \beta) + \alpha\right] \times \cos(\theta_{nN} + \beta) - \cos\left[(\theta_{nN} + \beta) + \alpha\right] \times \sin(\theta_{nN} + \beta)}{\cos\left[(\theta_{nN} + \beta) + \alpha\right] \times \cos(\theta_{nN+}\beta) + \sin\left[(\theta_{nN} + \beta) + \alpha\right] \times \sin(\theta_{nN} + \beta)} \qquad (4\text{–}4\text{–}6)$$

$R.H.S. \times \left(\frac{A \times B}{A \times B}\right)$:

$$\tan(\alpha) = \frac{B_y \times A'_x - B_x \times A'_y}{B_x \times A'_x + B_y \times A'_y}$$

$$= \frac{B_y \times [A_x \times \cos(\theta_{nN}) - A_y \times \sin(\theta_{nN})] - B_x \times [A_x \times \sin(\theta_{nN}) + A_y \times \cos(\theta_{nN})]}{B_x \times [A_x \times \cos(\theta_{nN}) - A_y \times \sin(\theta_{nN})] + B_y \times [A_x \times \sin(\theta_{nN}) + A_x \times \cos(\theta_{nN})]}$$

(4–4–7)

When n = N, then

$$\theta_{nN} = 2\pi$$

and

$$\cos(\ 2\pi\ ) = 1, \qquad \sin(\ 2\pi\ ) = 0$$

so the tan (α) can be simplified as

$$\tan(\alpha) = \frac{B_y \times A_x - B_x \times A_y}{B_x \times A_x + B_y \times A_y} \qquad (4\text{–}4\text{–}8)$$

Based on the above equations, the frequency tracking algorithm used in IGPS could be implemented as follows:

(1) calculate present positive sequence vector from the FFT results of the three phase voltages;

(2) take the last calculated vector (one cycle before) as the reference vector along with the present calculated vector to calculate tan (α);

(3) perform a $\tan^{-1}$ to obtain α from tan (α);

(4) use α to get $1/(1+\Delta\alpha)$;

(5) use above equations to get $T_{s(new)}$.

4–5 Implementation of $\Delta\alpha/\Delta t$ frequency tracking algorithm in IGPS

If the frequency tracking algorithm is implemented as above, it will involve two division and one "arc tan" calculations. As will be presented in the later chapters, the frequency tracking algorithm is implemented on a DSP chip of the first prototype of IGPS. As we know, for a DSP chip, such as NEC 77230 , one floating–point multiplication can be done in one instruction execution period in parallel with one addition or subtraction calculation, however a subroutine has to be executed for a division or other function calculations. To get "arc tan" takes more time than to do a division. Thus, implementing the above algorithm using the above procedure will be inefficient from the DSP chip point of view.

To fully use the power of the DSP chip, the algorithm implemented in IGPS uses the power series expansion method. The two power series used are as follows:

$$\arctan(x) = x - \frac{x^3}{3} + \frac{x^5}{5} - \frac{x^7}{7} + \cdots \qquad \text{for} \quad |x| \le 1 \qquad (4\text{–}5\text{–}1)$$

$$\frac{1}{1+x} = 1 - x + x^2 - x^3 + x^4 - \cdots \qquad \text{for} \quad |x| < 1 \qquad (4\text{–}5\text{–}2)$$

In practice, $|\alpha|$ is less than $4/\pi$ between two cycles even when the $f_{s(old)} / N$ has 5 Hz difference with the present "f". For example, when present f = 60 Hz and $f_{s(old)} / N = 65$ Hz, the phase difference will be

$$\alpha = \frac{65 \times 2\pi}{60} - 2\pi = \frac{6}{\pi} \qquad (4\text{–}5\text{–}3)$$

This is an unlikely situation as the sampling frequency is adjusted constantly (once a cycle in the first prototype of IGPS). So we have

$$|\tan(\alpha)| \leq |\tan(\frac{6}{\pi})| < 1 \qquad (4\text{–}5\text{–}4)$$

and

$$|\Delta\alpha| \leq \frac{\frac{6}{\pi}}{2\pi} \ll 1 \qquad (4\text{–}5\text{–}5)$$

Let

$$x = \tan(\alpha) \qquad (4\text{–}5\text{–}6)$$

Then

$$\begin{aligned} \alpha &= \arctan(\tan(\alpha)) \\ &= \arctan(x) \\ &= x - \frac{x^3}{3} + \frac{x^5}{5} - \frac{x^7}{7} + \cdots \end{aligned} \qquad (4\text{–}5\text{–}7)$$

This gives

$$\frac{1}{1+\Delta\alpha} = 1 - \Delta\alpha + \Delta\alpha^2 - \Delta\alpha^3 + \cdots$$

$$= 1 - \frac{\alpha}{\theta_{nN}} + \frac{\alpha^2}{\theta_{nN}^2} - \frac{\alpha^3}{\theta_{nN}^3} + \cdots$$

$$= 1 - \frac{1}{\theta_{nN}} \times \left(x - \frac{x^3}{3} + \cdots \right) + \frac{1}{\theta_{nN}^2} \times \left(x - \frac{x^3}{3} + \cdots \right)^2 - \frac{1}{\theta_{nN}^3} \times \left(x - \frac{x^3}{3} + \cdots \right)^3 + \cdots$$

$$= 1 - \frac{1}{\theta_{nN}} \times x + \frac{1}{\theta_{nN}^2} \times x^2 - \left(\frac{1}{\theta_{nN}^3} - \frac{1}{\theta_{nN} \times 3} \right) \times x^3 + \cdots$$

$$\approx 1-\frac{1}{\theta_{nN}} \times x+\frac{1}{\theta_{nN}^2} \times x^2-\left(\frac{1}{\theta_{nN}^3}-\frac{1}{\theta_{nN} \times 3}\right) \times x^3 \qquad (4\text{–}5\text{–}8)$$

The n can be fixed to N, N / 2 etc. to make $1/\theta_{nN}$ become a constant. In IGPS, n = N is used to get $1/\theta_{nN} = 1/2\pi$. Thus the above power series in IGPS becomes

$$\frac{1}{1+\Delta\alpha} \approx 1-a \times x+b \times x^2-c \times x^3 \qquad (4\text{–}5\text{–}9)$$

Where

$$a = \frac{1}{2 \times \pi} \qquad b = a^2 \qquad c = a^3-\frac{a}{3}$$

The above power series simplifies the calculations of $\tan^{-1}(\alpha)$ and $1/(1+\Delta\alpha)$ into multiplications, additions and subtractions, which can be done by the DSP chip very fast. Besides, the accuracy of the above approximation is excellent. Fig. 4.5.1 shows the actual $1/(1+\Delta\alpha)$ curve and the power series approximation in the practical α range (0° — 30°) when n = N. The dashed line is the actual curve and the solid line represents the power series approximation.

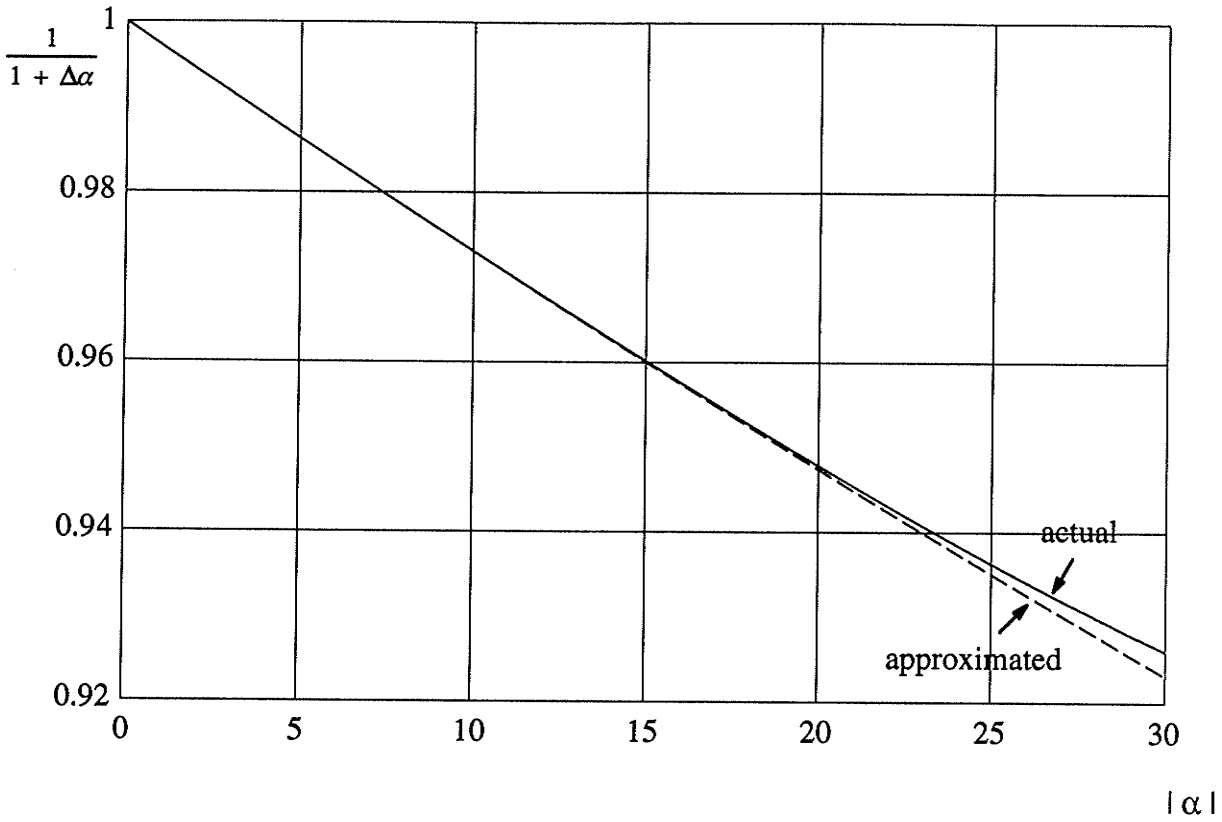

Fig. 4.5.1 Errors caused by the approximation

As can be seen from the diagram, the error increases as α increases. Both the absolute and relative error reach maximum at α = 30°. The absolute error at that point is 0.003 with the actual value equal to 0.923 (the power series one equal 0.926). The relative error at that point is 0.315%.

Using the above power series, the calculation of $T_{s(new)}$ in IGPS takes the following steps:

(1) calculate the present positive sequence vector from the FFT results of the three phase voltages;

(2) take the last calculated vector (one cycle before) as the reference vector along with the present calculated vector to calculate tan (α);

(3) use above power series equation to directly get 1 / (1 + Δα) from tan (α);

(4) multiply $T_{s(old)}$ to get $T_{s(new)}$.

Besides the calculation of $T_{s(new)}$, some other measures have been taken in the implementation to prevent the malfunctioning of the frequency tracking algorithm under certain abnormal conditions. These measures include (1) freezing sampling frequency when V_1 is less than a preset value, which may occur during a close–in fault to cause frequency tracking malfunctioning. The frequency tracking will be resumed when V_1 returns to above the preset value; (2) stop frequency tracking temporarily when the ΔV_1 exceeds a preset level. This condition may occur during any fault. As the angle and magnitude of system voltage waveform suddenly changes during the transition from pre–fault to post–fault state, the frequency tracking algorithm "sees" an apparent angle change and may malfunction. The frequency tracking will be resumed under this condition as soon as the ΔV_1 between current vector and reference vector falls within a preset level.

The above frequency tracking algorithm has been successfully implemented in IGPS. It has been tested using a variable frequency three phase signal generator. The test results show that it can correctly track the frequency change in the desired 45 to 90 Hz range and change the sampling frequency accordingly. It also works properly when one or two phase voltages are lost and during the transition of simulated faults. In the case that it loses all three phase voltages and then regains the three phase voltage, the algorithm can respond to such a condition correctly to freeze and resume the frequency tracking.

Fig. 4.5.2 is a recorded waveform which shows how the frequency tracking algorithm correctly responds to the loss of one phase voltage.

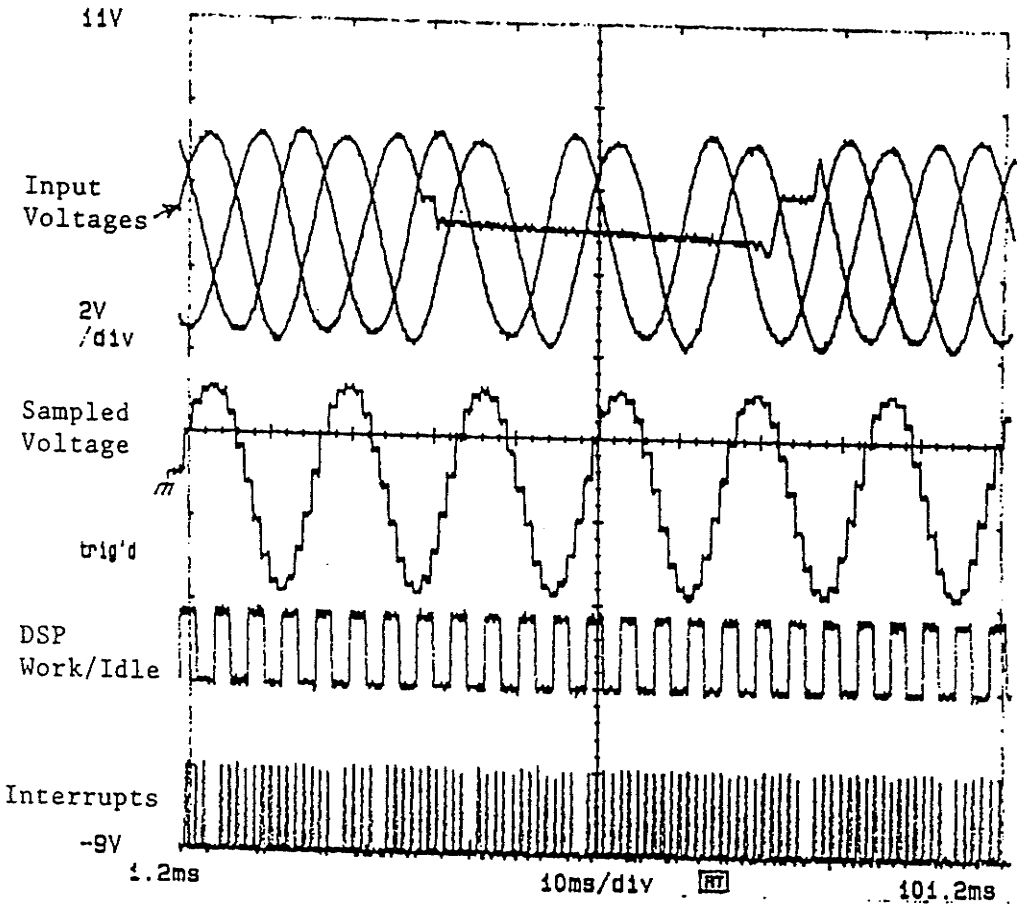

Fig. 4.5.2 Frequency tracking with one phase voltage temporary removed

In the Fig. 4.5.2, the top three traces are three phase voltages. A sampled waveform of one phase is shown in the 4th trace. The 5th trace shows the work/idle timing of the DSP chip and the 6th trace is the interrupt pulses for reading in sampled data from A/D converter. The 5th and the 6th trace are not important here, while the 4th trace is very important, which shows that the synchronized 16 sample/cycle sampling rate is kept unchanged during the temporary voltage drop of one phase. If the sampling frequency freezing measure is not used, such a voltage drop would have caused the

frequency tracking algorithm to lose tracking, as there will be an apparent phase change of V1 seen by the frequency tracking algorithm, while there is no frequency change in the system.

CHAPTER 5

SELF–EXCITATION IN GENERATORS CONNECTED TO DC LINE

5–1 Introduction

Self–excitation is an unique problem for generators carrying a dominantly capacitive load. The self–excitation problem for generators connected to HV/EHV AC transmission systems has been known and studied for many years [64] [65] [69] [70] [71]. A similar problem exists in a generating station connected to HVDC transmission lines.

Because of the nature of AC–DC conversion, the rectifiers of an HVDC transmission line consume large amounts of inductive VARs when converting AC power to DC power. The reactive power required for the conversion usually is in the range of 40 – 50 % of the active power converted. The rectification of AC power also generates high magnitude harmonic components.

The common practice is to design AC filters both to suppress the harmonics and at the same time to supply part or all of the reactive power required for the AC–DC conversion. When there is a full load rejection, generators will be left connected only to the capacitive filters on the rectifier AC busbar. The large capacitive load of the AC filters, previously consumed by the rectifiers, will have to flow into the generators. This exposes the generators to the danger of self–excitation and the consequent system overvoltage.

This self–excitation, resulting from load rejections, and the consequent system overvoltages in a generating station connected to DC lines are some of the many adverse effects on the generators and other station equipments. It also imposes strict limitations on the normal operation of the system. Though some problems caused by self–excitations in such a system, such as exciter stresses have been studied previously [61], there still are many other problems caused by self–excitation requiring further studies. The self–excitation problem in such a generating station is only similar to, but not exactly the same as, the self–excitation problem in a generating station connected to a HV/EHV transmission line. In fact, it has certain unique characteristics which enabled some useful results to be obtained in this research.

Considerable time has been spent and major efforts have been made in this research to further investigate other related aspects regarding the self–excitation and its proper protection in

such systems. As a result of these efforts, the classification between immediate and non–immediate self–excitations is introduced, the conditions under which a loss–of–excitation protection may misoperate are clarified, and the generator operating constraints as affected by the self–excitation considerations are established. These results will be presented in the following sections. A new predictive self–excitation protection system is also developed based on the results of the above analyses. This protection system and some related topics will be presented in the next chapter.

In the beginning of this chapter, the practical self–excitation criteria are described to provide the basis for later analyses. The model systems which are used in the self–excitation simulations are also briefly described.

5–2 Generator self–excitation criteria

The practical criteria used to determine if a generator is self–excited have been thoroughly studied previously in [64] [65] [69] [71]. It can be simply expressed as follows: the d–axis of a generator enters self–excitation when $X_c < X_d$, and the q–axis enters self–excitation when $X_c < X_q$, where X_c is the charging capacitance seen at the generator terminals. At the d–axis, the criterion corresponds to the field current going from positive to negative. Also, as X_d is always greater than or equal to X_q, and the X_c will be the same at both axes, the d–axis may enter self–excitation earlier than or at the same time as the q–axis does.

The physical explanation of the self–excitation is that the time constants governing the field flux dynamics become negative when the above criteria are satisfied [64] [71]. The time constants of d–axis and q–axis are

$$T_d = T_{do}\frac{X_c - X_d'}{X_c - X_d} \qquad \text{and} \qquad T_q = T_{qo}\frac{X_c - X_q''}{X_c - X_q} \qquad (5\text{–}2\text{–}1)$$

When the time constant is positive, any sudden change of field flux will decay exponentially. When the time constant becomes negative, any sudden change will cause the field flux to build–up exponentially, causing system voltage to rise limited only by the transformer saturation.

Although (5–2–1) shows that theoretically T_d and T_q may still remain positive if $X_c < X_d'$ and $X_c < X_q''$, such conditions are unlikely to occur in practical situations. Considering that X_d and

X_q normally are several times larger than X_d' and X_q", and $X_c < X_d$ and $X_c < X_q$ conditions are satisfied only under certain load rejection situations as will be discussed later, these make $X_c < X_d$' and $X_c < X_q$" unlikely to occur in real situations.

As can be seen from the constants equation, the negative time constants could be large or small depending on the values of X_d, X_q and X_c. The time constants are large when X_c is close to X_d or X_q. If $X_d > X_c > X_q$, only the d–axis becomes self–excited. When only the d–axis is self–excited or the time constants are large in both axes at the onset of self–excitation, the rate of field flux build–up will be slow. Under these conditions, the effect of field flux build–up could be nullified by the fast response of generator excitation systems with negative current capability [69]. That means the occurrence of overvoltages after generators entering the self–excitation condition could be postponed by providing negative current capability to the generator static excitation systems [69]. But if negative exciter current is not allowed to flow, the system voltage will start to increase immediately after generators become self–excited, i.e. immediately after their field currents reach zero.

5–3 Systems modelled in the self–excitation simulations

Figure 5.3.1 shows a system used in the self–excitation studies. Except for simulating generator tripping under self–excitation conditions, the system is simulated using only one generator. When a generator tripping under self–excitation condition case is simulated, two identical machines are connected in parallel on the bus, and one of them is tripped after the system becomes self–excited.

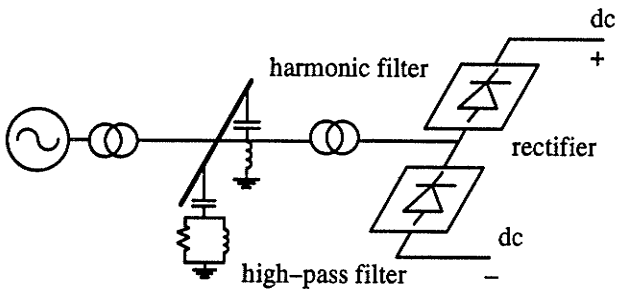

Fig. 5.3.1 Model system used in simulations

Machines in a generating station usually are of the same type. The common practice is to operate these generators sharing the active and reactive load equally during normal operations. When an HVDC load rejection occurs, the same amount of load change will be felt by each generator. Thus their dynamical processes will closely resemble each other after an HVDC load rejection. Analysis of one generator's behavior under an HVDC load rejection will reveal the behaviour of other generators.

The system is set up and simulated on an advanced graphical Electromagnetic Transients simulation software package PSCAD/EMTDC. The generators in the system are simulated using the machine model included in the PSCAD/EMTDC library and the data of an actual hydro generator at the Kettle station of the Northern Collector System. Table 5.3.1 lists the main data of this machine.

Table 5.3.1 Main data of the simulated generator

S (MVA)	V (kV)	X_d (pu)	X_q (pu)	H (pu)
120	13.8	1.106	0.642	3.42

In the above system, both generator governor system and excitation system are included and modelled in detail, as both systems greatly affect the self–excitation simulation results.

The reaction of the governor system and the counter torque produced by the generator losses and local load are the main factors preventing the system frequency from increasing indefinitely. The governor system functions to reduce the generator mechanical input power after a load rejection. Its action affects the frequency changing pattern considerably. The governor system modelled in the simulated systems uses the standard hydro generator governor system model provided by the PSCAD/EMTDC library.

The action of the excitation system affects the system voltage level, which in turn affects the local active and reactive load seen by the generator, thus indirectly affects the system dynamic process after a load rejection. The excitation system is simulated using the same data and structure of the actual system used by the simulated hydro generators of the Kettle station. The only difference is that the excitation system model used in the simulations can be chosen to have or not have negative current capability.

5–4 Immediate and non–immediate self–excitations

The self–excitations, resulting from load rejections, in a generating station connected to DC lines can be divided into two classes, immediate and non–immediate self–excitations. Fig. 5.4.1 shows how an HVDC load rejection is seen by a generator on a P–Q plane. In Fig. 5.4.1, two main generator operating constraints, i.e. maximum stator current and maximum field current limits, are also shown. In normal operations, the generator should be always operated within these limits. In Fig. 5.4.1, the circle is the maximum stator current limit, and the arc is the maximum field current limit. Fig. 5.4.1 is drawn using a per unit system, with the generator's rated MVA and voltage as the bases. As a generator always outputs electric power to the system, its normal operating area is enclosed by ABCDA shown in Fig. 5.4.1.

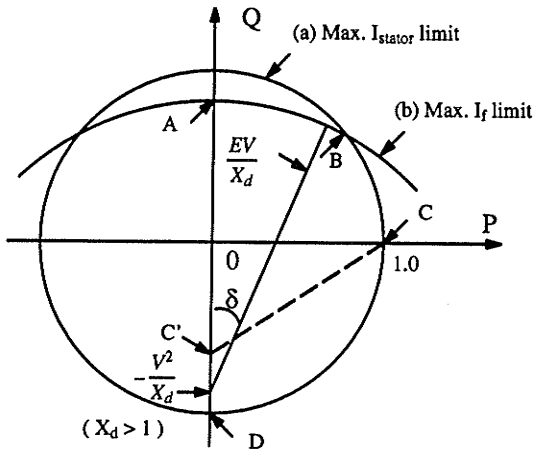

Fig. 5.4.1 HVDC load rejection seen by a generator

Fig. 5.4.1 does not show the common steady–state stability limit of a generator. The steady–state stability limit exists when a generator is connected to an AC transmission system. For generators connected to a DC transmission system, there is no such steady–state stability problem for them as they are operated asynchronously with the main system. Consequently, their operation does not have a steady–state stability limit.

Considering the rectifier load characteristic of a DC line in which the reactive power consumed is equal to 40 – 50% of the active power converted. A full HVDC load rejection occurring at the operating point C (Fig. 5.4.1) will cause the operating point to move to C' ($Q = V^2/X_c$)

immediately after the load rejection (assuming the system voltage and frequency remain unchanged).

The point $-V^2/X_d$ on the P–Q plane is a critical point when considering full load rejections. If the point C' is below $-V^2/X_d$, i.e. $1/X_c > 1/X_d$, the generator enters the self–excitation condition immediately after the load rejection. If the point C' is above $-V^2/X_d$, i.e. $1/X_c < 1/X_d$, then there is no immediate danger for the generator to become self–excited. But the generator may still enter the self–excitation condition later on due to system frequency increase after a load rejection. The self–excitations caused by the system frequency increase after load rejections are non–immediate self–excitation cases which will be discussed later.

Figure 5.4.1 indicates that an immediate self–excitation is possible if a generator has a large X_d (> 1 pu) and the generator is absorbing large VAR load when a load rejection occurs.

An immediate self–excitation will cause an immediate overvoltage in the generating station and induce extremely high reverse voltage across the thyristor bridges, if the generator excitation circuit does not have negative current capability (Fig. 5.4.2). The extremely high reverse voltage across the field circuit is induced by the field current attempting to go negative while the negative current is not allowed to flow in the exciter.

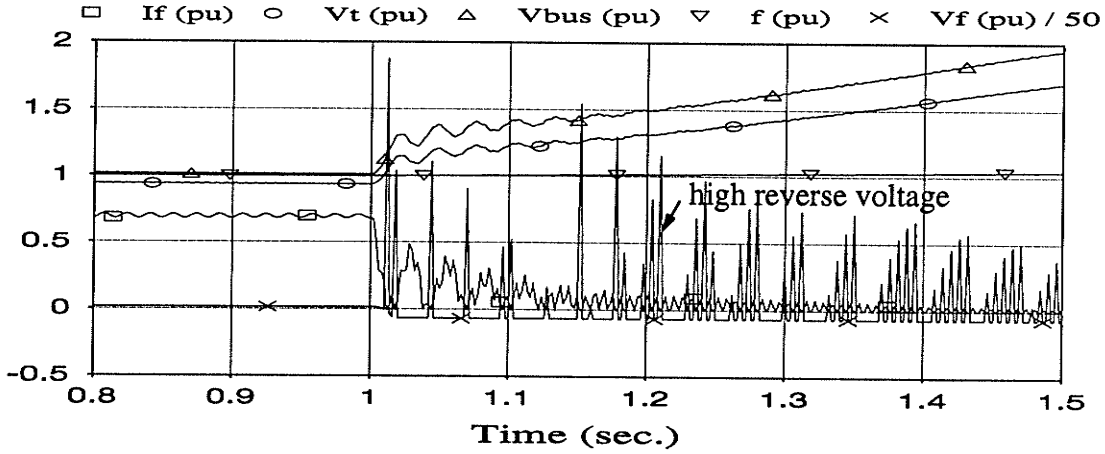

Fig. 5.4.2 Immediate self–excitation (no negative exciter current capability)

The field current attempting to go negative is the combined effects of two phenomena associated with the load rejection. The sudden increase of capacitive load after a load rejection in

such a generating station forces generator field current to drop to a very low level. Oscillations between generator inductance and the filter capacitances are initiated by the load rejection [61], which induces oscillating current components superimposed onto an already very low DC field current. If the field current is close to zero, this could result in field current attempting to go negative.

If negative current is allowed to flow in the excitation circuit, the immediate overvoltage of an immediate self–excitation could be postponed and the extremely high reverse voltage across the field circuit could be avoided (Fig. 5.4.3).

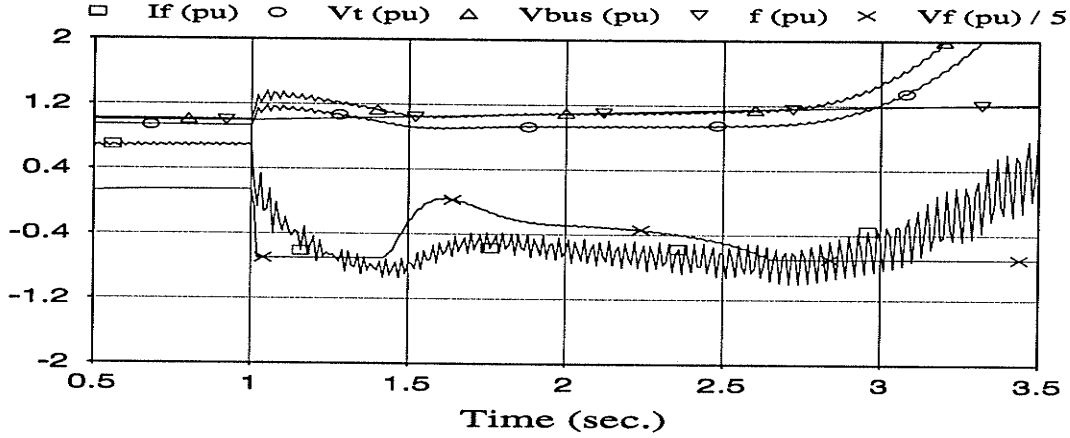

Fig. 5.4.3 Immediate self–excitation (has negative exciter current capability)

However, most self–excitation conditions are of the non–immediate type. The non–immediate self–excitations are different from the immediate self–excitations. Generators do not enter self–excitation conditions immediately following the load rejection (as in the immediate self–excitation cases) but later on due to the system frequency increase [64]. The frequency increase is the result of large torque unbalance caused by the load rejection. Due to the rapid change of the generator load and the slow response of the generator governor control system, the system frequency will start to increase after a load rejection. Though the system frequency could be finally brought back to the nominal value after it reached a maximum value by the reaction of the governor system and the effects of counter torque produced by the generator losses and local load, the maximum system frequency after a load rejection in such a generating station could still assume a very high value. In the Northern Collector System of Manitoba Hydro, the recorded maximum system frequency after a load rejection is 86 Hz [60]. With 60 Hz as its nominal system frequency, this represents more than 1.4 pu system frequency increase.

The increased system frequency increases $1/X_c$ and decreases $1/X_d$ at the same time, both in the direction to cause a self–excitation. On the P–Q plane (Fig. 5.4.1), the increase of frequency causes point C' to move downward and point V^2/X_d to move upward. When $1/X_c$ becomes greater than $1/X_d$ at a certain system frequency level, a self–excitation condition will occur. The criterion of self–excitation at the d–axis when considering the frequency change can be expressed as

$$\left(\frac{1}{X_{co}}\right)\frac{f}{f_o} \geq \left(\frac{1}{X_{do}}\right)\frac{f_o}{f} \qquad \text{or} \qquad \frac{1}{X_{co}} \geq \left(\frac{1}{X_{do}}\right)\left(\frac{f_o}{f}\right)^2 \qquad (5\text{–}4\text{–}1)$$

where f_o is the rated frequency of the generator, and X_{do} and X_{co} are X_d and X_c value at f_o. The critical frequency f_c after which a self–excitation will occur can be computed from

$$f_c = f_o \times \sqrt{X_{co} / X_{do}} \qquad (5\text{–}4\text{–}2)$$

Similar results can be easily obtained for the q–axis.

The system frequency does not rise indefinitely after a load rejection because of the counter torques of generator losses and remaining local load, as well as the action of the generator governor system. Thus if f_{max} is the maximum frequency which can be reached after a load rejection, a generator will become self–excited if $f_{max} > f_c$ but will not if $f_{max} < f_c$.

Figure 5.4.4 and Fig. 5.4.5 show two non–immediate self–excitation cases. In Fig. 5.4.4, the negative current is not allowed to flow in the exciter, while in Fig. 5.4.5, it is allowed. As can be seen from Fig. 5.4.4 and Fig. 5.4.5, the negative current capability of exciters helps to postpone the occurrence of a self–excitation. But the speed of voltage increase after it starts to rise is much faster than that in Fig. 5.4.4.

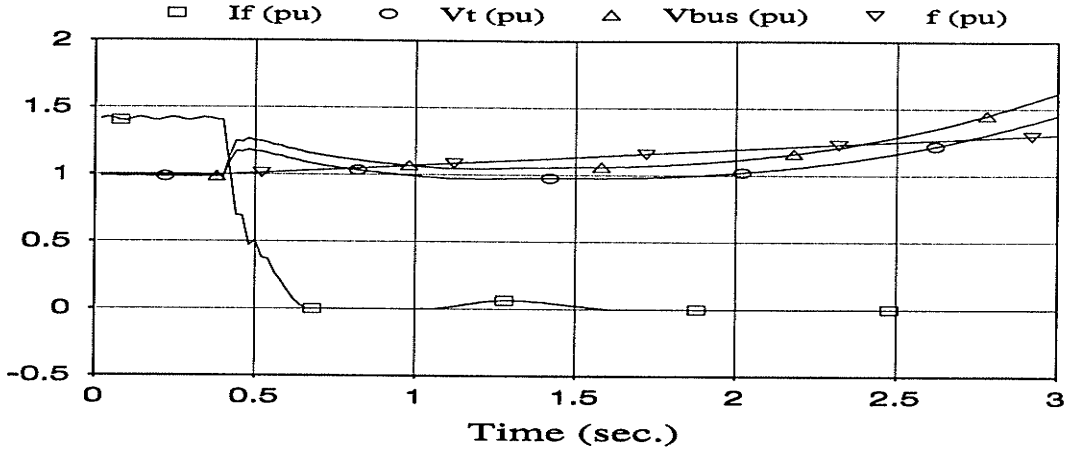

Fig. 5.4.4 Non–immediate self–excitation (no negative exciter current capability)

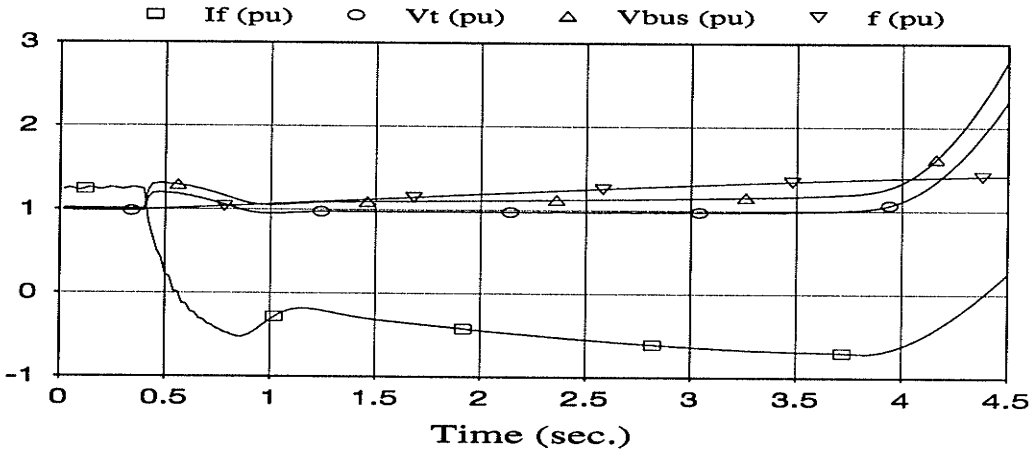

Fig. 5.4.5 Non–immediate self–excitation (has negative exciter current capability)

5–5 Problems other than system overvoltage caused by self–excitations

Besides the system overvoltage problems, there are other implications caused by the self–excitations in a generating station connected to DC lines.

One problem is the possible misoperation of the generator loss–of–excitation protection under self–excitation conditions. This problem can be analyzed as follows. The typical characteristics of impedance relays of a loss–of–excitation protection has been shown in Fig. 2.5.3.1. They can be converted into the P–Q plane as shown in Fig. 5.5.1 by

$$S = P - j\,Q = V^* \times \frac{V}{R + j\,X} = \frac{V^2}{R + j\,X} \qquad (5\text{–}5\text{–}1)$$

where R and X are bounded by

$$R^2 + \left(X + \frac{X_s - X_d}{2} \right)^2 \leq \left(\frac{X_s + X_d}{2} \right)^2 \qquad (5\text{–}5\text{–}2)$$

for the steady–state boundary, and by

$$R^2 + \left(X - \frac{X_d' + X_d}{2} \right)^2 \leq \left(\frac{X_d - X_d'}{2} \right)^2 \qquad (5\text{–}5\text{–}3)$$

for the asynchronous boundary. The shaded areas in Fig. 5.5.1 are the operating zones of the impedance relays of a loss–of–excitation protection.

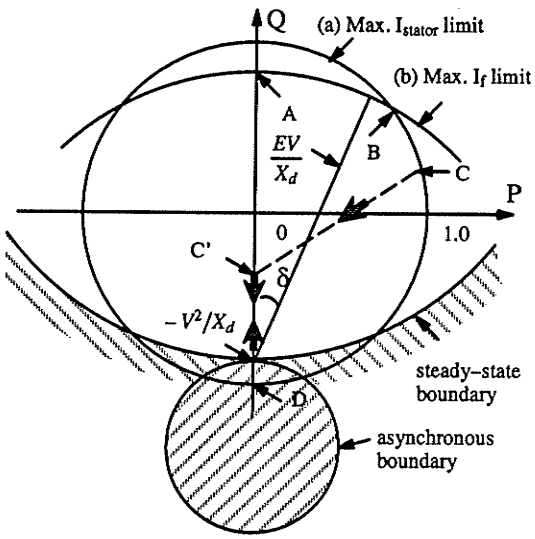

Fig. 5.5.1 Impedance relays' characteristics of a Loss–of–excitation protection on the P–Q plan

From Fig. 5.5.1, it is clear that the impedance seen by the relays enters both zones when the machine becomes self–excited at the d–axis. This will cause both relays to operate. Normally, the operation of impedance relays in a loss–of–excitation protection is safeguarded by an undervoltage relay with a setting around 0.8 pu generator terminal voltage. If system voltage temporally drops below the undervoltage relay's setting under this condition while the impedance relays operates, the generator loss–of–excitation protection will misoperate.

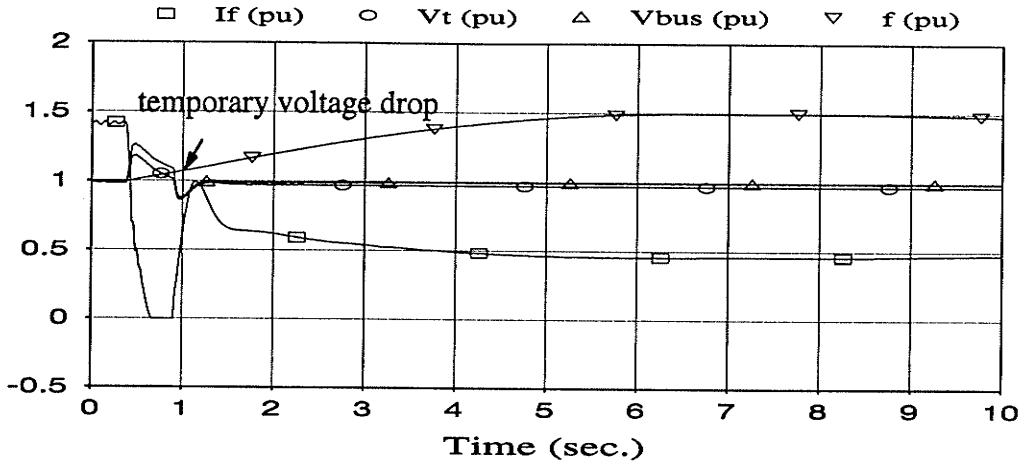

Fig. 5.5.2 Filter tripping after a load rejection causes temporary system voltage drop

The system voltage may drop only temporarily under self–excitation conditions. Overvoltages caused by the self–excitation could cause some filter overvoltage relays to operate. The sudden removal of some filters in the system will cause temporary system voltage drop due to sudden changes in generator armature reaction and the time delay in generator excitation systems' response. Fig. 5.5.2 shows the temporary system voltage drop when part of the filters are tripped after a load rejection.

In one severe load rejection incident at the Northern Collector System of Manitoba Hydro [59] [61], the loss–of–excitation protection at two tripped machines had operated (their undervoltage relays were set at 0.83 pu generator terminal voltage). The generator tripping occurred shortly after the high–pass filters in the system were tripped by the filters overvoltage relays. Due to the blocking of one DC converter, subsequently another converter was blocked. The analysis in [62] shows that the high–pass filter trip after these generators become self–excited results in the misoperation of these loss–of–excitation protection.

Generator tripping under self–excitation conditions causes further problems for the generators still remaining on the system, especially when these generators do not have the exciter negative current capability.

The generator tripping under self–excitation conditions causes more severe adverse effects than the immediate self–excitations after a load rejection. One obvious fact is that the more generators remain on the system, the less capacitive load each generator will take after a load

rejection. Tripping off some generators after load rejections forces the remaining generators to pick up more capacitive load, and at the same time initiates another burst of oscillations between generator inductance and filter capacitances.

Because the remaining generators have already entered self–excitation conditions, the combined effect of these two phenomena is more severe than that under an immediate self–excitation after a load rejection, if negative current is not allowed to flow in generator exciters. Sharper system voltage increase and much higher reverse voltages induced in the generator excitation circuit will be the direct results, which cause exciter circuit flashes and damage to the thyristor bridges of exciter. In the same load rejection incident mentioned above, the exciter of one generator was severely damaged with 12 out of 48 thyristors failed in the short circuit mode [61]. Figure 5.5.3 shows a simulated case where one generator in a two–machine system is tripped after the system enters a self–excitation condition due to a load rejection. The extremely high reverse voltage across the exciter of the remaining generator can be seen clearly from the Fig. 5.5.3.

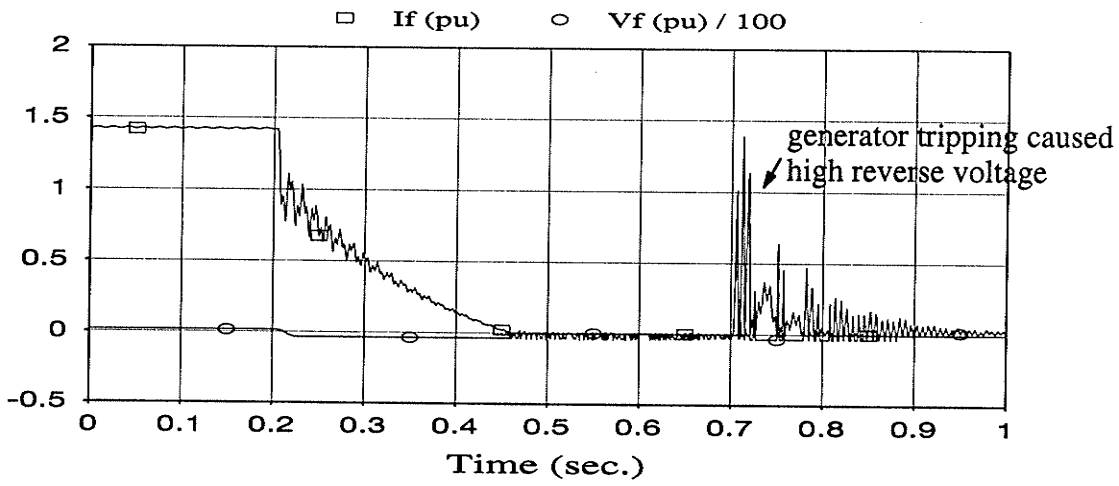

Fig. 5.5.3 Negative effects of generator tripping under self–excitation conditions

5–6 Self–excitation operating constraint for generators connected to DC lines

It is easy to see that the self–excitations in a generating station connected to DC lines could be avoided by keeping sufficient number of generators in operation, because each of them will take less capacitive load after a load rejection. This means that the generators in such a station should be operated under certain operating constraints taking the self–excitation possibility into account.

Though self–excitations in such a station have been known and some problems have been studied previously, the operating constraints as affected by the immediate and non–immediate self–excitation considerations for generators operating in such a system have not yet been clearly defined. These operating constraints have been derived as one of the results of this research. The immediate and non–immediate self–excitation operating constraints are presented as follows.

The operating constraint considering immediate self–excitation is easy to obtain. Simply draw a line utilizing the rectifier load characteristic of a DC line (assuming reactive power of a DC line is equal to 50% of the active power of it)

$$Q = -\frac{V^2}{X_d} + 0.5 \times P \qquad (5\text{–}6\text{–}1)$$

or

$$Q = -\frac{1}{X_d} + 0.5 \times P \qquad \text{in per unit system}$$

as shown in Fig. 5.6.1. When a generator is operated in the area above this line, there will be no immediate self–excitation danger to the generator after a full load rejection (assuming $Q_{DC} = 50\%$ P_{DC}).

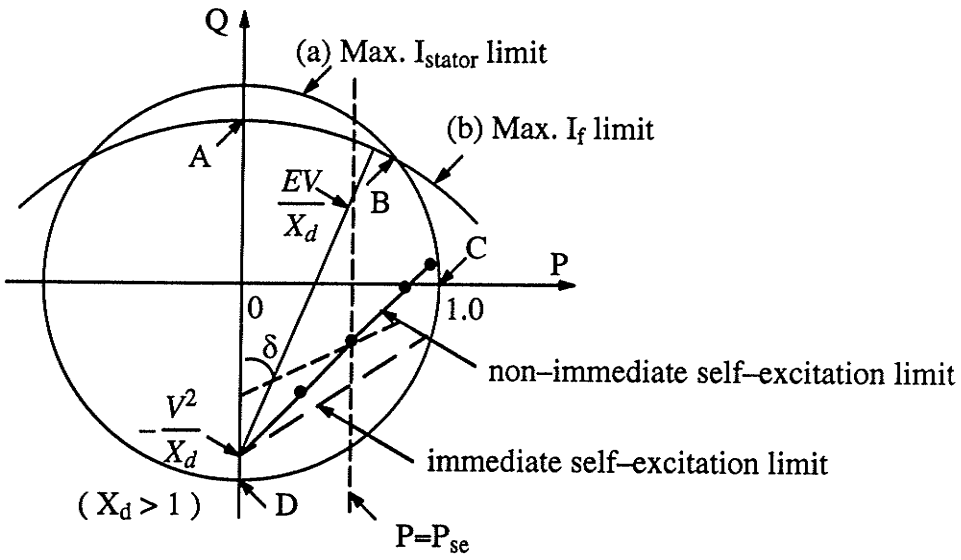

Fig. 5.6.1 Generator self–excitation operating constraints

The operating constraint considering non–immediate self–excitations is not as easy as the above one to obtain. The maximum system frequency, which could be reached after a load rejection, should be considered. There is no simple way to do it. The following describe the steps for obtaining such a constraint for a generator.

Step 1: Given an active power value P_{se} , draw the $P = P_{se}$ line on the P–Q plane (see Fig. 5.6.1);

Step 2: Conduct a full load rejection at this load level P_{se} to obtain the f_{max};

Step 3: Use f_{max}, V^2/X_d and (5–6–2) to obtain maximum V^2/X_{co} allowable immediately after load rejection. This is to ensure that at f_{max} the condition of $X_c(= X_{co} \times f_o/f_{max}) < X_d (= X_{do} \times f_{max}/f_o)$ will not be satisfied. If the operating point (P = 0, Q) is above this point (P = 0, Q = $-\max(V^2/X_{co})$) after a load rejection, a non–immediate self–excitation will not occur

$$\max\left(\frac{V^2}{X_{co}}\right) = \left(\frac{f_o}{f_{\max}}\right)^2 \frac{V^2}{X_d} \qquad (5\text{–}6\text{–}2)$$

Step 4: Draw a straight line based on the load characteristic of rectifiers from point Q = $-\max(V^2/X_{co})$, i.e.

$$Q = -\left(\frac{f_o}{f_{\max}}\right)^2 \frac{V^2}{X_d} + 0.5 \times P_{se} \qquad (5\text{–}6\text{–}3)$$

The intersection point of the line drawn in step 4 and the line $P = P_{se}$ is one (P, Q) point on the self–excitation operating constraint P–Q curve. If a generator operates above this point, it will not enter a non–immediate self–excitation condition after a full load rejection. Repeat above steps for different $P = P_{se}$, a P–Q curve can be obtained. Generators should operate above this curve to avoid entering non–immediate self–excitation after load rejections. This operating constraint is also shown in Fig. 5.6.1.

Both immediate and non–immediate self–excitation operating constraints in Fig. 5.6.1 are obtained using the data of the modelled generator of the model system simulated on the PSCAD/EMTDC. Table 5.6.1 shows the relationship between P_{se} and f_{max} of this generator. The time t_m for frequency to reach f_{max} is also included. It is assumed that after a load rejection, the losses of this generator and the local load is equivalent to 0.05 pu of its rated power. This means that the load rejected in P_{se} = 0.30 pu is ΔP = 0.25 pu.

Table 5.6.1 Relationship of f_{max} and P_{se}

P_{se} (pu)	0.30	0.55	0.80	0.95
f_{max} (pu)	1.14350	1.28780	1.44032	1.54961
t_m (sec.)	6.32	6.26	6.16	6.02
$\max(V^2/X_{co})$	0.6914687	0.5451902	0.4358398	0.3765304

Fig. 5.6.1 shows that the non–immediate self–excitation operating constraint poses a very strict limit on the normal operation of generators in such a system in the absence of a self–excitation protection system. By installing a self–excitation protection system, which can remove surplus filters when there is a danger of self–excitation after a load rejection, the above self–excitation operating constraints can be improved.

For generators having negative exciter current capability, the installation of a self–excitation protection system can both remove the non–immediate self–excitation operating constraint and improve the immediate self–excitation operating constraint, assuming it can remove surplus filters immediately after a load rejection when a self–excitation (non–immediate self–excitation cases) is going to occur or has already occurred (immediate self–excitation cases). Under immediate self–excitation conditions, the occurrence of system overvoltage is postponed by the negative current capability and there is no danger of high reverse exciter voltage being generated. Thus the self–excitation protection system will have sufficient time to respond.

For generators without negative exciter current capability, the non–immediate self–excitation operating constraint can be relaxed if a self–excitation protection system can remove surplus filters before a non–immediate self–excitation occurs. However, the immediate self–excitation operating constraint still exists and can not be improved by the installation of a protection system which detects the self–excitation and trips surplus filters after a load rejection. This is because the time delay of the protection system will make generators experience a short period of immediate system overvoltage and high exciter reverse voltage.

The self–excitation protection system for generators operating in such a generating station, as well as other related topics, will be further studied and discussed in the next chapter.

CHAPTER 6

SELF–EXCITATION PROTECTION

6–1 Introduction

The analysis results of some problems related to self–excitations in a generating station connected to DC lines have been presented in the previous chapter. This chapter is focused on the topics related to providing a proper self–excitation protection system for generators operating in a generating station connected to DC lines.

In this chapter, different measures which could be taken to prevent or eliminate self–excitations in such systems are discussed first. Some application problems of a commonly suggested "low field current + overvoltage relay" self–excitation protection system are analyzed. A new predictive self–excitation protection system is proposed based on the analysis results of the previous chapter. Some considerations in integrating this predictive self–excitation protection system into IGPS are discussed in the last section.

6–2 Protecting generators from damage by self–excitations

The surplus filter capacitive load or insufficient number of generators to absorb these surplus capacitive VARs is the fundamental cause of self–excitation problems. Increasing both the number of generators in operation or reducing the filters in the system could prevent a self–excitation from occurring or eliminate a self–excitation which has occurred.

As generators can not be started and operated to carry full load immediately after a load rejection, a sufficient number of generators has to be maintained in the system during normal operation to prevent self–excitations from occurring. This can be done by always keeping generators operating within their non–immediate self–excitation operating constraints under normal operations. However, as has been discussed in the previous section, this greatly limits the generator's normal operating area and poses a very strict operating constraint in the system operation and scheduling.

On the other hand, a sufficient number of filters has to be kept in the system during the normal operation of the system to suppress the harmonics and at the same time to supply required capacitive

VARs. Constantly switching filters in and out when the load changes to keep minimum number of filters in operation may partly, but can not completely, solve the problem. Doing so also shortens the life–span of filter breakers. Considering that it is the load rejection which makes the filters become "surplus" in a generating station connected to DC lines, and under a full load rejection there will be no need to keep filters in operation for harmonics suppression and capacitive VAR supplying purposes, removing surplus filters after a load rejection should be the best way to prevent self–excitation from occurring or eliminate a self–excitation in such a system.

However, simply tripping off filters whenever a load rejection occurs will result in many unnecessary filter trips, because not every load rejection will lead to a self–excitation. Intertripping filters after load rejections not only delays the restart process of an HVDC transmission system in many non–self–excitation load rejection cases, but also shortens the life–span of filter breakers.

Removing filters only when there is a real threat of self–excitation is a better solution to the above problem. This requires installing a dedicated self–excitation protection system for generators operating in such a system.

6–3 "Low field current + overvoltage relay" self–excitation protection system

"Low field current + overvoltage relay" self–excitation protection system is a commonly suggested self–excitation protection system [8] [59] [60] [69]. In fact, this is the only one studied previously.

Using an overvoltage relay alone to protect against self–excitations proved to be inappropriate. To avoid the misoperation of the relay under normal temporary system overvoltages, it requires a relatively high setting. This exposes generators and filters to self–excitation overvoltages before the filters are tripped, and the filter breakers will have to operate under unfavorable conditions.

Adding the generator "low field current" monitoring feature partly solves the above problem. Lower overvoltage relay settings can be used which will enable filters to be tripped at an early stage of self–excitation. However, this system is also operated on the basis of self–excitation detection, as it only operates when both the low field current condition and system overvoltage

condition occur at the same time. This may still expose generators and filters to a short period of overvoltages before surplus filters are tripped.

As the analysis in previous chapter shows, the system voltage usually can be kept at the nominal value by the action of generator excitation circuits after the load rejections. For generators without negative exciter current capability, the voltage can be kept at nominal value before the self–excitation occurs. For generators with negative exciter current capability, the voltage can be kept at the nominal value before the field flux build–up becomes faster than the field current change controlled by the excitation circuit.

The system voltage could increase very fast under the following two situations: generators have no negative exciter current capability but immediately become self–excited after a load rejection, generators have negative exciter current capability but finally lose their ability to control the voltage when the field flux build–up becomes too fast under both immediate and non–immediate self–excitations.

Any practical self–excitation protection system will take some time (include auxiliary relay and breaker time which are at least in tens of milliseconds) to finally trip the filters after its detection of the self–excitations. From the time the overvoltage relay operates to the time filters are tripped, the system voltage will be further increased if the voltage increase is very fast. This could cause the filter breakers to be operated under higher voltages and expose the system to a short period of overvoltages before the filters are removed from the system. Both are not desirable. Furthermore, the time delay may already cause damage to the exciters without negative current capability before the filters are removed, as the exciter reverse high voltage occurs immediately after the load rejection. These problems are the major obstacles in applying such a protection system. Other than these problems, there are some other concerns related to the application of such a protection system.

One concern is its possible misoperation under single generator loss–of–excitation. Generator low field current is not unique to self–excitation conditions. When a generator loses its excitation, it also experiences low field current. Tripping off filters under a single machine's loss–of–excitation could cause the system voltage to collapse, as the generator having no excitation absorbs a large amount of VARs from the system and tripping off filters further reduces the system

VAR supply. To avoid false tripping under a single machine's loss–of–field, such a system should only generate a filter trip signal when more than one generator detects low field current. This makes the system complicated to use.

Another concern is that this protection system may not be practical for a generator using a brushless excitation system. It will be difficult, if not impossible, to measure the field current of a generator using a brushless excitation system.

To input field current into a static or digital protection system could be a big problem. The field current flowing in the rotor winding is the one which correctly tells if a generator is self–excited. This is basically a DC signal. How to isolate the protection system from the field circuit, and how to accurately transfer this current signal from field winding to the protection system are two major problems which have to be solved for a static or digital self–excitation protection system. As most modern excitation systems are static, measuring AC field current instead of DC one may be a solution. However, to convert AC field current back to equivalent DC one will introduce extra time delay for the operation of protection systems, which will expose generators to a longer period of overvoltages.

In summary, the main problem of this protection system is caused by its operating principle of self–excitation detection. From the generator and system protection's point of view, it is better to trip the surplus filters before the self–excitation occurs. This requires a self–excitation protection system to have the ability of self–excitation prediction. Such a system has been studied and developed in this research, and will be presented in the following sections.

6–4 Predictive self–excitation protection system

Because of the drawbacks of the "low field current + overvoltage relay" self–excitation protection system, major efforts were made to develop a more suitable self–excitation protection system for generators connected to DC lines. The initial efforts were made to use non–harmonic oscillating components contained in the after–load–rejection field current to predict self–excitations. The results of the study show this method is not feasible. Many useful results have been obtained in the extensive studies of self–excitation phenomena in such a generating station, which lead to the development of a predictive self–excitation protection system.

6–4–1 Study of non–harmonic oscillating components

Initially, the possibility of using non–harmonic oscillating current components contained in the after–load–rejection field current to predict and detect self–excitations were studied. By non–harmonic oscillating components here means that the frequencies are not an integral multiple of the fundamental system frequency. The non–harmonic oscillating stator current components are the results of the oscillations between generator impedance and filter reactances initiated by the sudden load rejection [61]. Each of the oscillating current components contained in three phase stator windings produces a pulsating field which can be decoupled into two rotating fields rotating in the opposite directions. These two rotating fields then produce two non–harmonic oscillating current components superimposed onto the DC field current. If a non–harmonic oscillating component contained in the stator current has a frequency f_{osc}, the frequencies of two non–harmonic oscillating current components in the field current will be $f_{osc} + f_o$ and $f_{osc} - f_o$, where f_o is the system frequency.

Analyses and simulations show that it is difficult to use these non–harmonic oscillating components contained in after–load–rejection field current to predict and detect self–excitation conditions. This is because:

(1) The frequencies of these oscillating components are determined by the equivalent generator inductance and the filter capacitances at the time of load rejection. Thus they are not fixed values and vary with the system operation conditions.

(2) The oscillations between generator inductance and the filter capacitances are transient phenomena, thus the magnitudes of these oscillating components decay with time due to losses.

(3) The non–harmonic characteristic, non–fixed oscillating frequencies and the decaying magnitudes made it impossible to use the FFT algorithm to extract these oscillating components. They will be cross–represented in all harmonic vectors of an FFT calculation if an FFT is performed. Though some frequency zooming and digital filtering techniques may be used to extract these oscillating components, this will make it difficult to integrate a protection system using these oscillating components into IGPS.

(4) More importantly, these oscillating components, if they could be extracted accurately, may only be useful in detecting load rejections but not in detecting and predicting self–excitations. These oscillations are a load rejections related phenomenon. They also exist in non–self–excitation load rejection cases. Thus these oscillating components hardly can be used to distinguish self–excitation and non–self–excitation load rejections.

Because of the impossibility to use the above technique for self–excitation protection, major efforts were then directed to the study of the self–excitation phenomenon caused by load rejections in a generating station connected to DC lines. Several important results have been obtained. Some of them have already been presented in the previous chapter, such as classification of immediate and non–immediate self–excitations, self–excitation operating constraints for generators connected to DC lines, etc.. These results lead to the development of a new predictive self–excitation system which is one of the most important results obtained in this research. In the following sub–sections, the algorithms used by this system for predicting immediate and non–immediate self–excitations will be presented.

6–4–2 Predicting immediate self–excitations

The immediate self–excitations resulting from full load rejections in a generating station connected to DC lines can be predicted by utilizing the rectifier's load characteristic.

According to the analysis in section 5.4 and Fig. 5.4.1, if the reactive load Q_{lr} after a full load rejection seen by a generator is greater than $-V^2/X_d$, then this generator will not become self–excited immediately after a load rejection.

Assume that a load S = P + j Q is carried by the generator before a full load rejection. Immediately after the load rejection, P becomes zero and the reactive power changes from Q to Q_{lr} = Q – (50%/100) × P (a conservative consideration). Thus an immediate self–excitation can be predicted by

$$\left\{ Q_{lr} = Q - 0.5 \times P \right\} < -\frac{V^2}{X_d} \qquad (6\text{–}4\text{–}2\text{–}1)$$

using the P and Q during a generator's normal operation. This criterion actually checks to see if the immediate self–excitation operating constraint of a generator in such a system is violated.

When a generator enters the above condition during its normal operation and a full load rejection occurs, an immediate self–excitation, as well as an immediate system overvoltage if exciter has no negative current capability, will occur. This could be prevented by starting more generators in the system or removing some filter banks from the system (if allowed) until the above condition is no longer satisfied.

6–4–3 Predicting non–immediate self–excitations

In predicting a non–immediate self–excitation, the maximum frequency that a system reaches after a load rejection is the determining factor.

Extensive simulations were conducted using the modelled system to investigate the frequency increase pattern after a load rejection in such a generating station. Two important results were obtained.

Figure 6.4.3.1 shows the frequency change pattern of three load rejections at different load levels (P_o = 0.875, 0.625 and 0.375 pu) with the same amount of load rejection (ΔP = 0.25 pu).

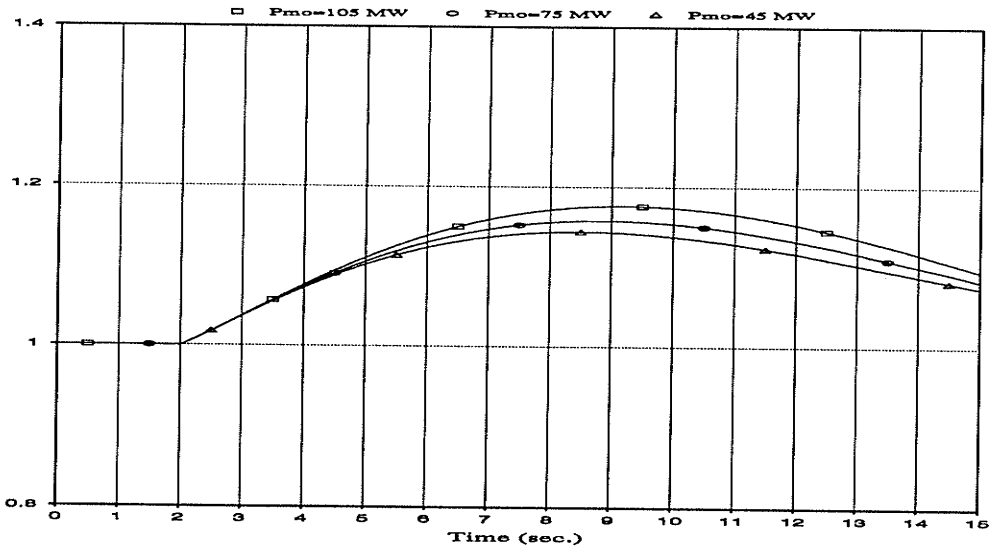

Fig. 6.4.3.1 f(t) curves for same ΔP but different P_o

As can be seen from the graph, the three f(t) curves in the Fig. 6.4.3.1 are only slightly different. This means that the frequency change pattern after a load rejection is mainly determined

by the amount of load rejected and less affected by the load level carried by a generator before the load rejection.

The second important result is that the maximum frequency which could be reached, and the speed of frequency increase after a load rejection are almost in proportion to the amount of load rejected.

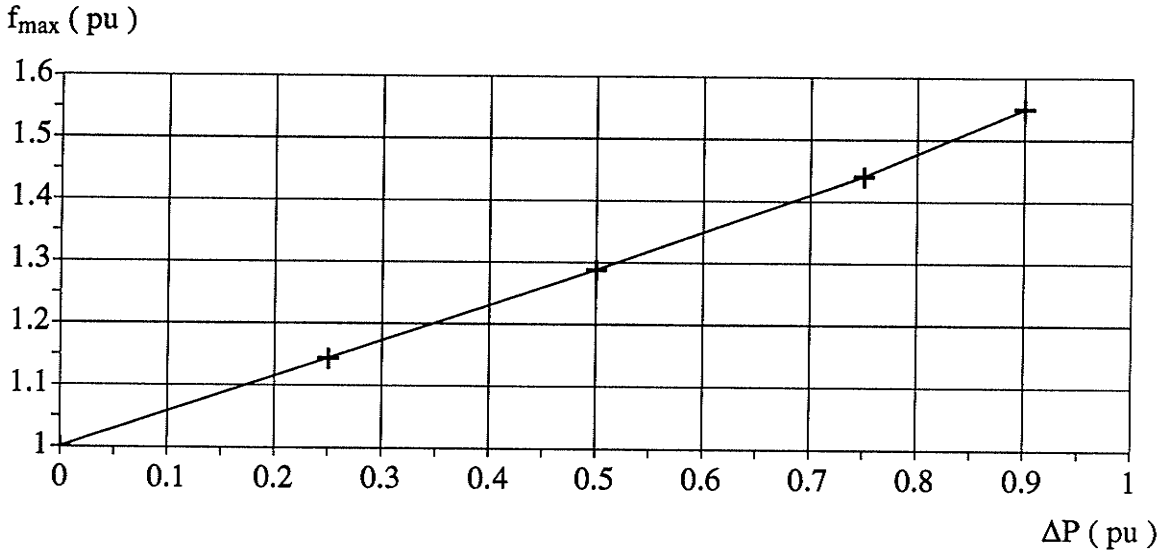

Fig. 6.4.3.2 f_{max} – ΔP curve (in per unit)

Using the data of Table 5.6.1 in section 5.6, a f_{max} – ΔP curve can be plotted in Fig. 6.4.3.2. As can be seen from the graph, it is very close to a straight line (the actual $f_{max}/\Delta P$ is slightly higher for a larger ΔP than that for a smaller ΔP). This means that the maximum frequency f_{max} after a load rejection could be predicted by using ΔP, which is the amount of load rejected. Using the $f_{max}/\Delta P$ at the $\Delta P = \Delta P_{max}$, the f_{max} of a load rejection with rejected load ΔP could be predicted by

$$f_{max} = \Delta P \times \left(\frac{f_{max}}{\Delta P}\right)_{\Delta P = \Delta P_{max}} \qquad (6\text{–}4\text{–}3\text{–}1)$$

which gives a slightly conservative estimation.

The same is true for the df/dt curve after a load rejection. Figure 6.4.3.3 (a) shows three f(t) curves corresponding to three different load rejections with different amount of load rejected (ΔP = 0.25, 0.5 and 0.75 pu). The frequency changing part of these three curves, when scaled by the following equation,

$$f(t)_{\Delta P} = f_o + \frac{f(t) - f_o}{\Delta P} \qquad (6\text{–}4\text{–}3\text{–}2)$$

are almost identical. This is particularly so in the initial phase when the frequency is increasing.

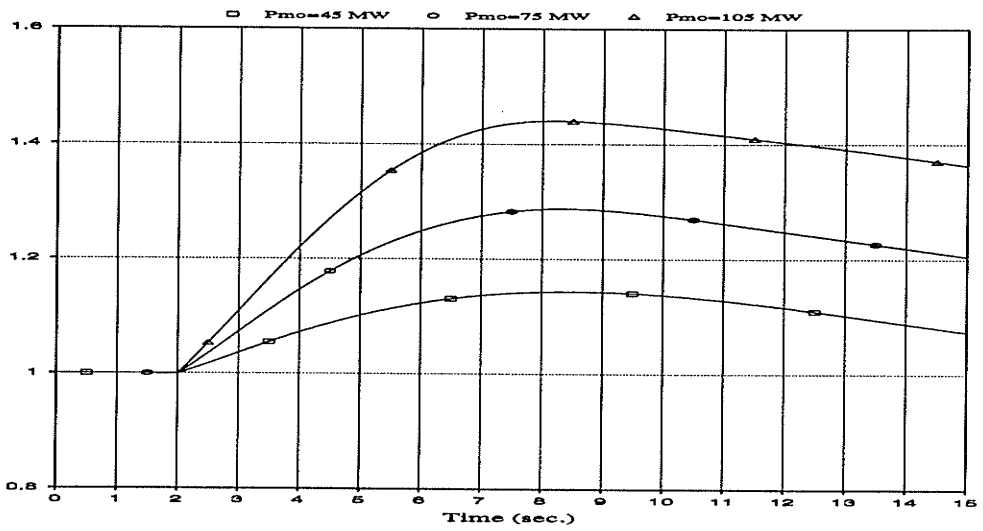

(a) Original f (t) curves

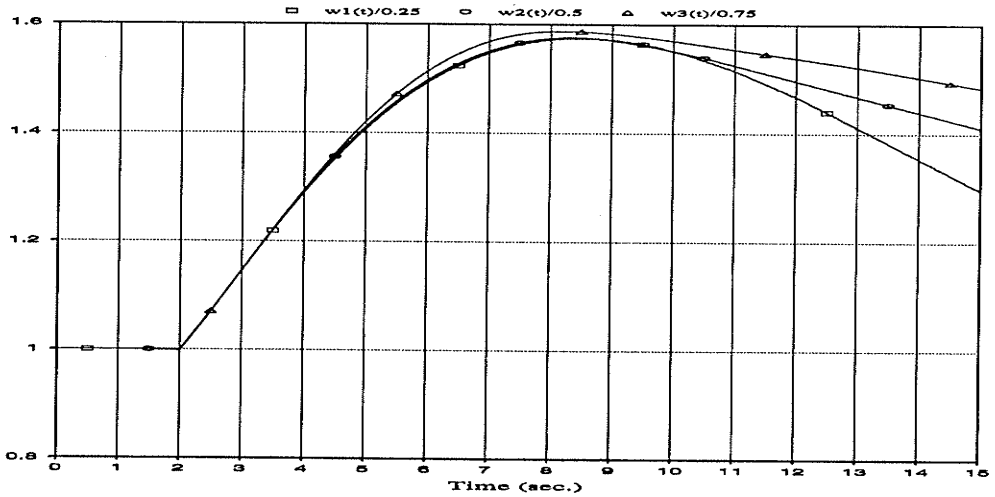

(b) Scaled f (t) curves

Fig. 6.4.3.3 f (t) curves corresponding to different ΔP

The above findings are very useful in predicting a non–immediate self–excitation and the system frequency change after a load rejection. The first finding indicates that in predicting non–immediate self–excitations after a load rejection, the effect of load level P_o before load rejection can be neglected and only ΔP is important. Using f_{max}–ΔP curve and $f(t)_{\Delta P}$ curve, three

important questions can be answered, i.e. "will a system become self–excited?", "at least how much filter load should be tripped?" and "how long does it take to self–excite?" after a load rejection.

"Will a system become self–excited?" can be predicted by first calculating the critical frequency f_c and the f_{max}, then comparing f_{max} with f_c. If $f_{max} > f_c$, a non–immediate self–excitation will occur after the frequency f eventually increases to a value greater than f_c. The f_c is calculated from f_o and X_{co} obtained immediately after the load rejection by using (5–4–2). The calculation of f_{max} is using ΔP and $f_{max}/\Delta P$ at the ΔP_{max} which was described above.

The minimum amount of filters which should be tripped after a load rejection to prevent self–excitation from occurring can be calculated from these values: f_c, f_{max}, f_o, X_{do} and X_{co}. To make $f_c = f_{max}$, the X_{co} should be changed to the value X_c

$$X_c = X_{do} \times \left(\frac{f_{max}}{f_o} \right)^2 \qquad (6–4–3–3)$$

this is equivalent to changing the capacitive VARs from $-V^2/X_{co}$ to $-V^2/X_c$ at f_o in the amount of

$$\Delta Q = - V^2 \times \left(\frac{1}{X_{co}} - \frac{1}{X_c} \right) \qquad (6–4–3–4)$$

Note that above calculation is based on one generator. When there are N generators in the system, the above results should be multiplied by N.

Normally, the capacitive VARs supplied by each filter bank at the f_o are known values. So that by tripping off filter banks with the total VARs greater than the value of $N \times \Delta Q$ of equation (6–4–3–4), a self–excitation could be prevented or eliminated.

Using f_c and the $f(t)_{\Delta P}$ curve, the time it takes from a load rejection to a self–excitation could also be predicted when $f_{max} > f_c$. Only one $f(t)_{\Delta P}$ curve at the maximum ΔP is needed, which also gives a slightly conservative estimation at a ΔP smaller than at the ΔP_{max}. By multiplying ΔP with $f(t)_{\Delta P}$, a curve is obtained for f(t). And the time from load rejection to the time when $f = f_c$ can then be calculated based on this curve.

Predicting the time needed for a load rejection to become a self–excitation may be useful in increasing the predictive algorithms' accuracy. When a calculated f_{max} is close to f_c, the errors caused by using $f_{max}/\Delta P$ at the ΔP_{max} could result in some unnecessary filter trips. As it will take several seconds for the self–excitation to occur when a calculated f_{max} is close to f_c, the unnecessary filter trip could be prevented by introducing a time delay and allow the protection system to check actual system frequency. The time delay should be less than the predicted self–excitation occurrence time with some safety margin. When large discrepancies are found between the actual system frequency change and the predicted one using $f(t)_{\Delta P}$ curve, the prediction should be modified to use the actual system frequency f(t).

The $f(t)_{\Delta P}$ curve could be stored in the computer memory so that a table–look–up method can be used to determine when f becomes equal to or greater than f_c. Curve–fitting is another possible solution, but the functions for fitting the $f(t)_{\Delta P}$ should be carefully chosen. They should enable the easy conversion of $f(t)_{\Delta P}$ to $t(f/\Delta P)$, so that the time consuming iterating calculations in finding a "t" for a given f_c and ΔP could be avoided. The $f(t)_{\Delta P}$ curve only needs to store up to the point of f_{max} because only the frequency increase part is useful for self–excitation prediction.

6–4–4 Proposed predictive self–excitation protection system

The predictive self–excitation protection system proposed for the first prototype of IGPS is based on the above findings. Overall, it consists of two major parts: one is the self–excitation prediction function implemented in generator protection system, another one is the filter trip selection device. The self–excitation prediction function contains both immediate and non–immediate self–excitation prediction functions.

The immediate self–excitation prediction part measures generator active and reactive powers continuously during the generator's normal operation. It calculates Q_{lr} ($= Q - 0.5 \times P$) and compares it with $- V^2/X_d$. When equation (6–4–2–1) is satisfied, a warning signal will be sent to inform the system operators that there is a danger of immediate self–excitation should a full load rejection occur. The signal goes off after the situation is corrected.

The non–immediate self–excitation prediction part stores X_{do}, and $f_{max}/\Delta P$ at the maximum ΔP of a generator. After a load rejection, the ΔP, f_o and X_{co} are measured and used to calculate the f_c and f_{max} with stored X_{do} and $f_{max}/\Delta P$ as described in the previous sub–section.

If $f_{max} > f_c$, a filter trip signal will be generated and sent to a filter trip selection device. At the same time, the operation of generator protections are blocked until filters are tripped and the system voltage has recovered from the temporary dip. The filter trip signal could be either a simple binary signal or a signal containing the information as to how much reactive VARs should be removed, depending on the actual structure and the requirement of the filter trip selection device.

The filter trip selection device is necessary for the self–excitation protection systems. It keeps track of operating status of all filter banks, and calculates capacitive VARs necessary to be removed by summing up those required by each generator, and decides the number of filters to be tripped. The filter trip selection device is also needed for a "low field current + overvoltage relay" self–excitation protection system, if it is used to protect generators in such a station. For "low field current + overvoltage relay" self–excitation protection system, its filter trip selection device must calculate the amount of VARs to be changed.

In the above proposed system, the $f(t)_{\Delta P}$ curve is not used. Though it can be used to further increase the accuracy of the self–excitation prediction and avoid some unnecessary filter trips, it also increases the complexity of the prediction algorithm. More studies are needed to determine the value of incorporating $f(t)_{\Delta P}$ into the self–excitation prediction algorithm.

6–5 Integrating predictive self–excitation protection system into IGPS

Figure 6.5.1 shows the functional block diagram of the above proposed self–excitation prediction function to be implemented in the generator protection system.

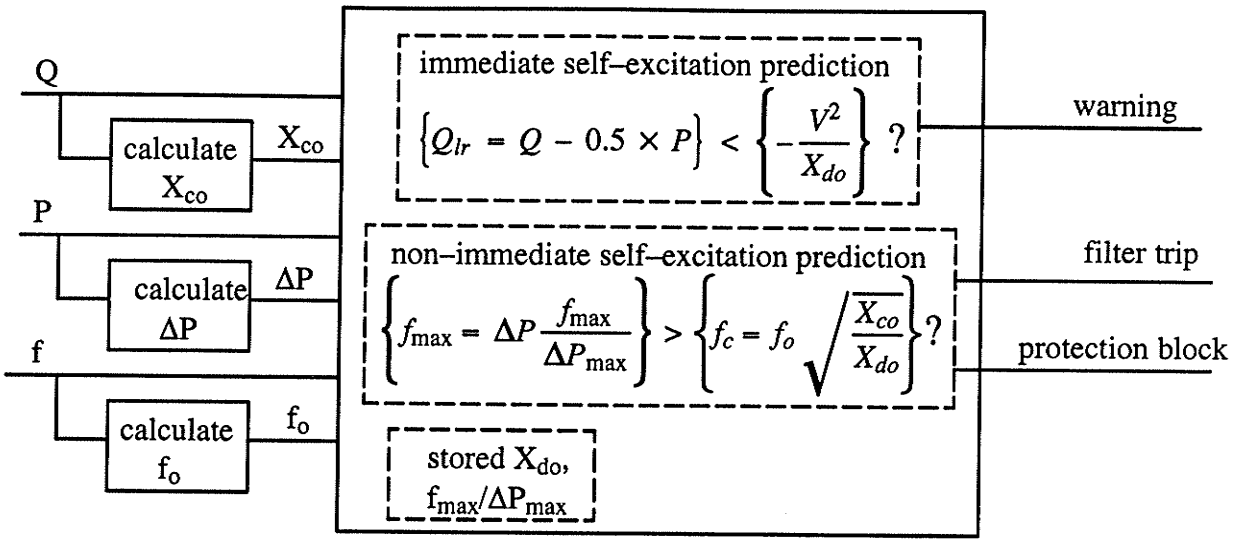

Fig. 6.5.1 Functional block diagram of proposed system

The integration of the predictive self–excitation protection function into IGPS is simple. P and Q are the preprocessing results and the f is measured in the frequency tracking algorithm, thus they are all readily available. The calculations of immediate and non–immediate self–excitation prediction algorithms are all simple except for the f_c calculation which involves a square–root operation. This could be simplified by comparing $(f_{max})^2$ with $(f_c)^2$ instead of comparing f_{max} with f_c in non–immediate self–excitation prediction. Also X_{do} can be stored as $1/X_{do}$ because both algorithms only use $1/X_{do}$.

With above changes, the calculations of these two algorithms become all multiplications and subtractions, which can be easily done by the DSP in the first prototype of IGPS.

By integrating the self–excitation prediction function into the IGPS, the blocking generator tripping task becomes trivial to implement. When it sends signals to trip filters, the operation of generator loss–of–excitation protection could be blocked at the same time. It will be blocked until the system voltage recovers from the temporary dip. Also as the filters are tripped before the self–excitation occurs, the impedance locus will not enter the operating zone of the impedance relays of a generator loss–of–excitation protection. Both indicate that the misoperation of generator loss–of–excitation protection under self–excitation conditions could be effectively prevented.

As mentioned before, the correct operation of such a self–excitation protection system needs the support of a filter trip selection device. The device should keep track of the operating status of

all filter banks in the station, and trips the appropriate number of filter banks when it receives the filter trip signal from the integrated generator protection system.

Comparing the above system with the commonly suggested "low field current + overvoltage relay" self–excitation protection system, it overcomes the major drawbacks of a "low field current + overvoltage relay" system by predicting self–excitation instead of detecting it and by not using the field current. Besides, it can calculate the amount of capacitive VARs to be removed which can not be done by the "low field current + overvoltage relay" self–excitation protection system. It is also easy to integrate into an integrated generator protection system.

As mentioned in the previous chapter, if such a system is installed, it can improve the self–excitation operating constraint of a generator from considering non–immediate self–excitations to only considering immediate self–excitations, no matter whether it is with or without negative current capability. This makes the system operation and scheduling become more flexible.

CHAPTER 7
INTEGRATED PROTECTION SYSTEMS

7–1 Introduction

Though one of the focuses of this research is to develop a prototype of an integrated generator protection system, there are many common problems related to integrated protection systems in general. These are economic aspects of integrated protection systems versus non–integrated systems, reliability concerns about integrated protection systems versus non–integrated systems, as well as what other advantages an integrated protection system would offer that a non–integrated would not.

To compare an integrated protection system with all existing protection systems is a very difficult task. This is due to the fact that existing protection systems utilize different technologies, such as electromechanical relays, static relays, digital or numerical relays. The comparisons made in this research are mainly focused on the digital protection systems, as this is the future direction of protection systems' development. And when a comparison is made, it is assumed that both integrated and non–integrated systems provide the same protection functions.

By an integrated protection system here is meant one protection system which could provide all protection and monitoring functions required for a single power system component, such as a generator, a transformer or a transmission line. And the system also has some computation power reserved for future modifications and/or additions of new functions. The system accesses all required input signals and has an unified output circuit.

In the following sections, the first two sections compare the economic aspects and reliability issues of integrated protection systems with non–integrated systems. The last two sections discuss some other major advantages of an integrated protection system, as well as the basic requirements for an integrated protection system.

7–2 Economical comparison

The economic advantage of an integrated protection system over a non–integrated protection system is not difficult to understand. In the early protection systems, different relays are

put into several closely located (usually are side by side) cabinets to reduce the cable length and simplify wirings, as well as for easy maintenance. In a static relay system, modular structures are commonly used to make several protection functions share power supply and input signals from auxiliary CTs and PTs. In a certain sense, these are early efforts made by the relay engineers to integrate protection systems.

When digital protection systems were developed, the economies of an integrated protection system over a non–integrated one become more obvious. This is due primarily to the more complicated structure of a digital protection system. Figure 7.2.1 shows the typical hardware structure required by a digital protection scheme or system.

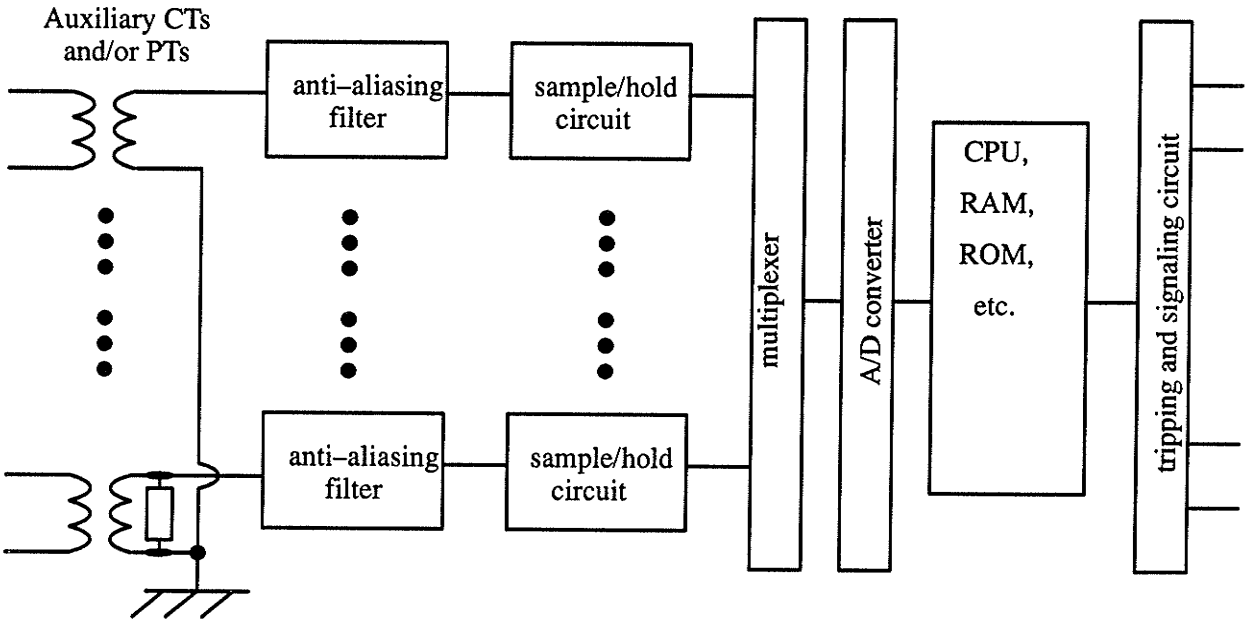

Fig. 7.2.1 Typical structure of a digital protection scheme

All functional blocks in Fig. 7.2.1 are the basic ones for a digital protection to accomplish its signal input, computation, protection and output tasks. When comparing an integrated system with a non–integrated system using this basic structure, the economic advantages of an integrated system become obvious.

Take the first prototype of IGPS as an example. The seven main protection and monitoring functions as well as the self–excitation protection and harmonics monitoring function have been implemented in it. If each function is implemented using a single function scheme, it would need

nine of these schemes. With the input signals required for these functions as shown in Table 7.2.1, a large amount of hardware will be needed.

Table 7.2.1 Input signals for generator protection functions in IGPS

Name of functions	Input signals										
	V_{ta}	V_{tb}	V_{tc}	I_{ta}	I_{tb}	I_{tc}	I_{na}	I_{nb}	I_{nc}	V_n	I_f
Differential stator protection				X	X	X	X	X	X		
Current unbalance protection				X	X	X					
Loss–of–excitation protection	X	X	X	X	X	X					
Motoring condition detection	X	X	X	X	X	X					
Over–voltage protection	X	X	X								
Over–current protection	X	X	X	X	X	X					
100% ground fault protection	X	X	X							X	
Self–excitation protection	X	X	X	X	X	X					X
harmonics monitoring	X	X	X	X	X	X	X	X	X	X	X

X: signal being used by this function.

As can be seen from the table, though in total only 11 input signals are used by these protection functions, 50 auxiliary CTs and PTs (except I_f which is a DC signal), 52 anti–aliasing filters, 52 sample/hold circuits, 9 multiplexers and A/D converters (assuming each scheme only uses one of them), at least 9 microprocessors and power supplies as well as supporting ROMs, RAMs and other interface circuits will be needed if single function schemes are used. But for an integrated system, it uses only 10 auxiliary CTs and PTs, 11 anti–aliasing filters, 11 sample/hold circuits, 1 multiplexer and 1 A/D converter, 1 or more microprocessors and one power supply. This will result in a substantial saving in hardware expenditures.

In an actual implementation, an integrated system may need to use more powerful CPU chips, more memory space and so on, while a single function scheme or system could use less powerful ones. An integrated protection system still is more economical than a non–integrated one when they provide the same protection functions. This is because the computation power needed by an integrated system does not increase in proportion to the number of protection functions which it includes.

As will be discussed in the later chapters, in a digital protection system, large portions of computation power are spent in the preprocessing computations, such as filtering, DFT and FFT computations, sequence components computations etc. The preprocessing results are then used by the protection algorithms to compare with stored settings. In a non–integrated protection system, these preprocessing computations have to be performed for each of the schemes on their input signals. In an integrated protection system, the results of these preprocessing computations can be shared by all protection functions of the system. Thus the computation power for preprocessing only needs to be increased slightly. In the above example, an average 6 input signals needs to be preprocessed for each scheme, while an integrated system needs only 11 input signals to be preprocessed.

The above comparison clearly shows that an integrated protection system is much more economical than a non–integrated one. Note that they are compared as far as the basic functionalities are concerned. When some more advanced functionalities are included in the comparison, an integrated protection system will have definite economic advantages over a non–integrated one. Some of these aspects will be discussed later in this chapter.

7–3 Reliability comparison

It is generally agreed that an integrated protection system has obvious economic advantages over a non–integrated one. But when the reliabilities of both systems are compared, a common perception is that a non–integrated protection system is more reliable than an integrated protection system, because the uneconomical redundancy in hardware and software of a non–integrated protection system seems to provide it with higher reliability than that of an integrated system.

It is true that if any major functional block shown in Fig. 6.2.1 fails in an integrated protection system, it could affect more than one or all protection functions of the system, while in a non–integrated system this usually affects only one protection function. Thus if a fault occurs, the non–integrated system will have a higher possibility to operate correctly than an integrated system. However, this comparison only compares the dependability of both systems, which is only one aspect of a protection system's reliability. The reliability of a protection has two aspects: dependability (function correctly when required) and security (no malfunction when not required

). Also this comparison assumes that both systems are used as a one–out–of–one stand–alone system. When other factors are considered, the conclusion will be different. To compare integrated protection systems with non–integrated ones, the following factors should be considered.

The major factors which should be considered are: (1) A complete protection system for any important component in a power system normally consists of two independent sub–systems, i.e. the one–out–of–two dual–system structure is a common practice in protecting important power system components; (2) All protection schemes of a non–integrated system in each sub–system share the same power supply source and output tripping circuit; (3) Consequently a non–integrated sub–system normally needs to be completely shutdown when any one of its protection schemes needs to be tested, replaced or repaired.

One thing which should be pointed out is that the comparisons made in the following sub–sections are not intended to perform a full range reliability comparison of both systems on a strict quantitative basis. It mainly points out several factors which could greatly affect the results of the reliability comparisons between the two systems. These factors should be considered for any detailed comparisons. A full comparison of both systems on a strict quantitative basis could be another major research project.

7–3–1 When one–out–of–two dual–system structure is considered

As has been mentioned, it is a common practice of utilities to provide two independent protection sub–systems for all important components, such as generators, in a power system. The two protection sub–systems usually provide almost the same level of protection for the component to be protected, so that sufficient protection could be maintained when one of them is out–of–service due to routine maintenance check, tests, repairs or other reasons. This is known as the one–out–of–two dual–system structure. Thus when integrated and non–integrated protection systems are to be compared, it could be assumed that this system structure is always used.

The dependabilities of both systems when one–out–of–one single sub–system structure is used have been analyzed in the beginning of this section. For this structure, an integrated protection system shows a lower dependability than a non–integrated protection system. However, by using

one–out–of–two dual–system structure, the dependability of a system using integrated sub–systems can be improved substantially.

The dependability of a protection system could be assessed using the system failure rate of a protection system and the fault rate of the protected equipment. If a protection system has a failure rate of p_{fail} and the protected equipment has a fault rate of p_{fault}, then the possibilities for the protection system failing to trip a fault will be $p_{fail} \times p_{fault}$. In the following analyses, it is assumed that any of the schemes in a non–integrated sub–system will have the same level of failure rate as an integrated sub–system, as their hardwares and softwares are of the same levels of complexity (refer to Fig. 7.2.1).

Now assuming a sub–system has a failure rate of $p_{fail-sub}$, then the possibility for a protection system using one–out–of–two dual–system structure to fail will be $(p_{fail-sub})^2$, as the whole system fails completely only when both sub–systems fail at the same time. Thus by using this structure, a protection system using integrated sub–systems will have a failure rate of $p_{fail} = p_{fail-sub} \times p_{fail-sub} = 0.0001$ if a single system has a failure rate of $p_{fail-sub} = 0.01$. This is a big improvement.

The failure rate calculation of a protection system using two non–integrated sub–systems is more complicated than that using integrated ones. Its total failure rate is the sum of its failure rate for loss of all protections and its failure rate for loss of single function or more functions.

Its failure rate for loss of all protections is easy to compute. For example, if each sub–system has N protection schemes and each of the schemes in one sub–system is assumed to have the same failure rate $p_{fail-scheme} = p_{fail-sub}$ of an integrated system, then the possibilities for whole system to fail completely is $((p_{fail-scheme})^N)^2$, which is much lower than a system using integrated ones.

However, its failure rate for loss of a single function or more functions is much higher and difficult to compute, because there are so many different combinations and each of them has to be dealt with separately. Though this failure rate will not be computed here, it is easy to see that the dependability of a protection system using two non–integrated sub–systems is not as high as commonly perceived when all failure possibilities are considered.

Also considering the fact that any one of the important components in a power system only has a limited fault rate of p_{fault} (e.g. once per year), i.e. they are not 100% of the time in the fault state, the possibilities of failing to trip a fault for a protection system using a dual–system structure will be even smaller. The above analysis shows that a protection system using a one–out–of–two system structure with two integrated sub–systems could have an acceptable dependability level.

7–3–2 When considering power supply source and tripping circuit sharing

The security is another important aspect of a protection system's reliability, as any false trip of an important component also has a severe impact on the normal operation of the power system. The failure rate calculation of a protection system for the security assessment here is different from that for dependability assessment. It is assumed that any functional block in an integrated sub–system or in a scheme of a non–integrated sub–system could cause a false trip of the sub–system. With this assumption, the failure rates of both systems can be computed directly based on a complete sub–system.

A digital protection system can be divided into four major parts as shown in Fig. 7.3.2.1: input circuit, main calculation and protection part, power supply and output tripping logic circuit. Its failure rate for security assessment thus is determined by the failure rate of these four parts.

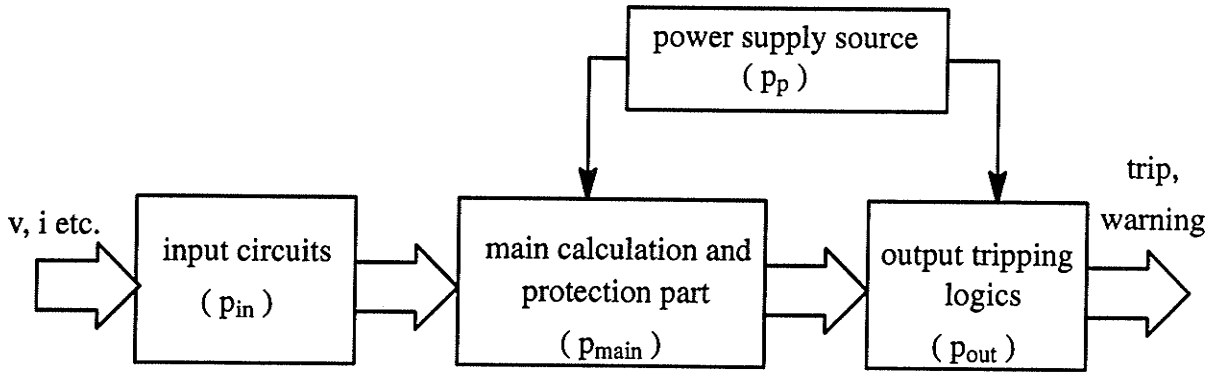

Fig. 7.3.2.1 Block diagram for system failure rate calculation (security)

A non–integrated protection system, as analyzed in the economic comparison, has more input signals (due to duplication for each scheme) than an integrated one. The complexity of its main calculation and protection part for each scheme is almost the same as the one used by an integrated protection system (as a digital protection system must have all the basic functional blocks

shown in Fig. 7.2.1 to work properly). Both integrated or non–integrated system use one power supply source, but the tripping circuit of a non–integrated protection system is more complicated than an integrated one. This is because the output signals of each scheme in a non–integrated system need to go through a tripping logic part to be delayed, "ORed" and "ANDed" to form the final tripping signal, while in an integrated system, the tripping logic part can be performed in the main calculation and protection part.

If above differences are considered, and the following are assumed (all "p"s are the failure rates): (1) all input signal channels for both systems have the same reliability p_{in}, (2) main calculation and protection part for each scheme in a non–integrated system has the same reliability p_{main} as the one used by an integrated protection system, (3) power supply sources for both systems have the same reliability p_p, and (4) the output circuit of a non–integrated system has a higher failure rate $p_{out.non-integrate}$ than $p_{out.integrate}$ that an integrated system. As the following calculation shows, a non–integrated protection system shows a much higher failure rate than that of an integrated system from the system security assessment point of view. The failure rate calculated below takes a system as a whole regardless whether it is an integrated one or not. This is correct when security is concerned, as any failure in one sub–system could cause a false trip of this sub–system.

For an integrated protection sub–system with N input signals, its system failure rate will be

$$p_{integrated} = N \times p_{in} + p_{main} + p_p + p_{out.integrated}$$

When a non–integrated structure is used such that it has M schemes and average N' input signals for each scheme ($M \times N' >> N$), its system failure rate will be

$$p_{non-integrated} = M \times N' \times p_{in} + M \times p_{main} + p_p + p_{out.non-integrated}$$

It is clear that $p_{non-integrated} >> p_{integrated}$. This means using a non–integrated structure will have higher failure rate or shorter MTBF (Mean Time Between Failure) than using an integrated structure, as far as security is concerned.

Though application of self–monitoring circuit/program in a digital protection system could greatly increase the system reliability, there is no guarantee that 100% of the problems can be

detected by the self–monitoring circuit/program. Any problem not being detected by the self–monitoring circuit/program could cause a false trip. If it is assumed that the self–monitoring circuit/programs work equally well in both integrated and non–integrated systems, then the percentage of problems not being detected by self–monitoring will be the same for both of them. As the calculated failure rate of a non–integrated system is higher than that of an integrated system, more false trips could be expected for a non–integrated one. Considering the fact that a protected component is in normal operation condition during most of its service time, this is a major drawback of using non–integrated systems.

Furthermore, the commonly used one–out–of–two dual–system structure can not prevent any false trip of its sub–systems. This makes the above security concerns more prominent for the protection systems using non–integrated sub–systems.

The above analysis shows that utilizing integrated sub–systems could increase the security level of a protection system using one–out–of–two dual–system structure. Other than that, the above calculated system failure rate also affects both systems' availability when the normal protection system shutdown procedure is considered, which will be discussed in the next sub–section.

7–3–3 When normal shutdown procedure for problem fixing is considered

In practice, if a problem is detected by the self–monitoring circuit/program of a protection sub–system, the sub–system will be blocked and a warning signal will be generated. The problem should be fixed before the sub–system can be put back into normal operation. No matter if a protection system uses integrated or non–integrated sub–systems, the faulty sub–system has to be shutdown completely to fix the problem. The need to completely shutdown an integrated sub–system is clear. For a non–integrated sub–system, because all schemes are put into the same or several nearby cabinets and share the same power supply source in the existing systems, it has to be completely shutdown to avoid any malfunctions of the system during the repair processes.

When this is considered, and the time needed for fixing any problem is assumed to be the same both for integrated and non–integrated systems, then a non–integrated system will have a lower availability than an integrated one has, because of its higher failure rate as analyzed in the previous sub–section.

The availability of a system is defined as [74]

$$A = \frac{MTBF}{MTBF + MTTR}$$

where, MTTR means "Mean Time To Repair". Both integrated and non–integrated systems could be assumed to have the same MTTR, but a non–integrated system has a smaller MTBF than an integrated one, as shown in the previous sub–section. This results in a lower availability for a non–integrated system.

7–3–4 When other factors are considered

Besides the above three major factors, there are some other factors which could affect the reliability comparison results when they are considered.

Among these, another important factor to consider is the low cost of an integrated system which would enable it to use some other reliability enhancement structures. Two of these possibilities are the two–out–of–three system structure and the duplication of input signals. Both are seldom considered by a non–integrated system because of the cost involved.

In the past, it is always a difficult balance between the system security and dependability when certain reliability measures are considered. A common problem is that they hardly can be increased by the same measure at the same time. The one–out–of–two dual–system structure increases system dependability but reduces the security. While the two–out–of–two dual–system structure suffers low dependability for increasing its security level [75].

The two–out–of–three system structure provides a much better compromise between the system security and dependability compared to the above two system structures [75]. If the cost is acceptable, the application of such a structure provides much higher reliability than the above structures.

Besides, duplication of input circuits could further increase the system reliability level. Some statistics [75] show that most of the protection system failures are caused by the input circuit and output circuit problems, such as PT open circuit, output auxiliary relay contacts problems, etc. Duplication of the input signal circuit increases the reliability of the input circuit, and makes it easy

to detect a faulty input channel. The cost of using a duplicated input signal structure is not acceptable for a non–integrated system, but could be considered for an integrated system. Take the first prototype of IGPS as an example. With duplicated input signals, it will have 22 input signals, which is still less than a single non–integrated system.

In conclusion, when all of the above factors are considered, a complete protection system using integrated protection systems has a higher security level and higher availability than the one using non–integrated systems. Its dependability level could be improved to an acceptable level when a one–out–of–two dual–system structure is used. Furthermore, the overall system reliability level of an integrated system could be improved by adopting some other reliability enhancement measures as discussed above.

7–4 Other advantages of integrated protection systems

There are many other advantages of using an integrated protection system over a non–integrated system, not just the economical one which has been discussed in 7–2. One important advantage, which is the primary goal of the development of an integrated generator protection system, is that it provides a solution for later system modification and addition of new functions. Among others, the most important ones are the much better fault recording function, the support for high level resources sharing, the great potential to implement more complicated protection and monitoring functions, and the ability to integrate some other measurement and control functions.

7–4–1 Better fault recording function

Fault recording function or disturbance recording function has become a "must–have" function for almost all digital protection systems. The built–in fault recording function in digital protection systems proves to be very useful in post–fault analysis of system disturbances and the performance analysis of the protection system itself. It also allows new relay algorithms and new relays to be tested using recorded fault waveforms which is also very useful.

The fault recording function of a non–integrated protection system has two main problems. One is the clock synchronizing problem and the other one is the unnecessary repetitive recording of the same signals.

For a non–integrated protection system, to synchronize all the clocks in all the schemes is a very difficult, if not an impossible, task. The problem exists even when highly stable crystal oscillators are used. As we know, many events of a system disturbance and the relay responses occur very fast in a very short time period (in tens of ms). Thus to be able to determine the sequence of events correctly, high time resolution (less than 1 ms) is required for the fault recording function of protection systems. Slightly out–of–synchronization of these clocks, say 10 ms, between different schemes, could result in false conclusions being drawn in the post–fault analysis.

The problem may be solved by installing a separate fault recording system, which records all input signals and relay operating states, so that there will be no clock synchronization problem existing for these schemes. But this solution has its own problems.

First, it is difficult for a separately installed fault recording system to obtain some internal transition states and some intermediate calculation results for the protection schemes of a non–integrated protection system. These internal transition states and intermediate calculation results may become very important for the post–fault analysis and relay performance evaluation under certain cases. Secondly, it requires additional capital cost for such a recording system and may require additional CTs, PTs, and wirings. Also, the fault recording starting algorithm of a separately installed system is almost as complicated as a protection system, because it can not rely on the relay signals from the protection system to start its fault recording if it wants to be operated independently. This may make a separate fault recording system become as complex as an integrated protection system. Thus installing a separate fault record system is not a good solution to solve clock synchronization problem.

Besides the clock synchronizing problem, the unnecessary repetitive recording of the same signals is another major problem for the fault recording function of a non–integrated protection system.

To form a complete fault record, each scheme in a non–integrated protection system must record all of its input signals and the protection function operating states. When no separate fault record system is installed and the clocks of these schemes are not synchronized, recording all input signals is very important, because it offers a means for adjusting the time difference between

different schemes by comparing the input signals. This, under some cases, could avoid false conclusions to be drawn.

But this will result in a large volume of multiple fault records for just one fault event, which are unnecessary for most cases. The total record size is almost in proportion to the total number of input signals being recorded (repetitive ones count as N if it is recorded N times), because protection function operating states occupy only a very small portion of a fault record. The large volume of multiple fault records for just one fault event causes problems in fault records archive and management.

Compared with non–integrated protection systems, the fault recording function of an integrated protection system does not have the above problems, as long as the protection system provides enough fault record space to accommodate the required fault record data. Providing large fault record memory is not a problem today, as high–density low–cost memory chips are widely available. This is a big advantage for using an integrated protection system.

Clock synchronizing is not a problem in an integrated protection system, as all events are recorded on the same time base. A separate fault recording system is not required, as with dual–system architecture the fault recording functions of each are backing–up each other. There will be no multiple fault records and there is no need to further duplicate the record of any input signals. This could result in substantial reduction in fault record volume, which makes it easy for archiving and managing fault records.

7–4–2 Resources sharing

Among major advantages of an integrated protection system, an important one is that it offers a great potential for resources sharing. The resource here include computer hardwares and softwares, such as hard disks, monitors, printers, as well as sophisticated analysis, display and database programs, etc.

A most notable development in the past few years in computer technologies is the networking technology. Any computer which has the network capability can be connected to a network and share all the resources available on that network.

However, to have network capability for a computer is not without cost. Special network hardware and software supports are needed for the computer wishing to connect to a network. Also the computer itself must have enough memory space to be able to run on the network satisfactorily and properly. The cost will be at least in hundreds of dollars and possibly more depending on the network capability requirement.

To provide better man–machine interface to protection systems directly with monitors, printers and hard disks has proved to be too costly, both for integrated and non–integrated protection systems. That is the main reason that most present–day digital protection schemes and systems only use very simple LCD displays and a very small keypad. But the functionality is also affected by doing so.

Providing an integrated protection system with network capability will cost less than providing it with hardware and software resources directly. But for a non–integrated system, the cost is still high as the network capability has to be provided to each scheme of the system.

Considering the trend in power utilities today is towards (1) the utilization of open–system architecture, which is strongly network based, in all major computer applications, such as SCADA/EMS, LMS and Database systems, for information sharing and easy upgrade, (2) the integration of planning, operation, control and protection functions, the network capability of a protection system could become another must–have function in the next few years.

With the network capability, the next generation protection systems will be able to use many more advanced technologies, such as visual relay characteristic analysis, visual setting adjustment, visual relay setting coordination, remote access fault records database, remote pooling relay operating status, run sophisticated simulation softwares remotely while working at the substations, ... the list can go on and on. In this sense, an integrated protection system has definite advantages over a non–integrated system.

7–4–3 Easy to implement more complicated functions

Another major advantage of using an integrated protection system is that it offers a great potential to implement more complicated protection and monitoring functions. One area an

integrated system can accomplish is its integration of the tripping logic part of a protection system into the main calculation and protection part.

If divided based on the functionality, a protection system has three major parts as shown in Fig. 7.4.3.1, i.e. measurement, comparison and tripping logic parts. Required electrical quantities are first measured and then compared with the settings. The results of these comparisons need to go through a tripping logic circuit to form the final tripping signals in a non–integrated system. This is because to form a final tripping signal usually requires more than one comparison result. It was not easy to design or modify a tripping logic circuit for a non–integrated system. It was also the major part prone to human errors and reliability problems for a non–integrated system.

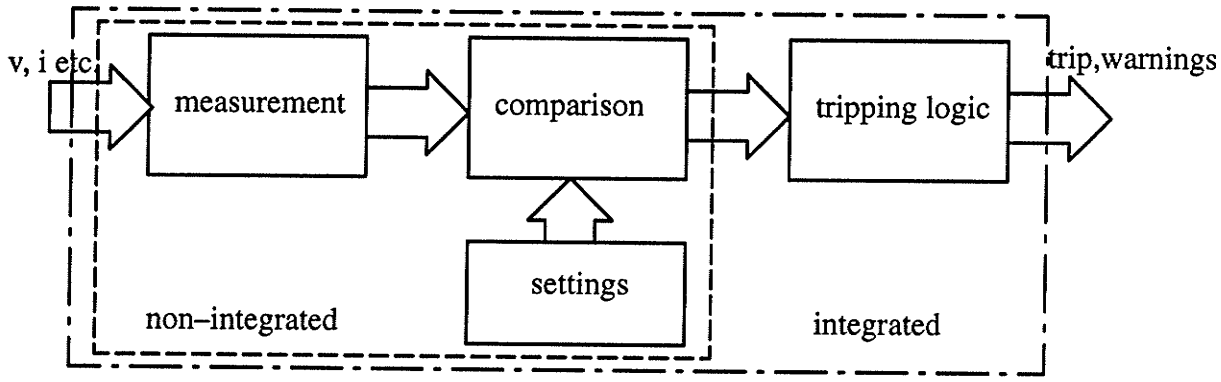

Fig. 7.4.3.1 Functional block diagram of a protection system

In an integrated system, the tripping logic part can be integrated into the main calculation and protection part, as all comparison results of different protection functions are available there. This makes implementation and modification of tripping logic of a protection system become easy. And more complex tripping logic could also be considered as no hardware cost will be involved.

One of the other areas the integrated system will be strong in is the implementation of adaptive protections, which are under active studies. A survey shows that the concept of adaptive relaying is widely accepted by the utilities [80]. An adaptive protection algorithm usually requires more input signals and other information. With all input signals accessible and resources sharing of the network capability if it is provided, an adaptive algorithm can be easily implemented in an integrated system. One example could be the generator overload protection.

As we know, the present generator overload protection mainly considers the overheating caused by the extended generator stator overcurrent. But there are many other heat generating

sources that will also cause generator temperature to increase, such as current unbalance and harmonics. These heat generating sources may exist at the same time so that the temperature increase is not determined by the overcurrent only. Also the actual temperature rise in a generator is not only determined by heat generating sources, but also the ambient temperature, actual generator internal temperature when additional heat generating sources occur, efficiency of cooling system and so on.

Thus an ideal overload protection should consider the combined effect of all these factors. A comprehensive temperature increase model should be studied and established. A more appropriate overload protection algorithm, which can automatically adapt to different situations, should also be developed on the basis of such a model. As current measurement, harmonics measurement and current unbalance measurement functions have all been included in an integrated generator protection system, the comprehensive overload protection function should have less difficulty to be implemented in it. But for a separate overload protection scheme, it may involve major efforts in adding harmonics measurement, current unbalance measurement and other functions or the development of a new scheme.

The above analysis shows that with all input signals accessible and the resources shared, more complicated functions can be easily implemented in an integrated system.

In conclusion, an integrated protection system has obvious advantages in many areas over a non–integrated system. It should become the main direction in the development of future protection systems.

7–5 Basic requirements of an integrated protection system

The following basic requirements are necessary for fully realizing the advantages of an integrated protection system.

1. Input all signals required for protecting an important equipment in power systems. This will result in a standard auxiliary CT and PT circuit design, and no need for rewiring when some protection function needs to be modified and/or new protection functions need to be added.

2. Sufficient hardware capability. In an integrated protection system, the hardware for the main preprocessing and protection part should be designed to have sufficient computation power

not only to be able to perform and implement standard protection and monitoring functions, but also have some reserve computation powers for future changes and new function additions. With this, the work of modifying implemented functions or adding new functions could be reduced to changing only parts of software, which will greatly reduce the cost and the time involved for modification/addition.

3. Provide suitable network capability. The advantages of providing network capabilities to any protection system has been discussed in section 7–4–2. This capability should be built into future integrated protection systems.

When an integrated protection system possesses these characteristics, it will have definite advantages over the non–integrated ones.

CHAPTER 8

IGPS HARDWARE

8–1 Introduction

Selecting a proper hardware platform is critical for developing a practical integrated generator protection system. In selecting a proper hardware platform, there are many considerations, such as the cost, computation power, system architecture, high level computer language support, system development tools, upgrading ability, and so on. Among them, the cost and the computation power are the two most important ones. Without sufficient computation power, the system would not be able to accomplish its tasks. On the other hand, if a selected hardware platform is powerful enough but costs too much, it would not be used.

The early development of digital protection systems in the 1970s and 1980s was greatly affected by these two factors. The powerful hardware, such as mini–computers, were too costly to be used by a digital protection system. While the costs of microcomputers or microprocessors were acceptable, they can only offer very limited computation power.

The computer technologies have advanced substantially in the past ten years. The computation power of current microprocessors is approaching the computation power of mini–computers in the 1970s and early 1980s. At the same time the price of these chips is kept at a reasonable level of several hundred dollars. During the same period, another major advancement of computer technologies was the development of Digital Signal Processors (DSPs). The DSPs typically have a hardware multiplier built in , and have parallel processing capability. This made it most suitable for computation intensive applications, such as real–time digital signal processing. Since the late 80s, floating point DSPs have also become commercially available, which greatly expands the application areas of DSPs. The DSPs have also found their applications in the digital protection systems, as these systems require substantial computation power.

State–of–the–art CPU and DSP chips are used in the first prototype of IGPS. The cost of the hardware platform being used is about $1,500 at the time the project was started, which is acceptable. The major objectives of implementing the first prototype of IGPS on this hardware platform are to

find out "if this hardware platform is powerful enough for a practical IGPS?" and "if it still lacks power, what level of computation power the next hardware platform should be looking for, while keeping the cost at the same level?". These will be discussed in the following sections.

8–2 Hardware platform used by the first prototype of IGPS

In selecting hardware for the first prototype of IGPS, the two main factors were first considered. To be able to make a replacement option for existing generator protection systems in the Northern Collector System, the cost of the hardware to be used will be a determining factor. There are a total of 22 generators in Kettle and Long Spruce generating stations. To provide two protection systems to each generator requires a total of 44 such systems. The number required will be more than 44 when spare units are included. Sufficient computation power is required by the system, as not only the standard generator protection functions, but also some special protection functions, need to be implemented. Those added special protections, particularly the harmonics monitoring function, require substantial computation power.

At the beginning of this research, there was a piece of hardware, called "Adaptive Microprocessor Protection System (AMPS)" board, available. It was developed by a graduate student to serve as a common hardware platform for different protection projects of Manitoba Hydro. This board contains a NEC 77230 chip which is the first commercially available 32–bit floating point Digital Signal Processor (DSP). The chip can perform a 32 bit by 32 bit floating point multiplication and up to 11 operations in parallel in one single instruction at 150 ns clock speed (6.6 MHz). The board also has a 32 bit Motorola 68000 CPU on it as a master processor.

Including both DSP and CPU on the original AMPS board is intended to utilize the strength of both chips and avoid their weaknesses.

A normal CPU, such as MC 68000, is strong in logical operation, fixed point addition and subtractions. It also has a well designed interrupt handling system (including stack mechanism and multiple interrupt input levels) and diverse addressing methods. It is good at general purpose applications such as logical control, timed sequence control, structured data manipulation and so on. In these applications, multiple interrupts and diverse addressing modes normally are required. It is also good at applications involving only fixed point addition and subtractions. But when it comes

to the multiplications, divisions and floating point addition/subtraction operations, the performance of a normal CPU is very unsatisfactory. Besides, most of the instructions of a normal CPU take more than one clock cycle to be executed.

On the other hand, a DSP is much faster than the normal CPU at multiplications and floating point calculations. It has a hardware multiplier built in and can perform one multiplication in parallel with some other operations in one clock cycle. If a DSP supports floating point operations, it can perform all above operations in floating point format without requiring any extra time. But the problem of most DSPs, including the NEC 77230, is that they are designed specifically for digital signal processing. The architecture of these DSPs is optimized to best conduct digital filtering, DFT, FFT as well as other digital signal processing algorithms. The result of such optimization is that these DSPs are weak in the areas where the normal CPUs are strong, such as interrupt handling, structured data manipulation and logical operations.

By including two powerful chips, the AMPS board is able to utilize the strength of both chips and avoid their weaknesses. At the time when the IGPS project was started, it was very powerful compared to some other boards, and more importantly it cost only about $1,500/board to build. It was chosen to implement the first prototype of IGPS, as it met the two main considerations in selecting a hardware platform for the IGPS.

The AMPS board does not have network capability, but can communicate with a PC through its serial port. The PC functions to provide man–machine interface and store fault records for the original AMPS board. As the main objective of building up a prototype is to verify the computation power required by the IGPS, this structure does not greatly affect the results of this feasibility study. But the network capability should be considered in the future development of a practical IGPS.

8–3 Structure of AMPS hardware

Figure 8.3.1 shows the functional diagram of an original AMPS board. It is divided into two major parts: the DSP part and the main CPU part. The dual port RAM links the DSP and the main CPU so that preprocessing data can be passed from the DSP to the main CPU. The input circuit is controlled by the DSP, while the multi–function interfacing chip MC 68901 is controlled by the main CPU.

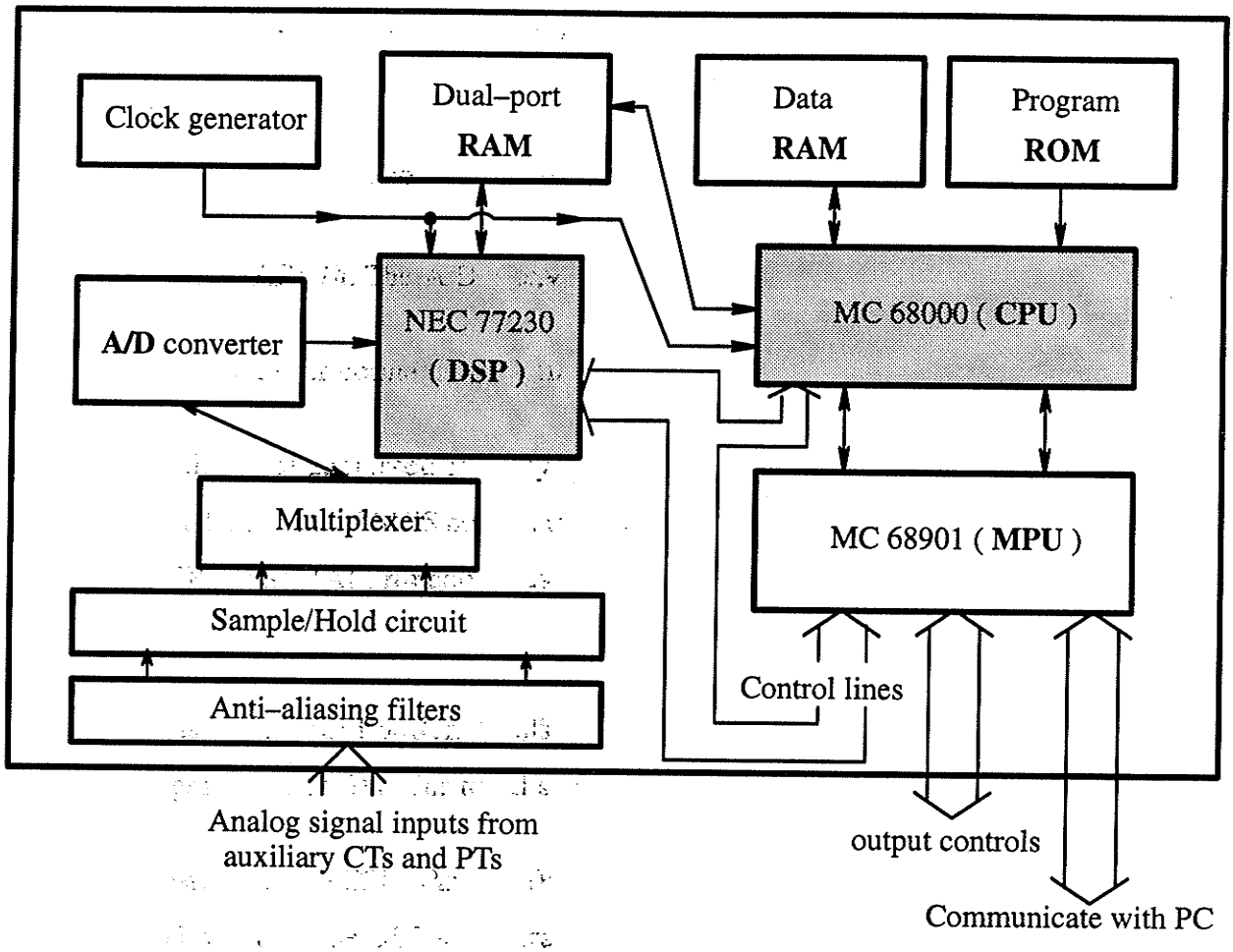

Fig. 8.3.1 Block diagram of AMPS hardware structure

The basic functions of these blocks are as follows:

(1) NEC 77230 (Digital Signal Processor): This is the first commercially available DSP having floating point operation capability. All instructions are executed in one main clock cycle of 150 ns (6.6 MHz clock speed). It can perform one 32 × 32 bit floating point multiplication along with a 32 bit floating point addition/subtraction, as well as other operations in parallel in one instruction. Depending on the instruction executed, up to 11 operations can be performed in one instruction. It can handle only 2 interrupt inputs, one is maskable and one is not. There is no built–in stack mechanism for interrupt handling. The chip comes in two versions, one is programmable with a built–in EPROM and another one is not programmable but has a built–in library of subroutines in its on–chip ROM.

(2) MC 68000 (Central Processing Unit): This is a true 32–bit common CPU. It can perform 32–bit fixed point addition/subtraction and multiplication/division, logical operations, and some other operations. One instruction can only accomplish one operation, and usually takes more than one CPU clock cycle to finish its execution (a multiplication/division takes more than 10 clock cycles to finish). It has a versatile addressing system supporting different addressing modes, and a strong multi–level interrupt handling system. Its clock speed was 6.6 MHz in the original original AMPS board, but was changed to 11 MHz in the first prototype of IGPS.

(3) MC 68901 (Multi–function Peripheral Unit): This chip provides a number of functions. It has an internal interrupt controller which can prioritize 16 interrupt inputs and send a corresponding interrupt request to one of the seven MC 68000 interrupt levels to which it is connected. It also has an 8–bit general purpose input/output interrupt port which may be operated as either inputs or outputs under software control. These input/output lines may optionally generate an interrupt on either a positive or a negative transition of the input signal. Four 8–bit timers are provided in the chip, which can be used to generate periodic interrupts, measure elapsed time, and count signal transitions. Two of them also have waveform generation capability. A universal synchronous/asynchronous receiver–transmitter (USART) is built into the chip. It is a single full–duplex serial channel with a double–buffered receiver and transmitter. This chip provides the necessary interfacing functions for the main CPU. The serial communication link between the board and a PC is also provided by this chip.

(4) Anti–aliasing filters: These are low–pass filters. They are used to filter out high frequency harmonics and white noise. According to the Nyquist Theorem, the sampling frequency must be twice as high as or higher than the highest frequency component contained in the signal. Else, frequency aliasing will occur.

(5) Sample/hold circuit: To reduce the cost, only one A/D converter is used. This circuit allows all signals to be sampled at the same moment, which is very important for obtaining the

correct phase angle relationships between different signals. The sampled signals are held until converted by the A/D converter one by one.

(6) Multiplexer: Used to select one input signal at a time to connect to the A/D converter.

(7) A/D converter: This is a 12 bit A/D converter AD574. The A/D conversion time is 12 μs.

(8) Clock generator: It generates a proper clock pulse for normal functioning of DSP and CPU.

(9) Dual–port RAM: This is a fast RAM which can be addressed both by the DSP and CPU. It serves as the external RAM for the DSP. In the original AMPS board, this RAM is also used as the DSP's program RAM. As for the CPU, this RAM functions as a normal RAM. The size of this RAM is 8 kB.

(10) Data RAM: Most of its space is used as fault record buffer. It also provides space for communication buffers and the CPU program's variables. The total space of it is 64 kB.

(11) Program ROM: In the original AMPS board, both the CPU's and DSP's program are stored in this ROM. At power up, the main CPU will load the DSP's program into the dual–port RAM and start running the DSP. In the first prototype of IGPS, the DSP's program has been put into the DSP's own on–chip EPROM, so that only the main CPU's program is stored in this ROM. The size of this ROM is determined by the ROM chips to be used. The size of it could be 8 kB to 32 kB.

The original AMPS board was designed to divide the pre–processing and main algorithm calculations between the DSP and the main CPU. To understand the functioning of each part, let us first look at the normal process of IGPS relay shown in Fig. 8.3.2.

In the Fig 8.3.2, the first three processes are called preprocessing. The purpose of preprocessing is to convert input signals into the required data format which can be used by the relay algorithms. As shown in the Fig. 8.3.2, these processes must be done before their results can be used by relay algorithms, thus the name preprocessing. The preprocessing and the computation of relay functions can only be done sequentially.

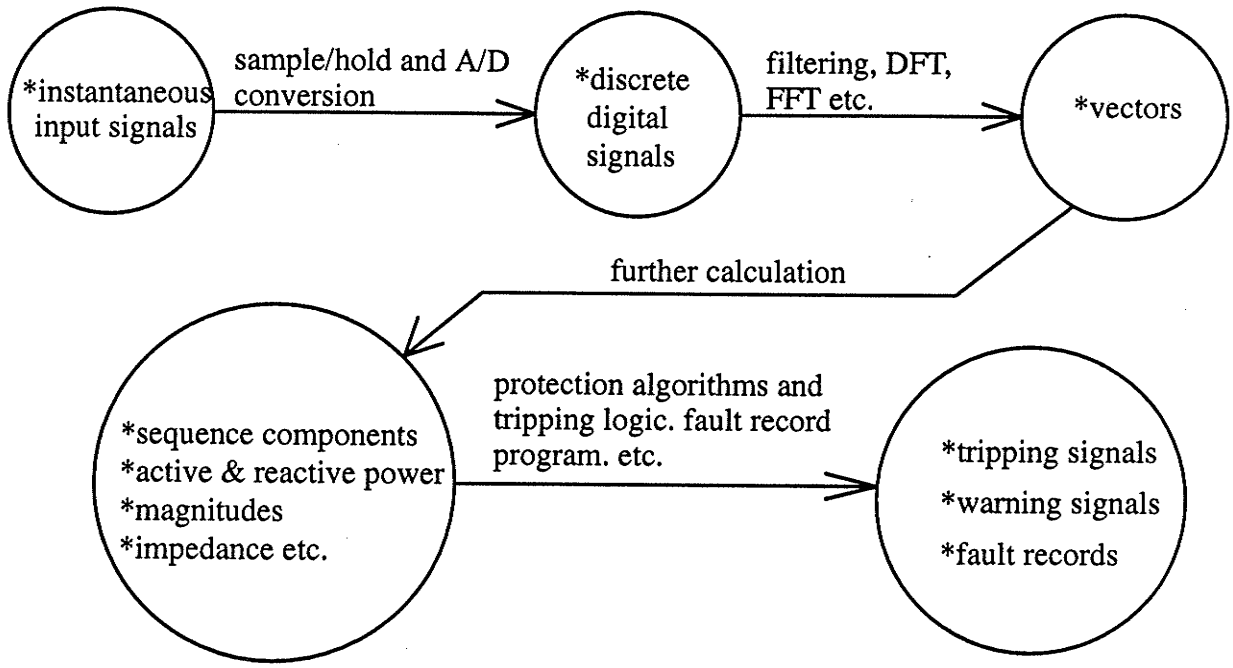

Fig. 8.3.2 Flowchart of normal program procedure

In a digital protection scheme or system, the preprocessing is the most time consuming part of the whole program. This is because filtering, DFT, FFT, magnitudes, sequence components calculations as well as other calculations involve extensive numerical operations, especially multiplications, divisions, square–root operations, and triangle function calculations. After the results of preprocessing are obtained, most of the protection functions may only involve simple comparisons of measured electrical quantities with stored settings and some logical operations, thus require very little time.

The original AMPS board design emphasizes separating the time consuming preprocessing part from the main protection functional part. This is due to the fact that the DSP is generally good at numerical calculations and the CPU is generally good at comparison and logical operations. The above processes shown in Fig. 8.3.2 are divided as follows in the first prototype of IGPS.

The DSP chip controls the A/D conversion and performs all the preprocessing. The task of frequency tracking was also done by the DSP chip because the anti–aliasing filters and the Sample/Hold circuit are under its control.

The main CPU MC 68000 was used to implement the protection and monitoring functions as well as fault record function. It also sends out control signals for tripping and warning, and controls other peripherals to communicate with the outside world such as a PC.

The DSP and main CPU programs are run independently. The data exchange is through dual–port RAM and it is initiated by the interrupt signals. The preprocessing results are put into dual–port RAM by the DSP after it finishes the calculations, and an interrupt signal is sent to the main CPU to inform it that data is ready. The main CPU responds to the interrupt signal by reading data from the dual–port RAM into normal data RAM, and then performs protection and monitoring functions as well as the fault record function on these data.

8–4 Modifications of original AMPS board

The initial goal for the first prototype of IGPS is to use a 32 point/cycle sampling rate, so that a 32 point FFT can be conducted on each of 11 input signals to obtain up to the 15th harmonic. Also all the computations, including preprocessing and protection algorithms calculations, were hoped to be updated at a rate of at least 1/4 cycle, preferably 1/8 cycle in the system operating frequency range of 45 – 90 Hz for fast response of the system.

An original AMPS board was wire–wrapped at the beginning of the project, based on the original AMPS board design. After the project was started, it was soon found that the original AMPS board, though it is powerful, is not powerful enough to accomplish all the tasks with above specifications. Efforts were made in the hardware modifications and software optimizations to further enhance the capabilities of the original AMPS board. The following details the main modifications to the original AMPS board. The software optimizations will be presented in the next chapter.

(1) Use programmable NEC 77230 chip instead of non–programmable one. The original AMPS board uses a non–programmable NEC 77230 chip to reduce the cost of building such a board. The non–programmable NEC 77230 chip comes with a preprogramed subroutine library in the non–programmable ROM inside the chip, which can be called by the user programs in the external memory. No user program can be stored in the chip. For the programmable NEC 77230, it has a programmable EPROM which does not contain the subroutine library. The

user program can be stored in the EPROM of the chip. Because the data read/write and the external instruction fetch both use the DR (data register) and AR (address register) of the NEC 77230, the execution of a non–programmable NEC 77230 is much slower than that of a programmable one and it was therefor replaced by a programmable NEC 77230.

(2) Make non–maskable interrupt input of NEC 77230 maskable. A major drawback of NEC 77230 is that it does not have a "stack" mechanism that most common CPUs have for interrupt handling. It only has two interrupt inputs, one is maskable and another one is not. Without stack, the non–maskable interrupt can not be used for common purposes but only for fatal failure handling. IGPS project needs to use at least two normal maskable interrupts to run the program more efficiently. A small circuit was added to the original AMPS board to make the non–maskable interrupt input become maskable.

(3) Raise main clock speed of the MC 68000 from 6.6 MHz to 11 MHz. In the original AMPS board, the MC 68000 shares the same system clock at 6.6 MHz with the NEC 77230 to simplify the circuit design. 6.6 MHz is the maximum speed the NEC 77230 DSP can run. But for the MC 68000, it could be run up to 12 MHz. It was found that 6.6 MHz is not sufficient for the MC 68000 to perform all the tasks required for IGPS. Another clock circuit was successfully added to the board to make the MC 68000 run at 11 MHz clock.

Besides the speed increasing enhancements, some other changes were made to the original AMPS board to improve its functionality. These changes include adding a battery–backed RAM with a time–keeper, and a protection operating status displaying circuit.

The battery–backed RAM is used to store settings of protection functions and some other important data. This simplifies the power–up process of the first prototype of IGPS and allows it to be operated more independently. The settings of the protection functions in IGPS need to be changed from time to time. It can not be put into the built–in EPROM of the DSP chip as this will require the EPROM to be re–programmed every time a setting needs to be changed. Putting these settings in normal RAM or dual–port RAM will require the PC to send correct settings to the board every time the system is powered up. This requires a PC always linked to it when it is powered up. The battery–backed RAM solves this problem.

The battery–backed time–keeper enables the first prototype of IGPS to keep an accurate time without getting it from the PC. In the original AMPS board, the date and time has to be sent by the PC to the board every time it is powered up, else it will have wrong date and time tagged to the fault record. Adding a battery–backed time–keeper solves this problem.

The original AMPS board does not have any display circuit for displaying protection function status. It is not convenient to conduct debugging and tests for the first prototype of IGPS without the protection status displaying circuit. The operations of different protection functions would have to be checked by examining the fault records, which is not easy to do without proper software support. Even with some powerful fault record displaying software, it is still fast and convenient to use a status displaying circuit while conducting the tests, as during the tests the most important thing to know is if the system correctly responds to the different faults.

The added protection status displaying circuit uses LEDs to display operating status for all the protection functions implemented in the first prototype of IGPS. For protection functions operated on each phase, additional status displaying LEDs were used to indicate the operating status for each phase of this protection function.

Though the hardware modifications and the software optimizations increased the capabilities of the original AMPS board substantially, the modified original AMPS board is still short of the power to accomplish all the tasks of the IGPS with the original specifications, particularly for the DSP chip. Fig. 8.4.1. illustrates the problem.

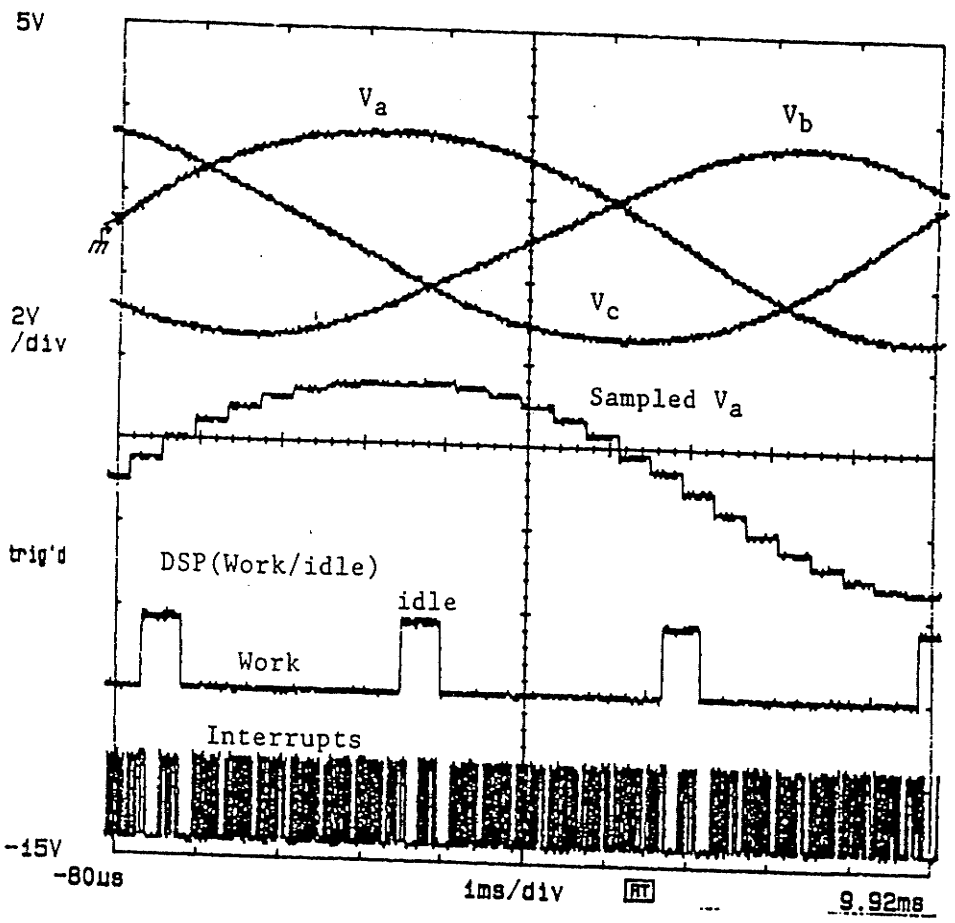

SAMPLING RATE: 32 points/cycle
UP-DATED: every 1/4 cycle
CALCULATED: 32-point FFT for all signals;
sequence components, Ps, Qs, Rs and Xs;
up to 3rd harmonics magnitude for Va,Vb, Vc and Vo;
up to 2nd harmonics magnitude for If;
only fundamental magnitude for all other signals.
RECORDED AT: f = 80 Hz

Fig. 8.4.1 Recorded DSP timing of modified AMPS board at 32 sample/cycle, f=80Hz

In the Fig. 8.4.1, the top set of three traces are the three phase voltages with the sampled version of one of the voltages just below (4th trace). The 5th trace shows the time during which the DSP is calculating (low) and the time to spare before the next set of calculations. The bottom trace is the

interrupt pulses which are generated each time a sample value is brought in from the A/D converter. Note that only the fundamental component's magnitude of all signals are calculated, except the three phase terminal voltages (Va, Vb and Vc), the neutral voltage (Vo) and the field current (If) for which up to 2nd (If) or 3rd (Va, Vb, Vc and Vo) harmonics magnitudes are calculated. This means that the harmonics monitoring function will not be able to be implemented. The waveform is recorded at the system frequency of 80 Hz. Even with the tasks reduced, the DSP chip is still short of the power to work properly to cover an upper frequency of 90 Hz. It can only run properly up to 86 Hz which is below the desired upper frequency limit.

It was found that reducing the sampling rate to 16 points/cycle and using an updating rate of 1/4 cycle will allow all required protection functions of IGPS to be performed. This can be seen clearly from the Fig. 8.4.2 which shows another recorded DSP timing with 16 samples/cycle sampling rate. The DSP chip now can perform all required calculations and work properly up to f = 98 Hz at the updating rate of 1/4 cycle. This sampling rate and the updating rate are thus adopted in the current IGPS prototype..

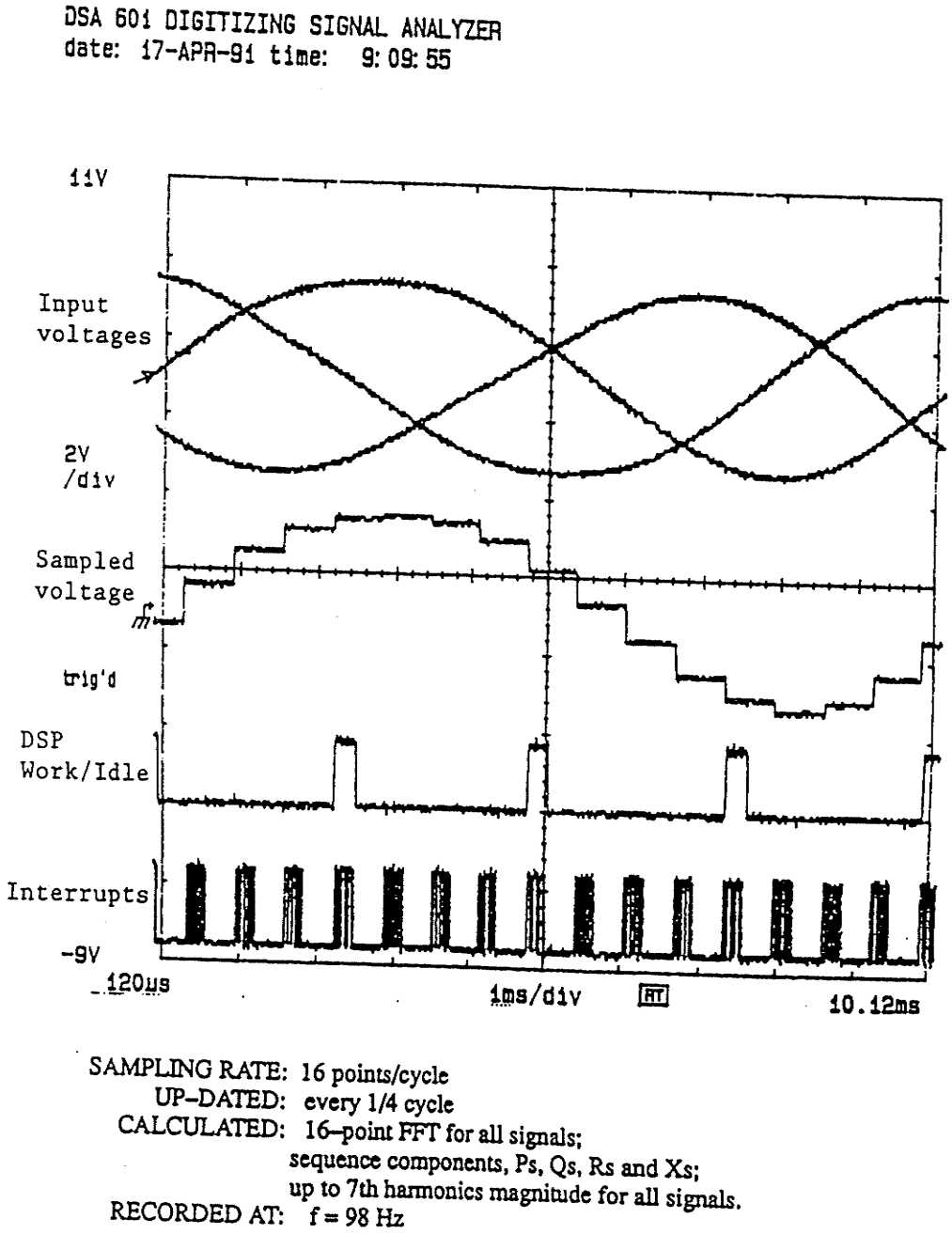

Fig. 8.4.2 Recorded DSP timing of modified AMPS board at 16 sample/cycle, f=98 Hz

The reduction of sampling rate does not affect the implementation of IGPS protection functions except for the harmonics monitoring function, which is partially affected. With a 16 point/cycle sampling rate, only up to the 7th harmonics can be obtained. The software structure is

not greatly affected by the sampling rate reduction either due to the following facts: (1) The FFT subroutine can be used by either a 16 point or a 32 point FFT. This is because the FFT subroutine is designed to be used by the FFTs with the number of input points being a power of 2. (2) Other sampling rate related calculations, such as harmonics magnitude calculation, are all designed to have two cascaded loops. The inner loop is the same for all harmonic components and the outer loop controls how many harmonics are to be calculated. Thus it can be easily adjusted to different sampling rates. In fact, the software development is started using a 32 point/cycle sampling rate but later changed to use the sampling rate of 16 point/cycle.

With all the hardware modifications and software optimizations, as well as the changed sampling rate, the modified original AMPS board now offers the following capabilities for the first prototype of IGPS:

In the DSP part, it can sample up to 16 input signals at the rate of 16 points/cycle; it can perform a 16 point FFT on up to 12 input signals; it also can calculate other quantities using the FFT results, such as magnitudes of harmonic and fundamental components, sequence components, active and reactive powers, and impedances. All the calculated results can be updated every 1/4 cycle in the system operating frequency range from 45 to 90 Hz.

In the main CPU part, it can transfer all the results from dual–port RAM to its own RAM, perform all seven main protection and monitoring functions, harmonics monitoring function (up to 7th harmonics)self–excitation protection function as well as fault record function in 1/4 cycle in the system operating frequency range from 45 to 90 Hz. It also communicates with a PC to receive settings and send fault records while performing above tasks.,

Other than the AMPS board modification and the software optimization, the modified AMPS board, the auxiliary PTs & CTs and the power supply of the system were all put into two metal boxes for easy test and field installation.

8–5 Selecting a more powerful hardware platform for future IGPS

Although the modified original AMPS board is more powerful than the unmodified one, the implementation results show that it still lacks the required power to achieve the initial goal for a

practical IGPS. A more powerful hardware platform is needed for developing a practical integrated generator protection system.

The implementation experience of the first prototype of IGPS provides a good basis in selecting a new platform. In selecting a new platform for IGPS, the most important thing is to determine how much computation power is needed for a practical IGPS while keeping the cost at the same level.

To achieve the initial goal for the first prototype of IGPS requires a hardware platform having at least four times the computation power as the modified original AMPS board. With this power, a 32 point FFT on each of the input signals can be performed and all the results can be updated in less than 1/8 cycle.

The computation power required for FFT calculations is roughly in proportion to the number of input data points to be transformed. That is, a 32 point FFT requires double the computation power of a 16 point FFT. As the FFT calculation is the most time consuming part among all other computations, and some other computation, such as the harmonic magnitude calculation, will also be doubled when a 32 point FFT is used, a doubled computation power is needed so that 32 point FFTs can be performed on all input signals.

It is obvious that to increase all computation results updating rate from 1/4 cycle to 1/8 cycle, the computation power must be doubled.

However, a new hardware platform for a practical integrated generator protection system requires more computation power as outlined above because of the following facts.

One fact is that the number of input signals could be well over 11, which is the number of input signals used by the first prototype of IGPS. In one generator protection system example described in [4],a total of 36 input signals are used. This does not mean three times the power is required, because most of the added signals in the above example may not require harmonics monitoring, thus less time consuming DFT can be used instead of using FFT. While the above example is an extreme case, a further doubling of the power may still be a proper hardware

requirement for accommodating more input signals into a practical integrated generator protection system.

Another fact is that in the first prototype of IGPS, only main protection and some special protection functions have been implemented. There are many other optional and special protection functions which also need to be implemented for a practical integrated generator protection system. A conservative estimate is that the number of protection and monitoring functions will be double the number of that implemented in the first prototype of IGPS. However, this does not require doubled computation power for doubled number of protection functions, as protection algorithm calculations use less time than preprocessing and the computation power required by the protection function does not increase with the increase of sampling rate.

Besides the protection and monitoring functions, the run–time self–monitoring function is a must–have function for any practical digital protection system. This function has not been implemented in the first prototype of IGPS. But the computation power needed by this function should be considered when selecting a new hardware platform for a practical IGPS.

Plus, if network capability is provided to a practical integrated generator protection system, it also requires some more computation power to handle the data transfer.

Also as an integrated protection system, one of its goals is to solve the problems of existing protection systems in modifying and adding new functions. It requires some computation power to be reserved for the future modification and addition of new protection functions.

With all these factors counted, at least another 2.5 times power or more is required on the top of the quadrupled power just discussed. That means at least 10 times the computation power of the modified original AMPS board is required for a practical integrated generator protection system. If high level programming languages, such as C, are to be used for developing a practical IGPS, even more powerful hardware will be required (at least twice as powerful as the one using Assembly language, since the program code generated by a high level language compiler is not as efficient as that written in the Assembly code).

In the past ten years, the computation power of a single chip CPU or DSP has been doubled in every 2 – 3 years, while the price for single chip did not increase in proportion to its computation

power but only increased slightly. If this trend holds, in 3 – 4 years from now (the original AMPS board was built in 1989), a board containing one CPU and one DSP could have 10 times the power of the modified original AMPS board, and its cost could be expected to be at the same level. At that time, a practical integrated generator protection system will become a reality.

It is possible to obtain the required computation power now by using parallel processing techniques, though it will cost more to build such a board and the hardware as well as the software will be more complicated than a non–parallel processing one. If the cost increase is acceptable, this could be another option. But this option should be evaluated very carefully, especially the extra development efforts involved in it, as the hardware and software structures become more complicated. This problem needs more studies and will not be further discussed in this thesis.

CHAPTER 9

IGPS SOFTWARE

9–1 Introduction

The software of a digital protection system typically consists of these programs: main program including preprocessing, protection and fault recording functions; man–machine interface program for changing the settings of protection functions, testing and diagnosing the system; run–time self–monitoring program; as well as fault record analysis programs.

Among them, main program and man–machine interface program are the core programs which make the digital protection system hardware work. The main program is presently dominantly programmed using Assembly language to achieve high efficiency, due to the fast response time requirement (in the range of several milliseconds to several tens of milliseconds) and the limited computation power of present hardwares. The man–machine interface program allows relay engineers to easily interact with the main program in changing the the settings of protection functions, testing the system and diagnosing the problems of the system.

The run–time self–monitoring program is a must–have program for any practical digital protection system, which ensures reliable operations of the system. It is not implemented in the first prototype of IGPS. Building–up a prototype is mainly to verify the feasibility, especially the computation power, of the hardware being used. The run–time self–monitoring program runs at the lowest priority in the background, and uses very little computation time. Without this program, the results of the verification would not be greatly affected.

Fault analysis programs, which may range from a very simple fault record print–out program to a complicated fault waveform display and analysis software, are very important for post–fault analysis and protection system performance evaluation. It is also important for a prototype system, as it provides a useful tool for debugging programs and facilitates the test of the system.

9–2 Overall software structure of the first prototype of IGPS

The overall software structure for the first prototype of IGPS is mainly determined by the hardware structure of the modified original AMPS board. As there is no on–board man–machine

interface circuit provided for the AMPS board, its man–machine interface is provided by a serial communication port which links the board to a PC and a man–machine interface program which runs on the PC.

The main program for the first prototype of IGPS consists of two parts: Assembly language preprocessing program for the NEC 77230 DSP chip, and Assembly language protection and fault record program for the MC 68000 main CPU chip. The man–machine interface program is programmed in TURBO PASCAL running under MS DOS on a PC. The fault record analysis program is an MS Windows program written in C using BORLAND C++ 3.1.

Except for the fault record analysis program, which is used independently, the other programs are interacting with each other while performing their specified tasks. The main tasks of these interacting programs and their relationships are shown in Fig. 9.2.1.

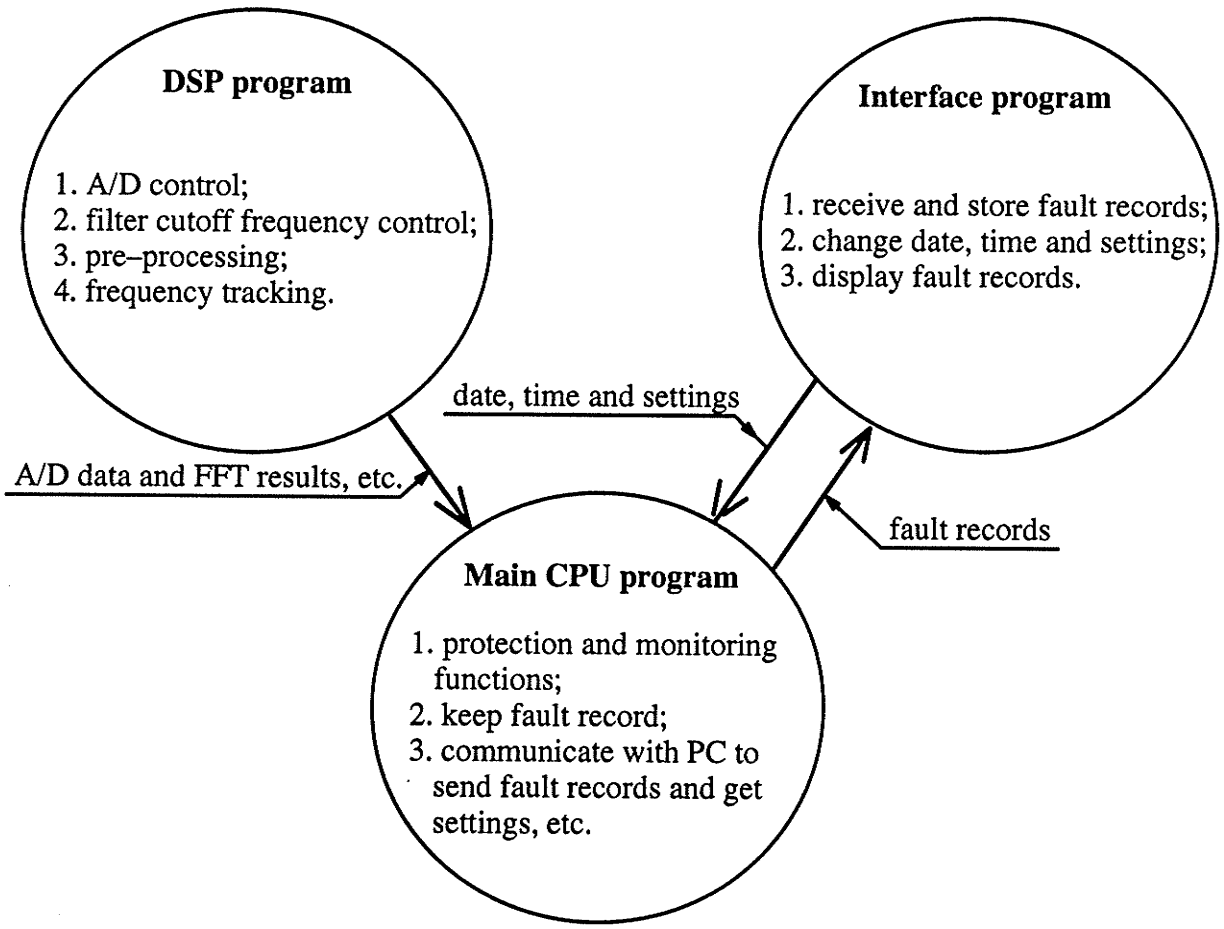

Fig. 9.2.1 Functions and relationships of IGPS programs

As Fig. 9.2.1 shows, the DSP program controls the A/D conversion and the cutoff frequency of anti–aliasing filters, performs pre–processing, such as FFT, sequence component calculation, etc., on the converted A/D data and keeps tracking the system frequency. It stores digitized input signals' data (by A/D conversion) and the preprocessing results in dual–port RAM for retrieval by the main CPU program.

The main CPU program performs several important tasks of the IGPS. It reads data from the dual–port RAM and performs all the required protection and monitoring functions once every 1/4 cycle. It constructs the fault record when there is a fault for post–fault analysis and the performance evaluation of the IGPS. It also communicates with the PC to send fault records and receive protection function settings.

The man–machine interface program on the PC has two main tasks. It provides the interface for changing the settings of protection functions as well as the date and time of the AMPS board. It also receives fault records from the AMPS board and stores them to the disks for later post–fault analysis and system performance evaluation.

As has been described in the previous chapter, to be able to accomplish major protection functions, the first prototype of IGPS uses a 16 point/cycle sampling rate, performs a 16 point FFT on each of 11 input signals and updates all results in every 1/4 cycle.

9–3 Main preprocessing and relay programs

The main preprocessing and protection program, as mentioned above, consists of two programs. One is the preprocessing program running on the DSP and the other one is the protection function program running on the main CPU. Both programs are programmed in the Assembly language to achieve the highest efficiency.

Major efforts were made to optimize these two programs, particularly the DSP program. Without the optimization, it would be impossible for them to accomplish their tasks on the modified AMPS hardware.

9–3–1 Assembly language preprocessing program for the NEC 77230 DSP

This program performs the most time consuming preprocessing computations for the first prototype of IGPS. The main tasks of this program are controlling input signal sampling and A/D conversion, preprocessing and frequency tracking.

It controls the sampling and A/D conversion of all 14 input signals (the terminal three phase currents have dual ranges to accommodate wide dynamic range requirement). The sampling rate is 16 point/cycle. After the A/D conversion, the dual–ranged terminal currents were autoscaled to become one scale thus reducing the number of the input signals to 11.

A 16 point FFT was conducted on each of the 11 input signals. The results of the FFT are used to calculate the magnitudes of fundamental and harmonic components, sequence components, active and reactive powers, as well as impedances. All preprocessing results are converted from the floating–point format to the fixed–point format before they are stored in the dual–port RAM for passing to the main CPU. The float–to–fix conversion is necessary as MC 68000 can handle only fixed point data. Also the float–to–fix conversion is more efficient in DSP (one instruction) than in main CPU which needs a subroutine to do the same job.

Once every system cycle, the frequency tracking subroutine was called to synchronize the sampling frequency with the system frequency, so that exact 16 point/cycle sampling rate can be maintained.

As mentioned before, all these preprocessing calculations should be done within 1/4 cycle with the maximum system frequency up to 90 Hz. At 90 Hz, the maximum time available for all preprocessing calculations including sampling and A/D conversion of 14 input signals in 1/4 cycle is only 2.78 ms. With 150 ns execution time per instruction, a total of 18533 instructions could be executed in this time period.

Though the NEC 77230 is very powerful, and using a programmable NEC 77230 further increased its power, the program will still have difficulties to finish all the calculations in 1/4 cycle at 90 Hz if the software is not optimized. Several programming and algorithm optimization techniques were used which make the program able to run properly at 90 Hz system frequency.

(1) Use of A/D conversion time. The A/D conversion time of the AD574 chip used on the AMPS board is 12 μs. In 12 μs, 80 instructions can be executed in the DSP. Selecting input signal channel, starting A/D conversion and reading back converted data use only an average of 10 instructions/channel. If pooling method is used, more than 80% (70/80) of the time will be wasted in waiting for converted data to become ready.

In the first prototype of IGPS, the interrupt method is used. Using the interrupt method, the program reads converted data and starts conversion of the next channel only when an interrupt signal indicating "converted data ready" is received, so that no time will be wasted in waiting. Adding the overhead of interrupt handling, an average of 30 instructions/channel is needed every time the interrupt subroutine is called. To be able to use the interrupt method, a small circuit was added to the original AMPS hardware to change the non–maskable interrupt input to a maskable one, which has been described in the previous chapter.

The time saved is significant. With 4 samples taken in every 1/4 cycle on 14 input signals, $4 \times 14 \times (80 - 30) = 2800$ more instructions can be executed in the 2.78 ms period, which is about 15% (2800/18533) improvement at 90 Hz system operating frequency.

(2) Maximize the use of internal RAM. For the DSP NEC 77230, reading/writing data from/to external RAM (i.e. dual port RAM) will take 4 to 5 instruction times compared to one instruction time required for reading/writing data from/to internal RAM of the DSP. In IGPS, some intermediate preprocessing results (such as FFT vectors), which are used by some later preprocessing calculations (such as powers, impedances etc.), are also used by the protection functions of the main CPU directly. If these results are stored in dual–port RAM after they are obtained, then the later preprocessing calculations would have to retrieve them from the dual–port RAM, which is very time consuming.

Similar efforts were made in programming DSP subroutines. As long as internal RAM space is available, the intermediate results which are required both by main CPU and the later calculations are stored into internal RAM at the same time when they are stored into dual–port RAM. No extra time is needed by doing so as the DSP can perform both storing operations in parallel. Applying the above technique speeds up the subroutine's execution considerably by saving the time in reading

back intermediate data from the external RAM. This technique results in about another 10% improvement.

(3) Perform two input signals' FFT in one FFT calculation. The FFT calculation on all 11 signals is one of the most time consuming parts of this program. An optimization technique described in section 3.6 is used in the first prototype of IGPS. It fully uses the properties of an FFT when it is applied to pure real data set or pure imaginary data set. With this technique implemented, two signals' FFT results can be obtained by only performing one FFT calculation.

When the above method is utilized, the calculation of 11 FFTs is reduced to 6 FFTs plus the conversion processes which only involve addition/subtraction operations. The improvement is significant. For a 16 points FFT, the time used by the above method is 15% less than that of the two direct FFT's. For the 32 point FFT, it uses 30% less time.

With all the above optimization, the DSP program can perform not only its main control functions and FFT calculations, but also some further calculations such as impedances and sequence components, which were originally assigned to the MC 68000 program.

9–3–2 Assembly language 68000 relay program

The 68000 program has three major tasks: reading data from dual–port RAM and performing desired protection and monitoring functions of IGPS; keeping fault records and communicating with the PC to send fault records and get date, time and settings.

The structure of the 68000 program is more complicated than that of the DSP program. It fully uses its powerful multiple interrupts handling system to make it perform all three tasks more efficiently.

The main program loop, which has the lowest priority, constantly checks its receiver buffer and transmitter buffer to see if there is any command received from the PC or there is any fault record waiting to be transmitted to the PC. When it finds a predefined command, it will jump to the appropriate subroutine to perform the corresponding task, such as receiving new date and time, or receiving new settings of protection functions. Or it will send the fault record to the PC if it finds one.

All the data received from the PC and the data sent to the PC are first put into receiver buffer and transmitter buffer respectively. The communication subroutines, which are interrupt driven, perform the actual transformation. The interrupt signals of these subroutines are assigned the highest priority level to ensure that no single byte will be missing during the transferring.

The data reading and protection functions subroutine was started by an interrupt signal from the DSP. Each time the DSP has finished one preprocessing process, it will send a "data ready" signal to interrupt the main CPU. Upon receiving the interrupt request, the main CPU first reads data from the dual–port RAM and puts these data into its own RAM, then performs all protection and monitoring functions. The priority level of this interrupt is higher than the main program loop but lower than the communication interrupts.

The data reading part supplies data both for constructing the fault records and for comparisons with the settings of the protection and monitoring functions.

A multiple circular buffer structure was used in this program for fault recording. The fault record buffers can hold up to two fault records in the data RAM at the same time. This allows the CPU to construct another fault record while it is in the process of transmitting a previously constructed one. At any time, only one buffer is "active" for the CPU to construct a fault record. When there is no fault, every time the data reading and protection function subroutine was executed, the oldest data in the active buffer will be replaced by the newest data. If a fault occurs or a "T" (Test) command is received, the subroutine will continue to store fault data into the buffer until a complete fault record is constructed with the specified lengths of pre–fault and post–fault data. Then the main CPU will switch to another circular buffer and leave this buffer for fault record transfer.

The protection and monitoring function part will start to work after the data reading. Currently, seven main protection and monitoring functions, which are described in Chapter 2, as well as the harmonics monitoring and the self–excitation protection function, are implemented in the first prototype of IGPS. The implementation details, though important, are omitted here as they are less related to this research's objectives.

9–3–3 Fault record structure

The current design of fault record structure for the first prototype of IGPS aimed for easy fault record construction as well as the post–fault analysis and its system performance evaluation.

A fault record contains digitized input signals, time and date when the fault record was taken and the protection operating status just as the fault record functions in other digital relays. It also includes two more data types.

Some intermediate and final computation results are included in the IGPS fault record. These data are included mainly for system performance evaluation and program debugging purposes. It has been found that this information is very useful in finding programming mistakes and some hard–to–find run–time bugs, as some software bugs only occur under certain conditions and thus are very difficult to find by examining the program.

The protection settings at the time when a fault occurs are also included into the fault record. This is an important feature as protection settings may change from time to time, especially during the prototype tests where the settings could be changed constantly for different test cases.

The structure of the fault record for the first prototype of IGPS is shown in the Fig. 9.3.3.1. All data are stored in binary format and each fault record has a size about 32 kB.

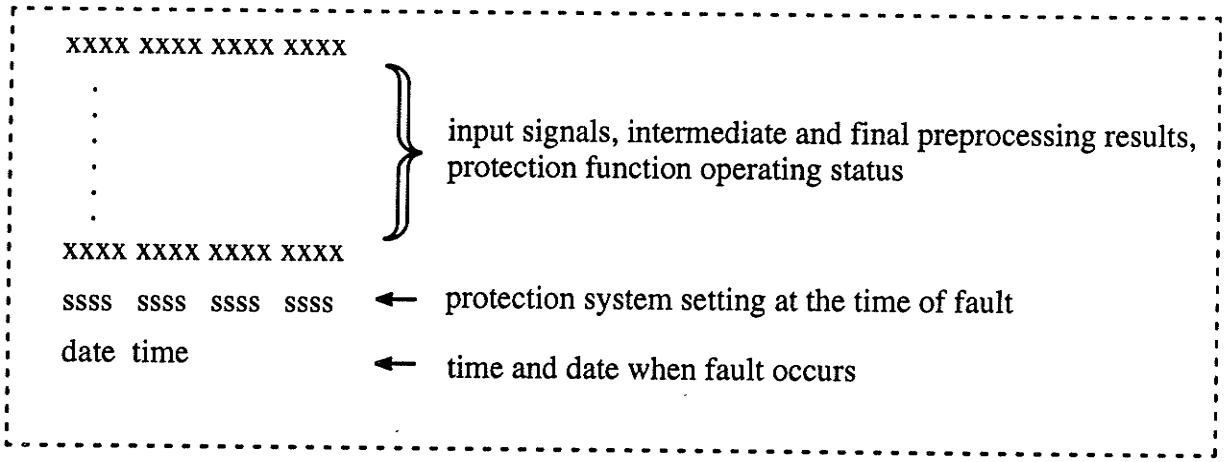

Fig. 9.3.3.1 Fault record structure of the first prototype of IGPS

The present fault record in the first prototype of IGPS consists of 2 pre–fault cycles and 14 post–fault cycles. The length of fault record can be increased to total 64 cycles if only input signals

and protection operating status are recorded. This is because the intermediate and final preprocessing results can be removed from the fault record after the system debugging and testing are finished.

9–4 Man–machine interface program

The man–machine interface program which interfaces operators with the AMPS board is a PASCAL program run under the MS DOS operating system on a PC. It allows the operator to check and change the settings of protection and monitoring functions on the AMPS board, and also allows the operator to set the date and time of the AMPS board. It automatically receives the fault records from the AMPS board and stores them permanently on the PC's hard disk for post–fault analysis and performance evaluation of the protection systems.

The design of this program aimed to provide a basic and easy–to–use man–machine interface. The program uses a multi–level menu–driven structure. The use of a multi–level menu is due to the fact that the protection function settings adjustment involves multiple protection functions and a sub–menu is needed to select the protection function whose settings need to be adjusted.

When the program is started, it always displays the main menu. Under this menu, four commands can be chosen. The four commands are "C" for "send PC's date and time to AMPS board", "S" for "change settings and send them to AMPS board", "T" for "test AMPS board" and "Q" for "quit the program". The total number of fault records received by the program since it started running is also displayed at the upper left corner of the screen.

Under the main menu, when the "C" command is issued, the current PC's date and time will be sent to the board to update the date and time on the board. If the "T" command is issued, the AMPS board is asked to send back a testing fault record to see if the board is functioning properly. If the "Q" command is issued, the program immediately terminates its execution and exits to DOS.

When the "S" command is issued, a "setting adjustment sub–menu" will pop up to display all the protection and monitoring functions implemented in the first prototype of the IGPS as shown in Fig. 9.4.1.

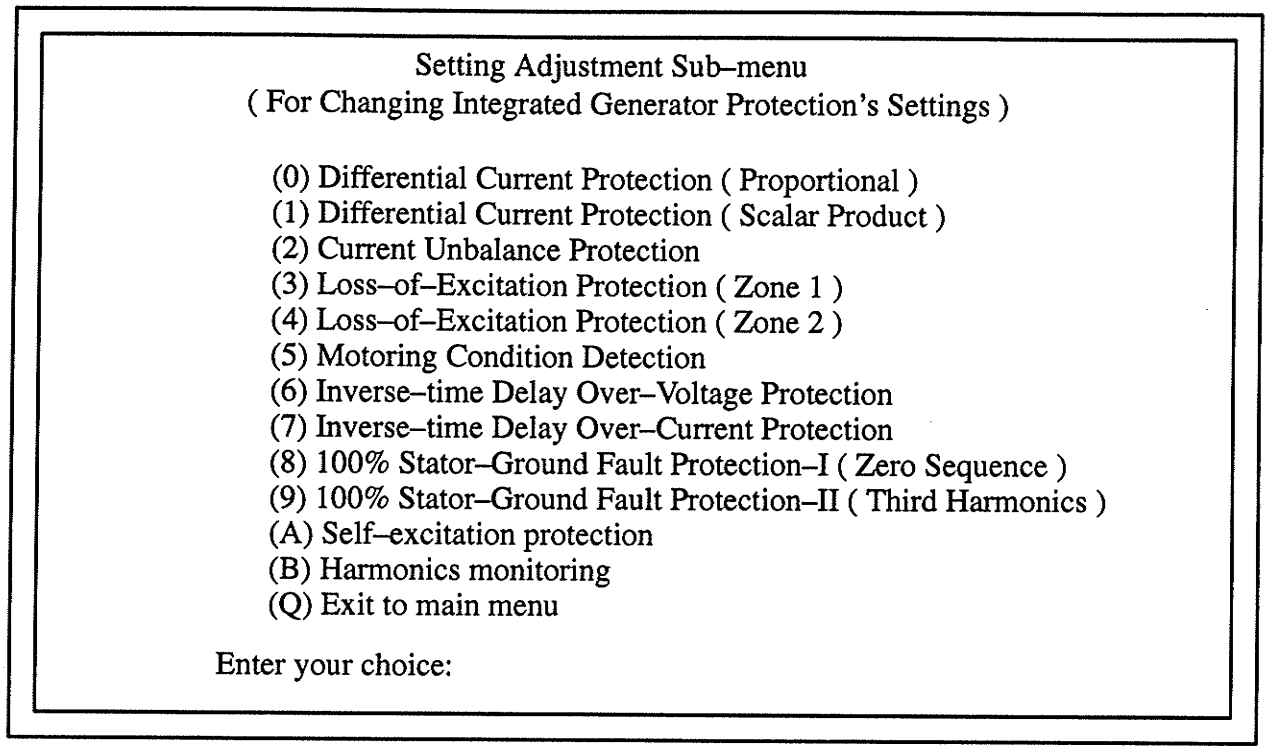

Fig. 9.4.1 Setting adjustment sub–menu screen

From the "setting adjustment sub–menu", any protection function, for which the settings need to be checked or changed, can be selected by typing in the number or letter of that function displayed on the screen. If the "Q" key is pressed, the program will send the changed settings to the AMPS board before it returns to the main menu. When a protection function is selected, a setting adjustment screen corresponding to this protection function will pop up so that the current settings of this protection function could be viewed and changed. A typical setting adjustment menu, which corresponds to loss–of–excitation protection, is shown in Fig. 9.4.2.

The setting adjustment screens for all protection functions have somethings in common. One is that other than displaying the name of the protection function, the criterion or algorithm used by this function is also displayed. This eliminates the need to memorize the criterion or algorithm used by this function. And the meaning of the displayed settings can immediately be understood by the operators or relay engineers. Also every time a new setting is typed in, the program asks for confirmation so that type–in mistakes can be corrected immediately.

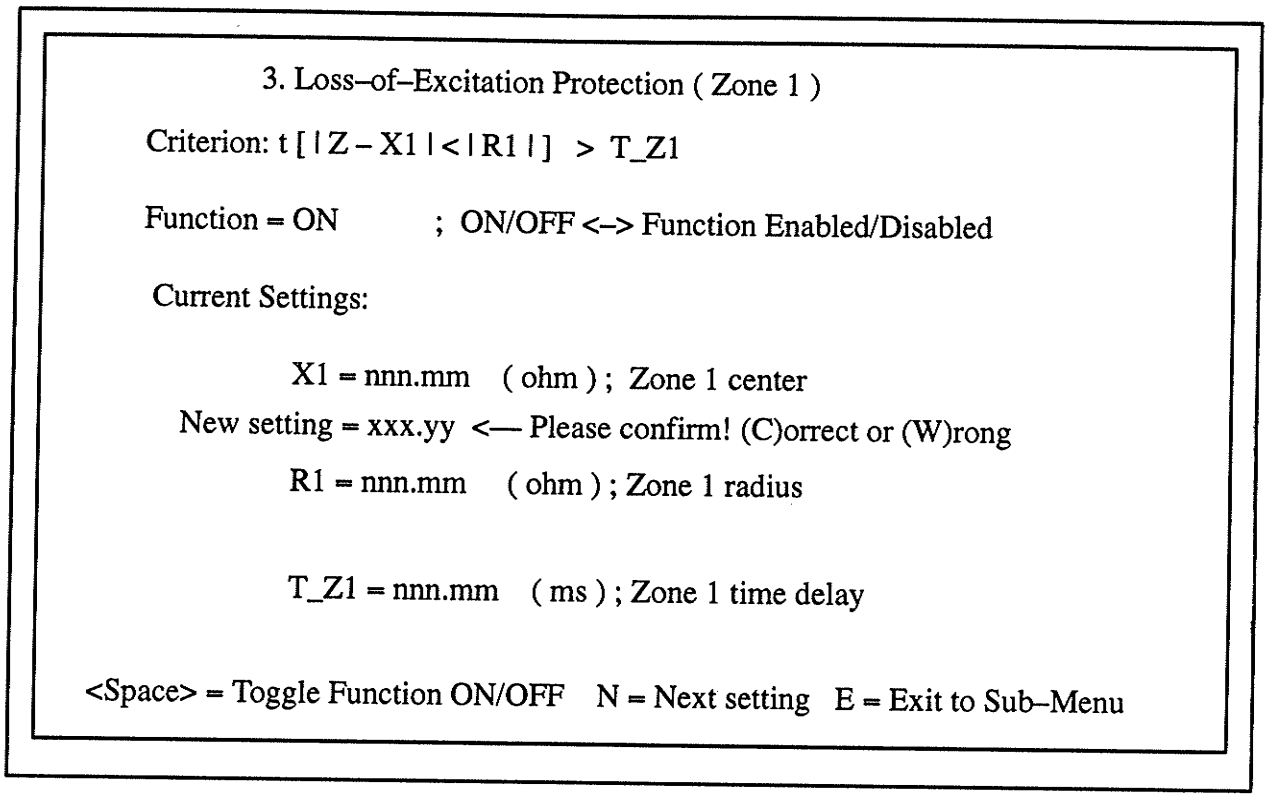

Fig. 9.4.2 Typical setting adjustment screen

Besides providing the man–machine interface, the program also performs another important task of receiving and storing fault records generated by the AMPS board.

While in "command waiting" state under main menu or in setting adjustment sub–menu, the man–machine interface program also periodically checks the communication input buffer to see if there is any request from the AMPS board asking for fault record transfer. If there is one, a fault record transfer process will be started to transfer the fault record from AMPS board to the fault record buffer of this program. After receiving a complete fault record, it will be written to the PC's hard disk and returns to the normal "command waiting" state. The number, which indicates how many fault records have been received since the program started its run, is also updated to reflect that a new record has been received.

9–5 Fault records display program

The fault record display program is an important tool for post–fault analysis and protection system performance evaluation. A fault record display program for an integrated protection system

requires more sophisticated features than a normal fault record display program for a single function protection scheme.

An MS Windows program written in C was developed for displaying multiple waveforms of fault records generated by the first prototype of IGPS. The program is aimed to provide a basic tool for viewing the fault records. Besides the normal fault record displaying functions in other waveform displaying programs, the program implemented some useful features for an integrated protection system.

(1) The ability to select and display two fault records at the same time. Most fault record display programs display only one fault record at a time. But for post–fault analysis, it will be very helpful if two fault records can be displayed at the same time and compared side by side, so that two different cases having slight differences can be compared.

(2) Two different waveform selection options. An integrated protection system stores all input signals which are obtained from the protected equipment and all implemented protection functions operating status in its fault records. It is very difficult and usually unnecessary to display all these signals and status at the same time in one screen. The program offers two different waveform selection options.

One waveform selection option is waveform–based. A dialog box is provided for this option. It lists all waveforms which can be displayed, including protection function characteristics and operating status, name by name. Any desired waveform to be displayed could be checked in this dialog box. Only those waveforms selected will be displayed when fault records are selected. This is a normal option similar to some other fault record display programs.

Another waveform selection option is the protection–function–based one. This is a preferred option for an integrated protection system. When this option is selected, one can select all waveforms related to one protection function (includes input signals, protection characteristics and operating status) by just selecting the name of that protection function. This greatly simplifies the waveform selection process when there is only one or two protection functions of interest.

To best suit the requirement of displaying fault records for integrated protection systems, some other features, such as waveform cut–and–paste, waveform analysis capability, were originally planned to be included. These features are equally important for a practical integrated protection system. However, due to the time limitation these features have not yet been implemented.

CHAPTER 10

CONCLUSIONS AND FUTURE DEVELOPMENT OF IGPS

10–1 Achievements and conclusions

The work completed in this research has achieved its original goals. The special generator protection problems related to generating stations connected to DC lines have been studied and their solutions provided. The first prototype of an integrated generator protection system has been developed and some important results regarding its feasibility obtained. The main achievements and contributions of this research can be summarized as follows:

(1) Three special generator protection problems related to generating stations connected to DC lines have been thoroughly studied, and the solutions to these problems have been provided. These problems are studied with the focus of providing proper protections and easily integrating these protections into an integrated generator protection system.

(2) In addition to the "spectral leakage" problem of an FFT in accurate harmonic measurement caused by asynchronous sampling, this research has further discussed the problem of "sampling window moving effect" of an FFT caused also by asynchronous sampling. This, to the author's knowledge, has not been discussed previously in the literature.

(3) An efficient technique of implementing the FFT for real data series has been studied. It has been successfully applied to the implementation of an FFT subroutine for the first prototype of IGPS.

(4) A fast $\Delta\alpha/\Delta t$ frequency tracking algorithm has been studied and implemented successfully in the first prototype of IGPS. The algorithm can track system frequency change very quickly in a wide system operating frequency range from 45 Hz to 90 Hz with a higher rate of frequency change that is not covered by most of the frequency measuring and tracking algorithms seen in the literature. The power series expansion technique is used in the implementation of this algorithm, which introduces little error but greatly improves its computation speed when implemented on a DSP.

(5) Several aspects of the self–excitation problems in such a generating station are thoroughly studied and this is the major contribution of this study to the problem area. In this research, the difference between immediate and non–immediate self–excitations, the generator operating constraints as affected by the self–excitation protection considerations, the conditions under which a generator loss–of–excitation protection may misoperate, generator dynamic frequency changing characteristics after a load rejection and finally, some problems related to the application of a commonly suggested "low field current + overvoltage relay" self–excitation protection system are for the first time analyzed. Several important results were obtained. A predictive self–excitation protection system is also developed based on these results.

(6) Several common problems related to integrated protection systems have been analyzed. Besides the obvious economic advantages of an integrated system over a non–integrated one, the reliabilities of both systems are compared taking into account the consideration of several common practices of utilities. The other advantages of integrated systems over non–integrated ones are analyzed, and the basic requirements for an integrated system are discussed. The reliability comparison between the two systems, and the discussion of some advantages of an integrated system have not been seen previously in the literature.

(7) All desired main and special protection and monitoring functions have been successfully implemented into the first prototype of IGPS, except for the harmonics monitoring function. The number of harmonics which can be monitored has been reduced from DC — 15th to DC — 7th due to the reduction of sampling rate from 32 point/cycle to 16 point/cycle. The reduction of the sampling rate is the result of the original AMPS hardware limit.

(8) A requirement of at least 10 times more computation power of the modified original AMPS board for implementing a practical integrated generator protection system has been identified, based on the experience obtained in the development of the first prototype of IGPS and careful considerations of a practical integrated generator protection system's requirement.

Based on the work completed in this research, several conclusions can be stated as follows:

(1) An integrated protection system provides a cost–efficient solution for solving the problems of existing protection systems in modifying and/or adding new functions. When such a system is installed as a new system, no hardware change will be required for protection function modification and new functions addition. This system can also provide an economical replacement option for the existing system due to its low cost.

(2) A generator protection system using integrated sub–systems has higher security and availability than using non–integrated sub–systems. Its dependability can be enhanced by the use of a common one–out–of–two system structure. The reliability level of an integrated protection system can be further increased by adopting a two–out–of–three system structure and other reliability enhancement measures, such as dual input circuits structure.

(3) Integrated protection systems are also advantageous over non–integrated systems in other areas, such as better fault record function, high level resources sharing, ease of implementing more complicated protection functions, etc. Thus one of the main conclusions of this research is that integrated protection systems should be the main direction of next generation protection systems development.

(4) It is feasible in the next 3 – 4 years to implement a low–cost yet powerful integrated digital generator protection system having the required computation power by using state–of–the–art computer technology.

(5) The three special generator protection and monitoring problems of a generating station connected to DC lines can be solved cost–efficiently by utilizing integrated generator protection systems.

(6) The self–excitations in such a generating station could be prevented either by restricting the generators' operation to be within their self–excitation operating constraints, or by installing a filter–tripping self–excitation protection system.

(7) The predictive self–excitation protection system developed in this research can overcome major problems of the commonly suggested "low field current + overvoltage relay" system. It also can be easily integrated into an integrated generator protection system.

10–2 Suggestions for further research and development of IGPS

The work completed in this research has accomplished its original goals. There are several areas the author would like to suggest for further studies. These areas are all very important for the development and application of a practical IGPS and solving the special protection problems related to generators connected to DC lines. These areas are as follows:

(1) *Development of a practical integrated generator protection system.* This is the direct continuation of the development of the first prototype of IGPS. Any new computer platform with acceptable cost, as well as having at least 10 times more computation power than that of the modified original AMPS board, can be considered. But this time, the system structure, network capability, high level programming language support and some other important issues should also be considered. The new development is aimed to provide a practical integrated protection system for large generators. It not only can solve the common problems in modifying and/or adding new functions to existing systems, but also intends to realize all the advantages of an integrated protection system.

(2) *Further studies in self–excitation protection for generators connected to DC lines.* The self–excitation protection studies conducted in this research use a one–machine model system in most of the simulations. This is primarily due to the limitations of using the Electromagnetic Transient simulation program PSCAD/EMTDC in simulating self–excitation problems on the present SUN workstations. A self–excitation after a load rejection is a long dynamic electro–mechanical process. To obtain a stable excitation system response in the presence of non–harmonic oscillations caused by the load rejections, the self–excitation simulations have to use very short time steps. Both make each simulation case run on the current SUN workstations a painfully long process, even when a simple one–machine system is modelled. The study of self–excitation protection with a full system representation is preferred if it does not take too much time for simulating one case. Though most of the results could be expected to be in close agreement with the current studies, some practical issues, such as how small differences between generators will affect the accuracy of self–excitation prediction, can only be investigated by using a full system representation. Using digital simulations to study self–excitation problems probably is the only choice, as

the problem is difficult to study on an analog simulator and conducting field tests is almost impossible.

(3) *Further reliability studies for integrated protection systems.* The reliability comparison made in this research between integrated and non–integrated protection systems is not a full range comparison on a strict quantitative basis. As the reliability of protection systems is a major concern of utilities, it is better to have the reliability of integrated protection systems further studied in another research. The possible topics could be to compare both systems using actual statistical data to calculate the dependability and security level of several commonly used system structures and to study measures in enhancing the reliability of an integrated protection system. These studies should also take into account several practical factors, which have been pointed out in this research.

(4) *Developing a digital generator model for generator internal fault tests.* To test a generator protection system under actual internal fault conditions is still close to impossible nowadays, though the generator protecting system can be tested under close to real situations for external faults and abnormal conditions caused by external faults, load unbalance and other abnormal conditions on some analog or digital simulators. The difficulty is caused by the fact that any internal fault not only has electrical impacts on the generator, but also has magnetic impacts on the generator field which is machine dependent. One example is the interturn fault. The shorted turns not only directly reduces the EMF of this phase, but also interact with the generator rotating field thus affecting other phases. A digital generator model, which can model actual generator structure and produce close to real fault currents and voltages for all internal faults at the measurable points of a generator, will make the off–line or even real–time tests of generator protection systems become possible. It will also facilitate many other studies, such as investigating the adequacy of generator protection algorithms presently used, developing new generator protection algorithms as well as some other studies which may emerge when such a model is available.

REFERENCES

Universal (or integrated) generator protection systems

[1] G. Benmouyal, "Design of a universal protection relay for synchronous generators", CIGRE session 1988, No. 34–09

[2] G. Benmouyal, S. Barceloux and R. Pelletier, "Field experience with a digital relay for synchronous generators", IEEE Trans., PWRD–7, No. 4, Oct. 1992, 1984 – 1992

[3] J. H. Harlow, "A multifunction protective relay for the cogeneration industry", IEEE CAP, Oct. 1990

[4] Ilar and G.stranne, " Numerical protection systems for generators and generator transformer units ", ABB Review, No. 1 1993, pp.27

Generator protections (general)

[5] AIEE project committee on generator protection of the AIEE relay committee, "Relay protection of A–C generators", AIEE Trans., Part I, Vol. 70, 1951, pp 275–281

[6] Working group of the generator protection subcommittee of the AIEE relays committee, "A partial survey of relay protection of steam–driven A–C generators", IEEE Trans., PAS–81, No. 2, Feb. 1962, pp 954–957

[7] The AC generator protection guide working group of the IEEE power system relaying committee, "Summary of the 'guide for AC generator protection' ANSI/IEEE c37.102–1987", IEEE Trans., PWRD–4 No. 2, Apr. 1989, pp 957–964

[8] Working group of IEEE power system relaying committee, "Impact of HV and EHV transmission on generator protection", IEEE Trans., PWRD–8 No. 3, July 1993, pp 962 – 974

[9] G. Ziegler, "Developments in generator protection – design and application aspects of a new numerical relay range", Proceeding of IEE, Fifth International Conference on Development in Power System Protection, April 1993, pp. 111 – 114

[10] K. Khan and B. Cory, "Developments in digital generator protection", Proceeding of IEE, Third International Conference on Development in Power System Protection, April 1985, pp. 223 – 226

[11] J. Gantner, "New developments in the protection of large turbo–generators", Proceeding of IEE, First International Conference on Development in Power System Protection, March 1975, pp. 64 –70

Generator differential protection

[12] G. S. Hope, P. dash and O. P. Malik, "Digital differential protection of a generating unit — scheme and real–time test results", IEEE Trans., PAS–96, No. 2, Mar./Apr. 1977, pp 502–512

[13] P. Dash, O. P. Malik and G. S. Hope, "Fast generator protection against internal asymmetrical faults", IEEE Trans., PAS–96, No. 5, Sept./Oct. 1977, pp 1498–1506

[14] P. McCleer and M. Mir, "A new technique of differential relaying: the Δ–differential relay", IEEE Trans., PAS–101, No. 10, Oct. 1982, pp 4164–4170

Generator loss–of–field protection

[15] The Working group of the rotating machinery protection subcommittee of the IEEE power system relay committee, "Loss–of–field relay operation during system disturbances, working group report – June 1971", IEEE Trans., PAS–94, No. , Sept./Oct. 1975, pp 1464–1472

[16] J. Berdy, "Loss of excitation protection for modern synchronous generators", IEEE Trans., PAS–94, No. , Sept./Oct. 1975, pp 1457–1463

[17] R. Tremaine and J. Blackburn, "Loss–of–field protection for synchronous machines", AIEE Trans., Part IIIA, vol. 73, Aug. 1954, pp 765–772

Generator stator ground fault protection

[18] The generator ground protection guide working group of the power system relaying committee, "Generator ground protection guide", IEEE Trans., PAS–103, No. 7, July 1984, pp 1743–1748

[19] X. Xin, O. Malik, G. Hope and D. Chen, "Adaptive ground fault protection schemes for turbo–generator based on third harmonic voltages", IEEE Trans., PWRD–5, No. 2, Apr. 1990, pp 595–603

[20] C. H. Griffin and J. W. Pope, "generator ground fault protection using overcurrent, overvoltage, and undervoltage relays", IEEE Trans., PAS–101, No. 12, Dec. 1982, pp 4490–4501

[21] R. J. Marttila, "Design principles of a new generator stator ground relay for 100% coverage of the stator winding", IEEE Trans., PWRD–1, No. 4, Oct. 1986, pp 41–51

[22] R. L. Schlake, G. W. Buckley and G. McPherson, "Performance of third harmonic ground fault protection schemes for generator stator windings", IEEE Trans., PAS–100, No. 7, July 1981, pp 3195–3202

[23] J. W. Pope, "A comparison of 100% stator ground fault protection schemes for generator stator windings", IEEE Trans., PAS–103, No. 4, Apr. 1984, pp 832–840

Harmonics and its measurement techniques

[24] J. Arrillaga, D. A. Bradley and P. S. Bodger, "Power system harmonics", Chichester [West Sussex], New York, Wiley, 1985

[25] P. Filipski and P. Labaj, "Evaluation of reactive power meters in the presence of high harmonic distortion", IEEE Trans. PWRD–7, No. 4, Oct. 1992, pp. 1793 – 1799

[26] R. Arseneau and P. Filipski, "Application of a three phase nonsinusoidal calibration system for testing energy and demand meters under simulated field conditions", IEEE Trans. PWRD–3, No. 3, July 1988, pp. 874 – 879

[27] M. Cox and T. Williams, "Induction VARhour and solid–state VARhour meters performances on nonlinear loads", IEEE Trans. PWRD–5, No. 4, Nov. 1990, pp. 1678 – 1686

[28] A. E. Emanuel, "Powers in nonsinusoidal situations — A review of definitions and physical meaning", IEEE Trans. PWRD–5, No. 3, July 1990, pp. 1377 – 1383

[29] L. S. Czarnecki, "Considerations on the reactive power in nonsinusoidal situations", IEEE Trans. IM–34, No. 3, Sept. 1985, pp. 399 –404

[30] Pan Wen, "A fast and high–precision measurement of distorted power based on digital filtering techniques", IEEE Trans. IM–41, No. 3, June 1992, pp. 403 – 406

[31] P. Filipski, "The measurement of distortion current and distortion power", IEEE Trans. IM–33, No. 1, Mar. 1984, pp. 36 – 40

[32] *IEEE Guide for Harmonic Control and Reactive Compensation of Static Power Converters*, IEEE Std. 519 – 1981

[33] A. Ferrero and R. Ottoboni, "High–accuracy Fourier analysis based on synchronous sampling techniques", IEEE Trans. IM–41, No. 6, Dec. 1992, pp. 780 – 785

[34] A. A. Girgis, W. B. Chang and E. B. Makram, "A digital recursive measurement scheme for on–line tracking of power system harmonics", IEEE Trans., PWRD–6 No. 3, July 1991, pp. 1153 – 1160

[35] CEA Research Report, "Power system harmonic measurement", No. 180, D 441, Nov. 1989

[36] J. S. Subjak, Jr. and J. S. McQuilkin, "Harmonics — causes, effects, measurements, and analysis: an update", IEEE Trans. IA–26, No. 6, Nov./Dec. 1990, pp. 1034 – 1042

[37] J. K. Winn, Jr. and D. R. Crow, "Harmonic measurements using a digital storage oscilloscope", IEEE Trans. IA–25, No. 4, July/Aug. 1989, pp. 783 – 788

[38] G. Andria, L. Salvatore, M. Savino and A. Trotta, "Techniques for identification of harmonics in industrial power systems",

[39] T. Grandke, "Interpolation algorithms for discrete Fourier transforms of weighted signals", IEEE Trans., Vol. IM–32, No. , June 1983, pp. 350 –355

[40] G. Andria, M. Savino and A. Trotta, "Windows and interpolation algorithms to improve electrical measurements accuracy", IEEE Trans., Vol. IM–38, No. , Aug. 1989, pp. 856 – 863

[41] A. Ferrero and R. Ottoboni, "A new approach to the Fourier analysis of periodic signals for the minimization of the phase errors", IEEE Trans., Vol. IM–40, No. , Aug. 1991, pp. 694 – 698

[42] L. Zu–Liang, " An error estimation for quasi–integer–period sampling and an approach for improving its accuracy", IEEE Trans., Vol. IM–37, No. , June 1988, pp. 219 – 222

[43] H. J. Nussbaumer, *Fast Fourier Transform and Convolution Algorithms*, Berlin, New York, Springer–Verlag, 1981

[44] E. O. Brigham, *The Fast Fourier Transform and Its Applications*, Englewood Cliffs, NJ, Prentice–Hall, 1974

Frequency measurement and tracking

[45] O. P. Malik et al, "Frequency measurement for use with a microprocessor–based turbine governor", Paper No. 91WM140–4EC, IEEE PAS Winter Meeting, New York, Feb. 1991

[46] S. A. McIlwaine, C. E. Tindall and W. McClay, "Frequency tracking for power system control", Proc. IEE, Vol. 133, Part C, No. 2, Mar. 1986, pp. 95 – 98

[47] A. A. Girgis and D, Hwang, "Optimal estimation of voltage phasors and frequency deviations using linear and non–linear Kalman filtering: theory and limitations", IEEE Trans. PAS–103, No. 10, Oct. 1984, pp. 2943 – 2949

[48] M. S. Sachdev, H. C. Wood and N. Johnson, "Kalman filtering applied to power system measurements for relaying", IEEE Trans. PAS–104, No. 12, Dec. 1985, pp. 3565 – 3573

[49] I. Kamwa and A. T. Johns, "Fast adaptive schemes for tracking voltage phasor and local frequency in power transmission and distribution systems", IEEE Trans. PWRD–7, No. 2, Apr. 1992, pp. 789 – 795

[50] M. M. Begovic, P. M. Djuric, S. Dunlap and A. G. Phadke, "Frequency tracking in power networks in the presence of harmonics", IEEE Trans., PWRD–8 No. 2, April 1993, pp. 480 – 486

[51] A. G. Phadke, J. S. Thorp and M. Adamiak, "A new measurement technique for tracking voltage phasors, local system frequency, and rate of change of frequency", IEEE Trans., PAS–102 No. 5, May 1983, pp. 1025 – 1038

[52] P. J. Moore, D. Carranza and A. T. Johns, "Performance of a new high speed digital technique for measuring power system frequency", Proceeding of IEE, Fifth International Conference on Development in Power System Protection, April 1993, pp. 73 – 76

[53] G. Benmouyal, "Design of a combined digital global differential and volt/hertz relay for step–up transformers", IEEE Trans., PWRD–6 No. 3, July 1991, pp. 1000 – 1007

[54] M. S. Sachdev and Jianping Shen, "A new digital technique for measuring frequency at a power system bus", Proceeding of IEE, Fourth International Conference on Development in Power System Protection, April 1989, pp. 102 –106

[55] M. Giray and M. S. Sachdev, "Off–nominal frequency measurements in electric power systems", IEEE Trans., PWRD–4 No. 3, July 1989, pp. 1573 – 1578

[56] M. S. Sachdev and M. Giray, "A Least Squares technique for determining power system frequency", IEEE Trans., PAS–104, Feb. 1985, pp. 437 – 443

[57] A. A. Girgis and W. Peterson, "Adaptive estimation of power system frequency deviation and its rate of change for calculating sudden power system overloads", IEEE Trans., PWRD–5 No. 2, April 1990, pp. 585 –594

[58] A. A. Girgis and F. Ham, "A new FFT–based digital frequency relay for load shedding", IEEE Trans., PAS–101, Feb. 1982, pp. 433 –439

Self–excitation problem and its protection

[59] System Planning Division, Transmission Planning Department (Manitoba Hydro Internal Report), "Report on Nelson river collector system operating restrictions and protection for self–excitation and second harmonic resonance", Interim report SPD 80–29, Spet. 30, 1980

[60] Memo from C. V. Thio to J. T. Atchison etc. (Manitoba Hydro Internal Report), "Collector system self–excitation protection", Dec. 29, 1982

[61] A. M. Gole, "Exciter stresses in capacitively loaded synchronous generators", Ph.D. Thesis, August 1982, University of Manitoba, Winnipeg, manitoba, Canada

[62] Yi Hu, P. G. McLaren, A. M. Gole, D. J. Fedirchuk and A. Castro, "Misoperation of hydro generator protections under HVDC load rejection", Proceedings of International Conference on The Development of Protection and Control Systems, May 1994, Beijing, P. R.China

[63] H. M. Rustebakke and C. Concordia, "Self–excited oscillations in a transmission system using series capacitors", IEEE Trans. PAS–89, No. 7, Sept./Oct. 1970, pp 1504–1512

[64] F. P. de Mello, A. C. Dolbec, and D. A. Swann, "Analog computer studies of system overvoltages following load rejections", IEEE Trans., pt. III, PAS–82, April 1963, pp. 42 – 49

[65] P. L. Dandeno and K. R. McClymont, "Extra–high–voltage system overvoltages following load rejection of hydraulic generation", IEEE Trans. PAS–81, No. 4, Apr. 1963, pp 49–

[66] F. Peer and R. Lubasch, "Unitrol static excitation equipment for the generators of the world's largest hydro power plant Itaipu", Brown Boveri Review, No. 82–3, pp 65–68

[67] H. Scheibengraf and H. Herzog, "Interaction of the various limit controllers of a static excitation system with reference to the equipment for the Itaipu power plant", Brown Boveri Review, No. 82–3, 1983, pp 69–72

[68] F. Peneder, H. J. Herzog and R. Bertschi, "Static systems for positive and negative excitation current", Brown Boveri Review,

[69] F. P. de Mello, L. M. Leuzinger and R. J. mills, "Load rejection overvoltages as affected by excitation system control", IEEE Trans., PAS–93, No. 2, Mar./Apr. 1975, pp 280–287

[70] S. Nishida, H. Suzuki and S. Takeda, "Analysis of overvoltages caused by self–excitation in a separated power system with heavy load and large shunt capacitance", IEEE Trans., PAS–102, No. 7, July 1983, pp 1970–1978

[71] V. Crastan, "Investigation of Self–excitation of Synchronous Machines", The Brown Boveri Review, Vol. 49, No. 3/4, pp. 80 –94, 1962

Digital protection systems

[72] IEEE Tutorial Course Textbook, "Microprocessor relays and protection systems", 1987

[73] M. S. Sachdev and M. Nagpal, "A recursive Least Error Squares algorithm for power system relaying and measurement applications", IEEE Trans., PWRD–6 No. 3, July 1991, pp. 1008 – 1015

Reliability of protection systems

[74] H. Hubensteiner and H. Ungrad, "Reliability of protection equipment in operation", Brown Boveri Review, 1/2 1983, pp. 111 – 116

[75] H. Ungrad and E. Wildhaber, "Methods of ensuring the reliable performance of protection equipment", Brown Boveri Review, 6 1978, pp. 348 – 357

[76] M. Tonnes, "Quality assurance for products used in protection and control systems", Brown Boveri Review, 1/2 1983, pp. 117 – 119

[77] F. Ando, H. Ohta and Y. Oura, "Protection Relays With Automatic Supervision And Inspection", Proceeding of IEE, First International Conference on Development in Power System Protection, March 1975, pp. 392 –398

Miscellaneous

[78] J. Arrillaga, *High Voltage Direct Current Transmission*, London, Peregrinus, 1983.

[79] J. Arrillaga, C. Arnold and B. Harker, *Computer Modelling of Electrical Power Systems*, Chichester, New York, Wiley, 1983

[80] J. S. Thorp et al, "Feasibility of adaptive protection and control", IEEE Trans., PWRD–8 No. 3, July 1993, pp 975 – 983